



12-2009

Design and Synthesis of Novel Tylophorine Analogs and their Biological Activity

Julio Gutierrez
University of Tennessee - Knoxville

Follow this and additional works at: https://trace.tennessee.edu/utk_graddiss

 Part of the [Chemistry Commons](#)

Recommended Citation

Gutierrez, Julio, "Design and Synthesis of Novel Tylophorine Analogs and their Biological Activity." PhD diss., University of Tennessee, 2009.
https://trace.tennessee.edu/utk_graddiss/603

This Dissertation is brought to you for free and open access by the Graduate School at TRACE: Tennessee Research and Creative Exchange. It has been accepted for inclusion in Doctoral Dissertations by an authorized administrator of TRACE: Tennessee Research and Creative Exchange. For more information, please contact trace@utk.edu.

To the Graduate Council:

I am submitting herewith a dissertation written by Julio Gutierrez entitled "Design and Synthesis of Novel Tylophorine Analogs and their Biological Activity." I have examined the final electronic copy of this dissertation for form and content and recommend that it be accepted in partial fulfillment of the requirements for the degree of Doctor of Philosophy, with a major in Chemistry.

David C. Baker, Major Professor

We have read this dissertation and recommend its acceptance:

Michael D. Best, Ziling (Ben) Xue, Engin H. Serpersu

Accepted for the Council:

Carolyn R. Hodges

Vice Provost and Dean of the Graduate School

(Original signatures are on file with official student records.)

To the Graduate Council:

I am submitting here with a dissertation written by Julio Gutierrez entitled "Design and Synthesis of Novel Tylophorine Analogs and their Biological Activity." I have examined the final electronic copy of this dissertation for form and content and recommend that it be accepted in partial fulfillment of the requirements for the degree of Doctor of Philosophy, with a major in Chemistry.

Dr. David C. Baker
Major Professor

We have read this dissertation
and recommend its acceptance:

Dr. Michael D. Best

Dr. Ziling (Ben) Xue

Dr. Engin H. Serpersu

Accepted for the Council:

Carolyn R. Hodges
Vice Provost and Dean of the
Graduate School

(Original signatures are on the file with official student records.)

**Design and Synthesis of Novel Tylophorine Analogs and
their Biological Activity**

A Dissertation

Presented for the

Doctor of Philosophy Degree

The University of Tennessee, Knoxville

Julio Gutierrez

December 2009

Dedication

I dedicate this work to my family who has always supported me. I want to thank my daughter Amy Andrea Gutierrez whose smile, love and role as a great dance partner motivated me to finish this degree. I want to deeply thank my beautiful wife Yolanda Emperatriz Cabrejo whose unconditional support helped me to obtain this work. Without her this would not exist.

Acknowledgments

First, the author would like to thank my adviser Dr. David D. Baker for his unconditional support since I started working in his lab in 2002 as an undergraduate student for a summer internship.

Second, he wants to thank past members of the Baker group for their advice, especially Mr. Conrad Kaczmarek who was my adviser during my first months as a synthetic chemist.

Third, he wants to thank Dr. Carlos Steren for his immense support using the 300 NMR and the author appreciates his knowledge in the characterization of compounds.

Finally, the author acknowledges his parents Oscar Gutierrez and Hermelinda Nava, and his sister Eva Gutierrez for their constant support and love. Also, his wife Yolanda Cabrejo and daughter Amy Gutierrez is deeply appreciated for their unconditional love and support throughout his graduate school.

Abstract

Alkaloids containing the nitrogen atom in the bridgehead position of two rings, such as indolizidine, pyrrolizidine, and quinolizidine alkaloids, have a wide and varied distribution in nature. Some of these alkaloids demonstrate a broad range of pharmacological activities and have generated substantial synthetic interest. This thesis covers the total synthesis of novel tylophorine analogs called DCB 3503, DCB 3506, DCB 3507, DCB 3508, DCB 3509, and a derivative with a biotinylated chain attached to DCB 3506 for use as a biological probe. This thesis discusses the biological activity of these compounds as well.

Table of Contents

List of tables.....	ix
List of figures.....	x
List of schemes.....	xii
Abbreviations and acronyms.....	xiii
1. Chapter One: Synthesis of DCB 3503.....	14
1.1 Statement of problem.....	14
1.2 Introduction.....	15
1.3 Results and discussion: DCB 3503 scale-up.....	17
1.3.1 Synthesis of (<i>E</i>)-2,3-bis(3,4-dimethoxyphenyl)acrylic acid (3).....	19
1.3.2 Synthesis of (<i>E</i>)-methyl 2,3-bis(3,4-dimethoxyphenyl)acrylate (4).....	22
1.3.3 Synthesis of methyl 2,3,6,7-tetramethoxyphenanthrene-9- carboxylate (5).....	23
1.3.3.1 Method 1: VOF ₃	23
1.3.3.2 Method 2: FeCl ₃ anhydrous.....	26
1.3.4 Synthesis of (2,3,6,7-tetramethoxyphenylphenanthren-9-yl)methanol (6).....	28
1.3.5 Synthesis of (<i>S</i>)-methyl 5-oxo-1-((2,3,6,7)-tetramethoxyphenanthren-9- yl)methyl)pyrrolidine-2-carboxylate (7).....	29
1.3.5.1 Important NMR observation for diastereotopic hydrogens on C11 for product (7).....	18
1.3.6 Synthesis of (<i>S</i>)-5-oxo-1-((2,3,6,7-tetramethoxyphenanthren-9- yl)pyrrolidine-2-carboxylic acid (8).....	37
1.3.7 Synthesis of (<i>S</i>)-2,3,6,7-tetramethoxy-13,13a dihydrodibenzo[<i>f,h</i>]pyrrolo[1,2- <i>b</i>]isoquinoline-11,14(9 <i>H</i> ,12 <i>H</i>)-dione.....	38
1.3.7.1 Method 1: TFAA and BF ₃ ·Et ₂ O.....	38
1.3.7.2 Method 2: Oxalyl chloride and SnCl ₄	42

1.3.8 Synthesis of (13a <i>S</i> , 14 <i>S</i>)-2,3,6,7-tetramethoxy-9,11,12,13,13a,14 hexahydrodibenzo[<i>f,h</i>]pyrrolo[1,2- <i>b</i>]isoquinolin-14-ol (11).....	44
1.3.8.1 Molecular modeling and dihedral angle between H14 and H13a.....	45
1.3.9 Attempted cyclization of the free amide (29).....	47
2. Chapter Two: Synthesis of DCB 3507.....	49
2.1 Statement of problem.....	49
2.2 Introduction.....	50
2.3 Results and discussion: Total synthesis of DCB 3507.....	51
2.3.1 Synthesis of (<i>E</i>)-3-(3,4-dimethoxyphenyl)-2-phenylacrylic acid (13)	
2.3.1.1 Condensation reaction to give C.....	53
2.3.1.2 Condensation reaction to give (13).....	53
2.3.2 Synthesis of methyl 2,3-dimethoxyphenanthrene-9-carboxylate (15)	
2.3.2.1 Method 1 VOF ₃	58
2.3.2.2 Method 2 FeCl ₃ /SiO ₂	58
2.3.3 Synthesis of (2,3-dimethoxyphenanthren-9-yl)methanol (16).....	66
2.3.4 Synthesis of (<i>S</i>)-methyl 1-((2,3-dimethoxyphenanthren-9-yl)methyl)-5-oxopurrolidine-2-carboxylate (17).....	67
2.3.4.1 AB spin system.....	67
2.3.4.2 Geminal coupling ² <i>J</i> (H,H), bond angle, and effect of neighboring π electrons for methylene protons on C11 of (17).....	70
2.3.5 Synthesis of (<i>S</i>)-2,3-dimethoxy-13,13a dihydrodibenzo[<i>f,h</i>]pyrrolo[1,2 <i>b</i>]isoquinoline-11,14(9 <i>H</i> , 12 <i>H</i>)-dione (19).....	72
2.3.5.1 Method 1 TFAA and BF ₃ ·Et ₂ O.....	72
2.3.5.2 Method 2 (COCl) ₂ and SnCl ₄	72
2.3.6 Synthesis of (13a <i>S</i> , 14 <i>S</i>)-14-hydroxy-2,3-dimethoxy-12,13,13a,14 tetrahydrodibenzo[<i>f,h</i>]pyrrolo[1,2- <i>b</i>]isoquinolin-11(9 <i>H</i>)-one (20).....	77

2.3.7 Synthesis of (13a <i>S</i> , 14 <i>S</i>)-2,3-dimethoxy-9,11,12,13a,14-hexahydrodibenzo[<i>f,g</i>]pyrrolo[1,2- <i>b</i>]isoquinolin-14-ol (21).....	80
2.3.8 Karplus equation and molecular modeling applied to DCB 3507.....	82
2.3.8.1 Dihedral angle analysis.....	82
2.3.8.2 Vicinal coupling constant analysis.....	83
2.3.8.3 Karplus equation analysis.....	83
2.3.8.4 Molecular modeling (Tripos: SYBYL 8.0).....	86
3. Chapter Three: Synthesis of DCB 3508.....	90
3.1 Statement of problem.....	90
3.2 Introduction.....	91
3.3 Results and discussion: Total synthesis of DCB 3508.....	92
3.3.1 Synthesis of (<i>S</i>)-methyl 1-(2,3,6,7-tetramethoxyphenanthren-9-yl)methylpyrrolidine-2-carboxylate (24).....	93
3.3.2 Synthesis of (<i>S</i>)-1-((2,3,6,7-tetramethoxyphenanthren-9-yl)methylpyrrolidin-2-yl)methanol (25).....	97
4. Chapter four: Synthesis of DCB 3509.....	101
4.1 Statement of problem.....	101
4.2 Introduction.....	102
4.3 Results and discussion: Total synthesis of DCB 3509.....	103
4.3.1 Synthesis of Preparation of (13a <i>S</i> , 14 <i>S</i>)-3-(3-hydroxypropoxy)-2,6,7-trimethoxy-9,11,12,13,13a,14 hexahydrodibenzo[<i>f,h</i>]pyrrolo[1,2- <i>b</i>]isoquinolin-14-ol (37).....	106
5. Chapter five: Synthesis of biotinylated tylophorine analog.....	111
5.1 Statement of problem.....	111
5.2	
Introduction.....	112
5.3 Results and discussion: Total synthesis of biotinylated tylophorine analog.....	113

5.3.1 Synthesis of (13a <i>S</i> , 14 <i>S</i>)-3-(6-bromohexyloxy)-14-hydroxy-2,6,7-trimethoxy-12,13,13a,14-tetrahydrodibenzo[<i>f,h</i>]pyrrolo[1,2- <i>b</i>]isoquinolin-11(9 <i>H</i>)-one (38).....	114
5.3.2 Synthesis of (13a <i>S</i> ,14 <i>S</i>)-3-(6-azidohexyloxy)-14-hydroxy-2.6.7- trimethoxy-12,13,13a,14-tetrahydrobibenzo[<i>f,h</i>]pyrrolo[1,2- <i>b</i>]isoquinolin-11(9 <i>H</i>)-one (39).....	117
5.3.3 Synthesis of (13a <i>S</i> ,14 <i>S</i>)-3-(6-aminohexyloxy)-2,6,7-trimethoxy-9,11,12,13,13a,14-hexahydrodibenzo[<i>f,h</i>]pyrrolo[1,2- <i>b</i>]isoquinolin-14-ol (40).....	120
5.3.4 Synthesis of <i>N</i> -(6-((13a <i>S</i> ,14 <i>S</i> -14-hydroxy-2,6,7-trimethoxy-9,11,12,13,13a,14-hexahydrodibenzo[<i>f,h</i>]pyrrolo[1,2- <i>b</i>]isoquinolin-3-yloxy)hexyl)-5-((3a <i>S</i> ,4a <i>S</i> ,6a <i>R</i>)-2-oxohexahydro-1 <i>H</i> -thieno[3,4- <i>d</i>]imidazol-4-yl)pentanamide (41).....	125
6. Chapter six: National Cancer Institute: Development Therapeutics Program	
tylophorine analogs.....	136
6.1 Statement of Problem.....	136
6.2 Background.....	136
6.2.1. Screening.....	136
6.2.2. In vivo testing cells.....	136
6.2.3. Concentrations parameters.....	136
6.2.4. The mean graph.....	136
6.3 DCB 3503 cytotoxic analysis and structure-activity relationships.....	137
6.4 DCB 3507 cytotoxic analysis and structure-activity relationships.....	144
6.5 DCB 3508 cytotoxic analysis and structure-activity relationships.....	151
6.6 DCB 3509 cytotoxic analysis and structure-activity relationships.....	154
6.7 Synthesis of biotinylated tylophorine analog cytotoxic analysis and structure-activity relationships.....	155
Conclusions.....	156
7. Chapter seven: Experimental.....	160

Experimental procedure to scale up DCB 3503	160
Experimental procedure for DCB 3503.....	160
Experimental procedure for DCB 3507.....	174
Experimental procedure for DCB 3508.....	180
Experimental procedure for DCB 3506.....	182
Experimental procedure for DCB 3509.....	187
Experimental procedure for biotinylated tylophorine analog.....	188
References.....	190
Appendix.....	194
Vita.....	385

List of Tables

Table 1: Partial table made by Halton and co-workers ¹⁸	25
Table 2: VOF ₃ and FeCl ₃ reaction time, toxicity, and price	28
Table 3: Comparison of ¹ H and ¹³ C NMR shifts for compound 8, 9, and 10	42
Table 4: SnCl ₄ and BF ₃ ·Et ₂ O reaction time, toxicity, and price	43
Table 5: DCB 3503 dihedral angle molecular modeling results.....	45
Table 6: VOF ₃ and FeCl ₃ /SiO ₂ reaction time, toxicity, and price	59
Table 7: Chemical shift, splitting, and <i>J</i> coupling for 15.....	60
Table 8: Comparison of ¹ H and ¹³ C NMR shifts for compound 18, 19, and 20	72
Table 9: DC 3507 dihedral angle molecular modeling results	83
Table 10: DCB 3507 and DCB 3503 dihedral angle molecular modeling results.....	83
Table 11: Partial table from the paper of Wei ²⁹	97
Table 12: Compound 40 theoretical and experimental mass	116
Table 13: Theoretical and experimental mass for compound 40.....	123
Table 14: DCB 3503 some relevant cell line and growth percent	133
Table 15: DCB 3507 relevant cell line, GI ₅₀ , and growth percent.....	140
Table 16: DCB 3508 relevant cell line and growth percent.....	147
Table 17: Lipinski's "rule of five" applied to DCB analogs	155

List of Figures

Figure 1: Structure of $R^1 = \text{OH}$, $R^2 = \text{H}$, $R^3, R^4 = \text{OMe}$ DCB-3503	16
Figure 2: Compound 3 (<i>E</i>) and (<i>Z</i>) isomer.....	21
Figure 3: Structure of compound 4 (<i>E</i>) and (<i>Z</i>) isomer	24
Figure 4: Coupling constant vs bond angle.....	33
Figure 5: <i>J</i> Coupling of compound 7 at 4.42 ppm	35
Figure 6: <i>J</i> Coupling of compound 7 at 5.51 ppm	36
Figure 7: Molecular modeling structure of compound 7	37
Figure 8: Compound 11 direct drawing and minimization molecular modeling.....	46
Figure 9: Structure of DCB 3507.....	49
Figure 10: Compound 13 (<i>E</i>) and (<i>Z</i>) isomers.....	54
Figure 11: Ring current effect in arenes and compound 13 in plane view	55
Figure 12: ^1H NMR spectrum for compound 13.	56
Figure 13: Compound 15, phenanthrene ring in bold.....	60
Figure 14: Ortho coupling constants for (15)	61
Figure 15: Naphthalene <i>J</i> coupling according to Friebolin	61
Figure 16: AB spin system (roof effect) of compound 17.....	67
Figure 17: Coupling constant vs bond angle.....	68
Figure 18: Structure of compound 17 from molecular modeling.	69
Figure 19: AB spin system (roof effect) of compound 19.....	71
Figure 20: C9 diastereomeric protons of compound 20	76
Figure 21: C9 diastereomeric protons of compound 21.....	78
Figure 22: Dihedral angle case A and case B	79
Figure 23: Karplus curve	81
Figure 24: <i>J</i> coupling of compound 21 at 4.78 ppm.....	82
Figure 25: Direct drawing and minimization molecular.....	85
Figure 26: Direct drawing non planar $\text{DH} = 69^\circ$ molecular modeling compound 21.	86
Figure 27: Structure of DCB 3508.....	87
Figure 28: Diastereotopic hydrogens of 24.....	91
Figure 29: <i>J</i> coupling of compound 24 at 3.53 ppm.....	92
Figure 30: <i>J</i> coupling of compound 24 at 4.48 ppm.....	93
Figure 31: R_f values for compound 11 and 25.	95
Figure 32: Tylophorine derivatives containing prolinol.....	97
Figure 33: Structure of DCB 3509.....	98
Figure 34: Possible substitutions for compound 37.....	104
Figure 35: Chemical shifts for alkylation of 37.....	105
Figure 36: Molecular modeling structure for compound 37.....	106
Figure 37: Biotinylated tylophorine analog structure	107
Figure 38: Characteristic peak intensities for a monobrominated compound	110
Figure 39: Compound 38.	111
Figure 40: Mass spectrum of compound 38.....	112
Figure 41: R_f values for compound 38 and 39.....	113
Figure 42: Mass spectrum of compound 39.....	114

Figure 43: R_f values for 39 and 40.....	115
Figure 44: Molecular weight and fragment ion for compound 40.....	116
Figure 45: Mass spectrum of compound 40.....	117
Figure 46: Chemical structure for HBTU, DCC, DIC, and EDC.....	120
Figure 47: QUATRO II mass spectrum for compound 41.....	125
Figure 48: MALDI mass spectrum with 6.7 ppm error for compound 41.....	126
Figure 49: MALDI mass spectrum with 2.6 ppm error for compound 41.....	128
Figure 50: HPLC results for compound 41 with method 79:21 (MeOH:H ₂ O).....	129
Figure 51: HPLC–mass spectrometer results for compound 41.....	130
Figure 52: Molecular modeling of the structure for compound 41.....	131
Figure 53: Structures of tylophorine, tylocrebine, and DCB 3503.....	134
Figure 54: DCB 3503 mean graph.....	136
Figure 55: DCB 3503 dose–response curves (all cell lines).....	137
Figure 56: DCB 3503 dose–response curves (by cell line).....	138
Figure 57: DCB 3503 in-vitro testing results.....	138
Figure 58: Tylophorine derivative with R substituents.....	141
Figure 59: DCB 3507 One–dose mean graph.....	142
Figure 60: DCB 3507 dose–response curves (all cell lines).....	143
Figure 61: DCB 3507 dose–response curves (by cell line).....	144
Figure 62: DCB 3507 In-vitro testing results.....	145
Figure 63: DCB 3507 mean graphs.....	146
Figure 64: DCB 3503 and DCB 3508 structures.....	147
Figure 65: DCB 3508 One–dose mean graph.....	150
Figure 66: Structre of DCB 3509.....	151
Figure 67: DCB 3503, 3507, 3508, and 3509.....	154

List of schemes

Scheme 1: The synthetic route to DCB 3503.....	19
Scheme 2: Proposed mechanism for the formation of (<i>E</i>)-2,3-bis(3,4-dimethoxyphenyl)acrylic acid (3).	23
Scheme 3: Synthetic conditions to obtain 5.....	25
Scheme 4: VOF ₃ reaction of compound 4 with R substituents.....	25
Scheme 5: Proposed general mechanism for the formation of ring coupling.....	27
Scheme 6: Proposed mechanism for the conversion of 4 (<i>E</i>) and (<i>Z</i>) isomers to 5.....	29
Scheme 7: Procedure to transform OH to Br.....	31
Scheme 8: Alkylation of amino acid side chain.....	32
Scheme 9: Closing amino acid side chain.....	33
Scheme 10: Cyclization of compound 8 at reflux.....	40
Scheme 11: Proposed mechanism for formation of 9.1.....	40
Scheme 12: Mechanism for the formation of compound (9) at room temperature.	41
Scheme 13: Proposed mechanism for the SnCl ₄ -mediated synthesis of 9.....	44
Scheme 14: Attempted cyclization of 28.....	48
Scheme 15: The synthetic route to DCB 3507.....	51
Scheme 16: Condensation reaction to obtain C.....	53
Scheme 17: Condensation reaction to obtain 13.....	53
Scheme 18: Proposed mechanism for the formation of (<i>E</i>)-3-(3,4-dimethoxyphenyl)-2-phenylacrylic acid (13).	57
Scheme 19: VOF ₃ reaction to obtain 15.....	58
Scheme 20: FeCl ₃ /SiO ₂ to obtain 15.....	59
Scheme 21: Proposed mechanism for the synthesis of 15 using VOF ₃ or FeCl ₃	62
Scheme 22: FeCl ₃ reaction in the presence of hydroxyl group.....	63
Scheme 23: Proposed mechanism for FeCl ₃ reagent in the presence of OH group.....	64
Scheme 24: Reduction of compound 15.....	65
Scheme 25: Akué-Gédu's reaction example.....	73
Scheme 26: Reaction mechanism for the synthesis of 19.....	74
Scheme 27: DCB 3503, 3501, and undesired product.....	75
Scheme 28: The synthetic route to DCB 3508.....	89
Scheme 29: Synthesis of 25 by two routers.....	94
Scheme 30: Reaction route for by-product 25.....	96
Scheme 31: The synthetic route to DCB 3509.....	100
Scheme 32: Alkylation of 36 to obtain 37.....	103
Scheme 33: Alkylation of 36 at the tertiary amine.....	105
Scheme 34: The synthetic route to synthesis of biotynilated tylophirine analog.....	109
Scheme 35: Alternative route to obtain 44.....	119
Scheme 36: The carbodiimide activated ester rearrangement.....	121
Scheme 37: Mechanism using HATU.....	121
Scheme 38: Mechanism using HBTU.....	122
Scheme 48: Condensation reaction to obtain C.....	188
Scheme 49: Condensation reaction to obtain 13.....	189

List Of Attachments

Attachment One.....Table Characterizations and NMR spectra.doc

Abbreviations and acronyms

Ac	Acetyl
Ac ₂ O	Acetic anhydride
AcOH	Acetic Acid
COSY	Correlated spectroscopy
DCM	Dichloromethane
DMF	<i>N,N</i> -dimethylformamide
DMSO	Dimethyl sulfoxide
Et	Ethyl
EtOAc	Ethyl acetate
EtOH	Ethanol
HSQC	Heteronuclear single-quantum coherence
MALDI	Matrix-assisted laser-desorption ionization
MeO	Methoxy group
MeOH	Methanol
Me	Methyl
MS	Mass spectrometry
NMR	Nuclear magnetic resonance
NOESY	Nuclear Overhauser effect spectroscopy
TEA	Triethylamine
TFA	Trifluoroacetic acid
TFAA	Trifluoroacetic anhydride
THF	Tetrahydrofuran
TLC	Thin-layer chromatography
TMS	Tetramethylsilane
TOCSY	Totally correlated spectroscopy
VOF ₃	Vanadium(V) oxitrifluoride

Chapter One: Synthesis of DCB 3503

1.1 Statement of Problem

The objective was to develop a scale-up synthesis of DCB 3503. The National Cancer Institute showed in its anticancer screen that DCB 3503 (a synthetic compound, Figure 1) had a potent growth inhibitory effect ($GI_{50} \sim 10^{-8}$ M). To evaluate its antitumor potential, synthesis and large scale preparation was required.

**Figure 1: Structure of $R^1 = OH, R^2 = H, R^3, R^4 = OMe$ DCB-3503
 $R^1 = H, R^2 = H, R^3, R^4 = OMe$ Tylophorine
 $R^1, R^4 = H, R^2, R^3 = OMe, Tylophora crebriflora$**

This highly potent anticancer compound needed to be synthesized in scale-up conditions in order to do more biological analysis. This compound, DCB 3503, requires at least 10 steps that involve reactions such as Perkin condensation¹, cyclization through oxidative couplings,¹⁸ diastereoselective reduction², intramolecular Friedel–Crafts cyclizations¹, hydrolysis, peptide bonds, alkylations¹, and amino acid couplings. These reactions required specific temperatures and molecular equivalent.

In the past, the synthesis of DCB 3503 took longer time to be synthesized and the final compound yield was approximately 40–50 mg, therefore, the synthetic route had to be improved.

1.2 Introduction

Tylophorine and its analogs are phenanthroindolizidine alkaloids.^{3,4} These natural compounds have been isolated primarily from the genera *Cynanchum*, *Pergularia*, and *Tylophora* in the Asclepiadaceae family, but they have also been reported from *Hypoestes verticillaris* (Acanthaceae), *Cryptocarya phyllostemmon* (Lauraceae), as well as *Ficus hispida* and *Ficus septica* (Moraceae).

DCB 3503 is an analog of tylophorine and has an added secondary alcohol moiety. Tylophorine is a pharmacologically active⁵ phenanthrolizidine alkaloid. It is the major constituent of the plant *Tylophora indica* (Asclepiadaceae). Its common names are anthrapachaka (Sanskrit), country ipecac, and Indian ipecac, and it is a perennial plant native to southern and eastern India.

Tylophorine has medicinal properties. It has been proved to have antitumor activity,⁶ such as in breast cancer.^{2,7-9} It is an effective drug for bronchial asthma. This plant is used to treat respiratory diseases. It is useful as a bronchodilator, an emetic, and an expectorant. A similar compound from *Tylophora crebriflora* shows high activity against leukemia L1210 in mice.⁷

Tylophorine has anti-inflammatory properties.¹⁰ The molecular mechanism for the anti-inflammatory of phenanthroindolizidine alkaloids has been examined as an *in vitro* system.¹¹ Tylophorine exhibited a potent suppression of nitric oxide production and did not show a significant cytotoxicity to the lipopolysaccharide interferons (LPS)/IFN- γ stimulated RAW264.7 cells. The RAW264.7 cell line is used in an assay of IFN- γ that measures the concentration of nitric oxide (determined by nitrite accumulation in the culture medium) generated by RAW264.7 cell line.¹¹

Tylophorine and its analogs such as DCB 3503 are commonly called tylophora alkaloids. These analogs have been targets of synthesis and modification for their significant cytotoxic activities.⁴ Tylophora alkaloids can be naturally extracted from its natural source only in small quantities; therefore, DCB 3503 needed to be synthesized, along with its prospective analogs, to find their molecular mechanism of action with cancer cells.^{12,13}

The Baker group has focused its efforts on the synthesis of DCB 3503 and analogues for evaluation as anti-cancer,³ anti-arthritic,¹¹ and anti-lupus drugs.¹⁴ Work by Dr. S. Zhong, C. Kaczmarek¹⁵ and others have laid the foundation for this dissertation. Biological collaborators include Prof. Yung-Chi Cheng and his group at Yale University School of Medicine.

1.3 Results and discussion: DCB 3503 scale-up

Scheme 1: The synthetic route to DCB 3503.

Scheme 1, cont'd.

1.3.1 Synthesis of (*E*)-2,3-bis(3,4-dimethoxyphenyl)acrylic acid (**3**)

The synthesis of **3** was carried out by condensation of 3,4-dimethoxybenzaldehyde and (3,4-dimethoxyphenyl)acetic acid in refluxing TEA and Ac₂O in excellent yield. This condensation, also known as Perkin condensation, yielded a mixture of both (*E*) and (*Z*) isomers in a ratio of (10:1),¹⁶ but isomer (*E*) was obtained exclusively by recrystallization.¹⁸ It has been noted that even without recrystallization, isomer (*E*) and (*Z*) can be used for the subsequent intramolecular oxidative coupling in order to obtain **5**.¹⁷

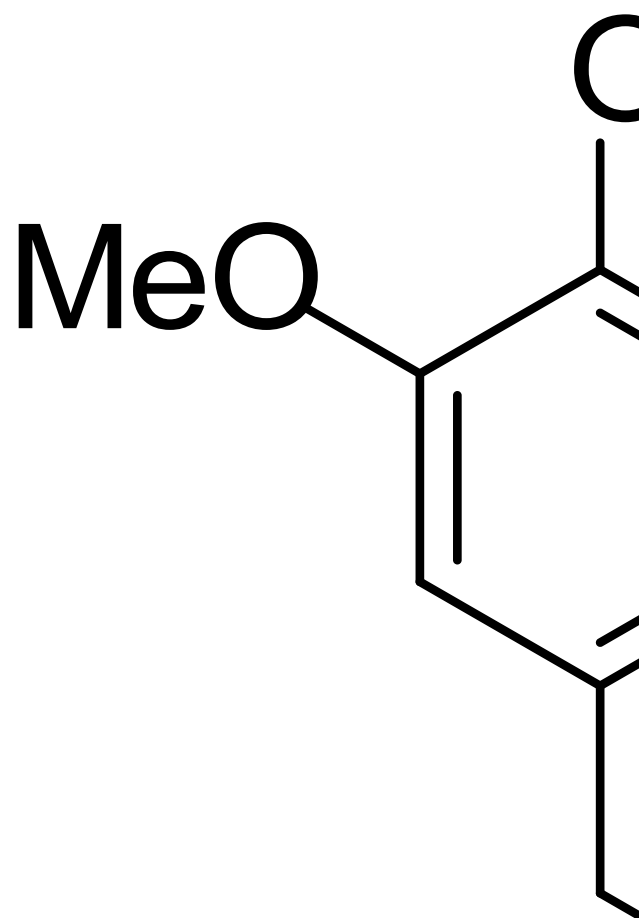
It has been reported that for product **3** the (*E*) isomer displayed a characteristic singlet resonance at 7.8 ppm for the vinylic β proton; the (*Z*) isomer for **3** displayed at approximately 7.1 ppm. This characteristic singlet for the (*E*) isomer has been found at 7.8 ppm in the ¹H NMR spectrum for product **3**. It is important to indicate that a singlet at 7.1 ppm was not found after recrystallization (see Figure 2).

Figure 2: Compound **3** (*E*) and (*Z*) isomer.

This condensation was improved in the following steps:

1. In a 15 g scale, addition of 3,4-dimethoxybenzaldehyde and Ac_2O were added until a solution was obtained. Then the TEA was added. At that moment, (3,4-dimethoxyphenyl)acetic acid was added, and the mixture was slowly heated until it reached $100\text{ }^\circ\text{C}$ (~1 h).
2. Slowly H_2O and a solution of $\text{K}_2\text{CO}_3/\text{H}_2\text{O}$ was added dropwise to the mixture (4–5 h).
3. The reaction was slowly quenched with 2 N HCl (2–3 h).

If these steps were followed, the product would always precipitate as yellow powder in high yield. If these steps were not followed or the solutions were added faster, the formation of a sticky oily product would occur, which stopped the stirring bar, and addition of 2 N HCl could not quench the reaction.



Scheme 2: Proposed mechanism for the formation of (*E*)-2,3-bis(3,4-dimethoxyphenyl)acrylic acid (3).

1.3.2 Synthesis of (*E*)-methyl 2,3-bis(3,4-dimethoxyphenyl)acrylate (**4**)

The esterification of **3** was achieved by addition of methanol under strongly acidic conditions. This reaction was improved to obtain high yields in the following steps:

1. The starting material was dissolved in methanol and left stirring until all components dissolved.
2. The solution was heated slowly until 60 °C was reached.

On the next day, the solution was left stirring until room temperature was reached. Then, solvent was removed by vacuum evaporation at not higher than 30 °C or the solution would turn into a purple oil. Under these conditions, the ester product **4** precipitated into a yellow powder in high yield and was washed quickly with cold methanol.

Product **4** (*E*) isomer displayed a characteristic singlet resonance at 7.8 ppm for the vinylic β proton. According to the literature, the (*Z*) isomer of **4** **would be** displayed at approximately 7.1 ppm.¹⁸ This characteristic singlet for the (*E*) isomer has been found at 7.8 ppm in the ¹H NMR spectrum for **4**. It is important to indicate that singlet around 7.1 ppm was not found in the product (see Figure 3).

Figure 3: Structure of compound 4 (*E*) and (*Z*) isomer.

1.3.3 Synthesis of methyl 2,3,6,7-tetramethoxyphenanthrene-9-carboxylate (5):

Product 5 was obtained by two methods:

1.3.3.1 Method 1: VOF₃

Scheme 3: Synthetic conditions to obtain 5.

Vanadium trifluoride oxide (VOF₃) with trifluoroacetic acid (TFAA) was useful for the cyclization of phenanthrene rings that contained methoxy groups as substituents.² It has been demonstrated by Halton and co-workers¹⁸ that from a survey of derivatives that oxygen functionality (-OMe groups) was necessary at the R⁴, R⁵ positions and/or the R¹, R² positions of (B) of the aromatic rings for cyclization to occur, as illustrated in Table 1.

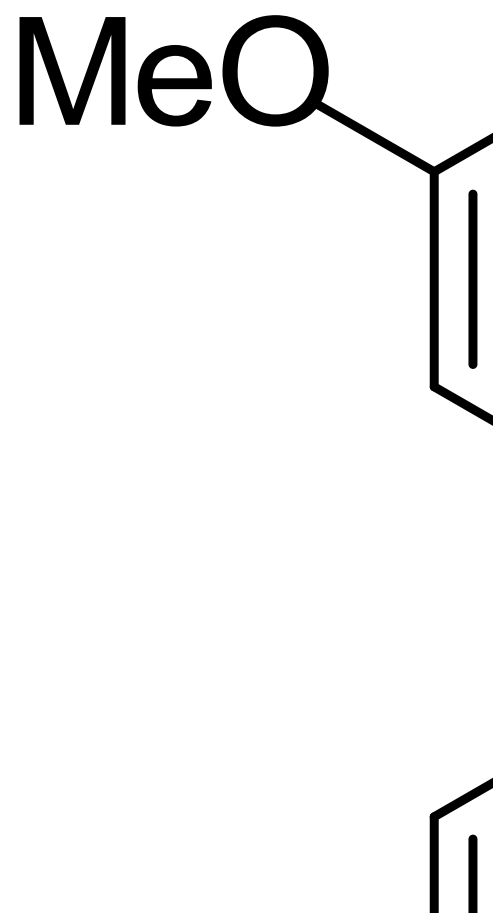
Scheme 4: VOF₃ reaction of compound 4 with R substituents
Table 1: Partial table made by Halton and co-workers¹⁸

	R ¹	R ²	R ³	R ⁴	R ⁵	R ⁶	VOF ₃ /TFA % yield	VOF ₃ /BF ₃ ·Et ₂ O % yield
--	----------------	----------------	----------------	----------------	----------------	----------------	-------------------------------	--

a	OMe	OMe	H	OMe	OMe	H	74	95%
b	OMe	OMe	H	H	H	H	44	65
c	H	H	OMe	OMe	H	H	61	82
d	H	H	H	OMe	OMe	H	0	5 to 95
n	H	H	H	H	H	H	0	0

Halton and co-workers¹⁸ suggested the formation of a radical cation as a possible mechanism using VOF₃/TFA. Vanadium trifluoride oxide is believed to affect the electron transfer and form radical cations with methoxy groups at the ortho position. It was experimentally demonstrated in Halton and co-workers¹⁸ and Jin and co-workers¹⁷ that the two groups should be in the ortho position or the reactions failed. Vanadium trifluoride oxide acts as an oxidizing agent. This substance can gain electrons in a redox chemical reaction and becomes reduced in the process.

This mechanism is believed to involve electron transfer and form radical cations on electron-rich substrates. Therefore, the aryl–aryl bond formation could occur by the coupling of a pair of radical cations in the presence of -OMe at the R¹, R², R⁴, and R⁵ positions, followed by a radical attack on a un-ionized aryl group. This hypothesis is also supported by Jin and co-workers.¹⁷ The cyclizations of phenanthrene rings with -OMe substituents at different position than R¹, R², R⁴, and R⁵ resulted in very low yield as reported by Halton and co-workers.¹⁸ This demonstrates the lower yield for product **15 (only 2 –OMe groups in R⁴ and R⁵, chapter 2)** compared to **5 (4 –OMe in R¹, R², R⁴, and R⁵ positions)**, because it shows that two methoxy groups or oxygen functionalities are necessary in at least one of the aryl groups. These mechanisms are a possible explanation for products **5** and **15** using VOF₃. This coupling occurred between these two aryl to give **5** which was evident for the newly formed of four ¹H NMR single peaks in the phenanthrene ring of compound **5**.



Scheme 5: Proposed general mechanism for the formation of ring coupling.

1.3.3.2 Method 2: Anhydrous FeCl₃

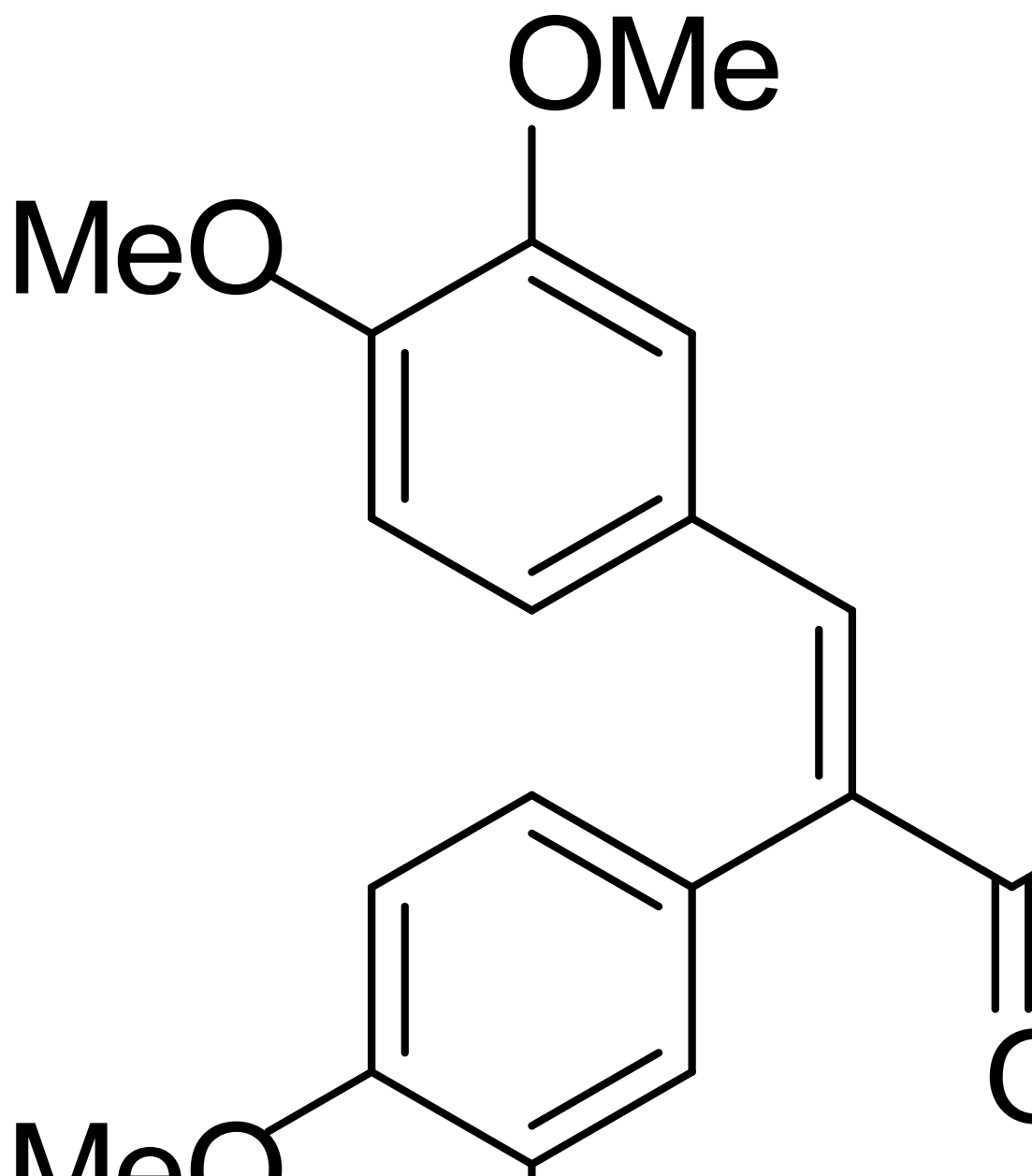
Anhydrous iron(III) chloride has been used to synthesize the phenanthrene ring substituted with polymethoxy groups. This product is achieved via intramolecular oxidative coupling of *E* and *Z* **5** isomers using anhydrous FeCl₃ in EtOAc. Vanadium trifluoride oxide (VOF₃) can be used to form the phenanthrene ring as explained above; however, this reaction was improved to use in the scale-up process. Vanadium trifluoride oxide reagent has been limited due to toxicity, rigorous conditions, and price (Table 2). Therefore, the use of anhydrous FeCl₃ was ideal for scale-up process.

The conditions for the intramolecular oxidative coupling were simple. First, the starting material was dissolved in DCM below -10 °C. It was noticed that at room temperature the reaction was not completed, and a large amount of starting material (60%) was detected by TLC. Secondly, a fresh solution containing FeCl₃ in EtOAc was added dropwise. The reaction was completed as soon as the addition of FeCl₃/EtOAc was finished. The product was monitored by TLC that gave a characteristic bright blue color on anisaldehyde–H₂SO₄ spray.¹⁹ It was also noticed that for scales higher than four grams the reaction was completed within 10 minutes.

Table 2: VOF₃ and FeCl₃ reaction time, toxicity, and price.

Reagent	Reaction time (1g scale)	Toxicity	Price (Fisher)
VOF ₃	4 h	Corrosive	\$25 (5 g)
FeCl ₃	10 min	Low toxicity	\$22 (500 g)

Anhydrous iron(III) chloride was added in large excess. Even though FeCl₃ was completely dissolved in EtOAc, a large excess was needed to form the phenanthrene ring. Lowering the mol equivalents of FeCl₃ has been attempted, but the presence of starting material was found. It is important to indicate that the FeCl₃ must be anhydrous. The use of FeCl₃·6H₂O resulted in low yields, apparently due to the presence of water. The use of FeCl₃·6H₂O on silica gel was also investigated, but the reaction gave a lower yield of product.



Scheme 6: Proposed mechanism for the conversion of 4 (*E*) and (*Z*) isomers to 5.

1.3.4 Synthesis of (2,3,6,7-tetramethoxyphenylphenanthren-9-yl)methanol (6):

The reduction of **5** required one molecular equivalent of LiAlH_4 to reduce the ester group to a primary alcohol. This simple reduction gave high yield and was quenched in by either of two methods:

1. EtOAc and 2 N HCl.
2. EtOAc and $\text{Na}_2\text{SO}_4 \cdot 10\text{H}_2\text{O}$ overnight

The second method provided perfect conditions to obtain high yield, because $\text{Na}_2\text{SO}_4 \cdot 10\text{H}_2\text{O}$ is one of the ideal quenching reagents for sensitive compounds, and the granular form of LiOH that resulted facilitated filtration and isolation of product.

The reduction of the ester formed homotopic methylene hydrogens. The ^1H NMR spectroscopy proved the complete reduction of the ester group to obtain the CH_2 hydrogens at 5.14 ppm, it was also noticed that the ester $-\text{Me}$ peak at 4.01 ppm from compound **5** was not present.

1.3.5 Synthesis of (S)-methyl 5-oxo-1-((2,3,6,7)-tetramethoxyphenanthren-9-yl)methylpyrrolidine-2-carboxylate (7):

This reaction required three steps:

1. Halogenation: bromination of the alcohol was accomplished with PBr_3 in chloroform at $-10\text{ }^\circ\text{C}$. The reaction was carried out in freshly distilled chloroform at cold temperatures, which was important in order to increase the final yield. Previously, chloroform was used directly from the bottle, and it gave a thick liquid as product, which gave unsatisfactory ^1H and ^{13}C NMR spectra and a low yield of the brominated product. Under these circumstances the crude product was used in the next step continued without any NMR characterization. However, after reading several papers with similar reactions, it was decided to distill the chloroform in order to remove any ethanol present (stabilizer) in the bottle. According to Fisher Scientific, chloroform only contains 0.75% of ethanol, but using this freshly distilled chloroform the brominated product gave a high yield and solid product that was easily characterized by NMR spectroscopy. Another important point to increase the yield was during quenching the reaction with ice. It was significantly important to let the ice melt completely and let the aqueous solution mix for at least 30 minutes before any organic extraction was attempted to significantly improve the quality of brominated product. If the organic extraction was separated in the presence of ice, the brominated compound did not turn solid even when distilled chloroform was used (see Scheme 7).

Scheme 7: Procedure to transform OH to Br.

2. Coupling of L-glutamic ester HCl: The coupling of the brominated compound with L-glutamic ester HCl was also significantly improved. In the past, this coupling was achieved by mixing the halogenated compound, the amino acid, and K_2CO_3 in DMF at the same time, and the reaction was run overnight at room temperature. The reaction was improved by mixing the brominated intermediate with the L-glutamic ester HCl completely and then adding K_2CO_3 ; the reaction was run from 65–70 °C overnight. This range of temperature was important, because it was found that any higher or lower heat will considerably lower the yield of the product. The ESI+ mass spectrometry for this intermediate was obtained and indicated complete coupling without any brominated starting material.

Scheme 8: Alkylation of amino acid side chain.

3. Closing of the amino acid side chain: This final step was achieved by mixing the amino adduct in MeOH and AcOH. This reaction was improved as well. In the past, this reaction was accomplished by mixing MeOH and AcOH overnight at room temperature. The final product yield was improved by adding a 1:1 molar ratio of MeOH:AcOH and increasing the temperature up to 35 °C overnight. The temperature in this step was crucial. From experience, any temperature greater than 40 °C would decrease the yield.

Scheme 9: Closing amino acid side chain.

1.3.5.1 Important NMR observation for diastereotopic hydrogens on C11 for product 7.

Geminal coupling $^2J(\text{H,H})$, bond angle, and effect of neighboring π electrons for diastereotopic hydrogens on C11.

Bond angle

Geminal coupling or 2J coupling is dependent upon the bond angle between the nuclei. Generally, the smaller the angle the bigger the coupling constant. The bond angle for the geminal hydrogens on C11 was 109.5° . This bond angle was calculated by drawing the structure in Tripos: Sybyl 8.0 molecular modeling program (molecular dynamics and MM4 minimization were used), as shown in Figure 4. The Figure 4 indicates the dependence of the coupling constant on bond angle.

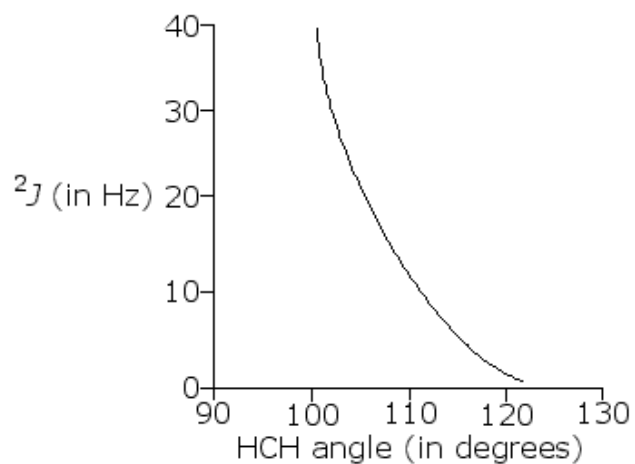


Figure 4: Coupling constant vs bond angle.

Dependence of the magnitude of the geminal coupling constant on C11, $J = 14.60$ Hz, and the HCH angle = 109.5° correlated with the expected values according to the graph above.

Geminal coupling $^2J(\text{H,H})$

The diastereotopic hydrogens on C11 showed two distinct chemical shifts at 4.4 and 5.5 ppm, $^2J(\text{H,H}) = 14.60$ Hz as shown in Figure 5 and 6. It was noted that these hydrogens were homotopic in starting material **6** before coupling to obtain product **7**.

The effect of neighboring π electrons.

There are several major factors that affected the geminal coupling constant:²⁰

1. The hybridization of the atoms involved in the coupling.
2. Bond angles and torsional angles.
3. Bond length.
4. The presence of neighboring π -bonds.
5. Effects of neighboring electron lone-pairs.
6. Substituent effects.

The diastereotopic hydrogens on C11 have different chemical shift primarily due to the neighboring π -bonds and electron lone-pairs from the amide group. This effect was clearly present when the amide was formed in the intermediates, but the difference in chemical shifts was noticeably smaller when the amide was reduced to a tertiary amine by LiAlH_4 to obtain compound **11**. The new chemical shifts for the diastereotopic hydrogens on C11 were 2.8 and 3.1 ppm for compound **11**.

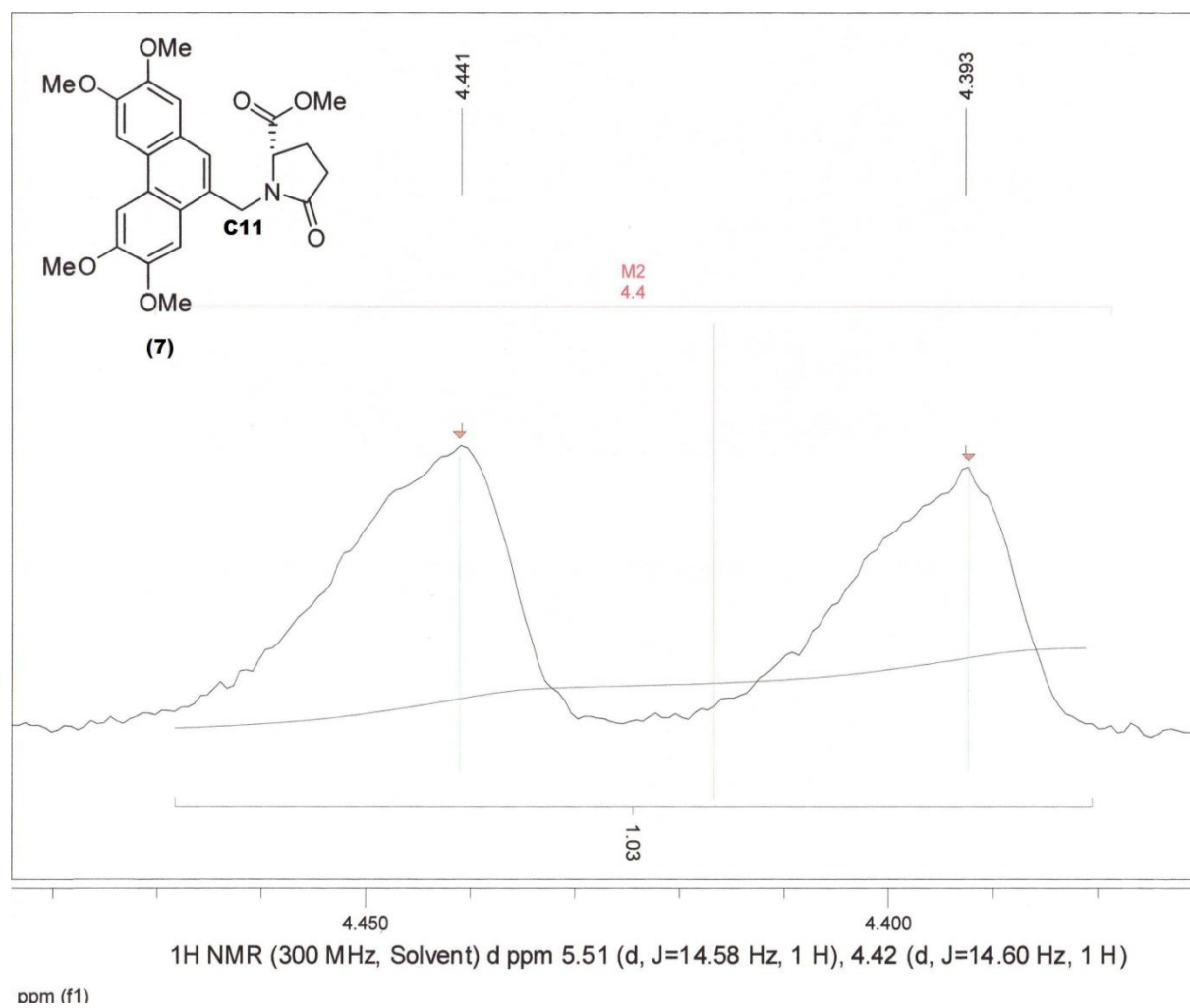


Figure 5: *J* Coupling of compound 7 at 4.42 ppm.

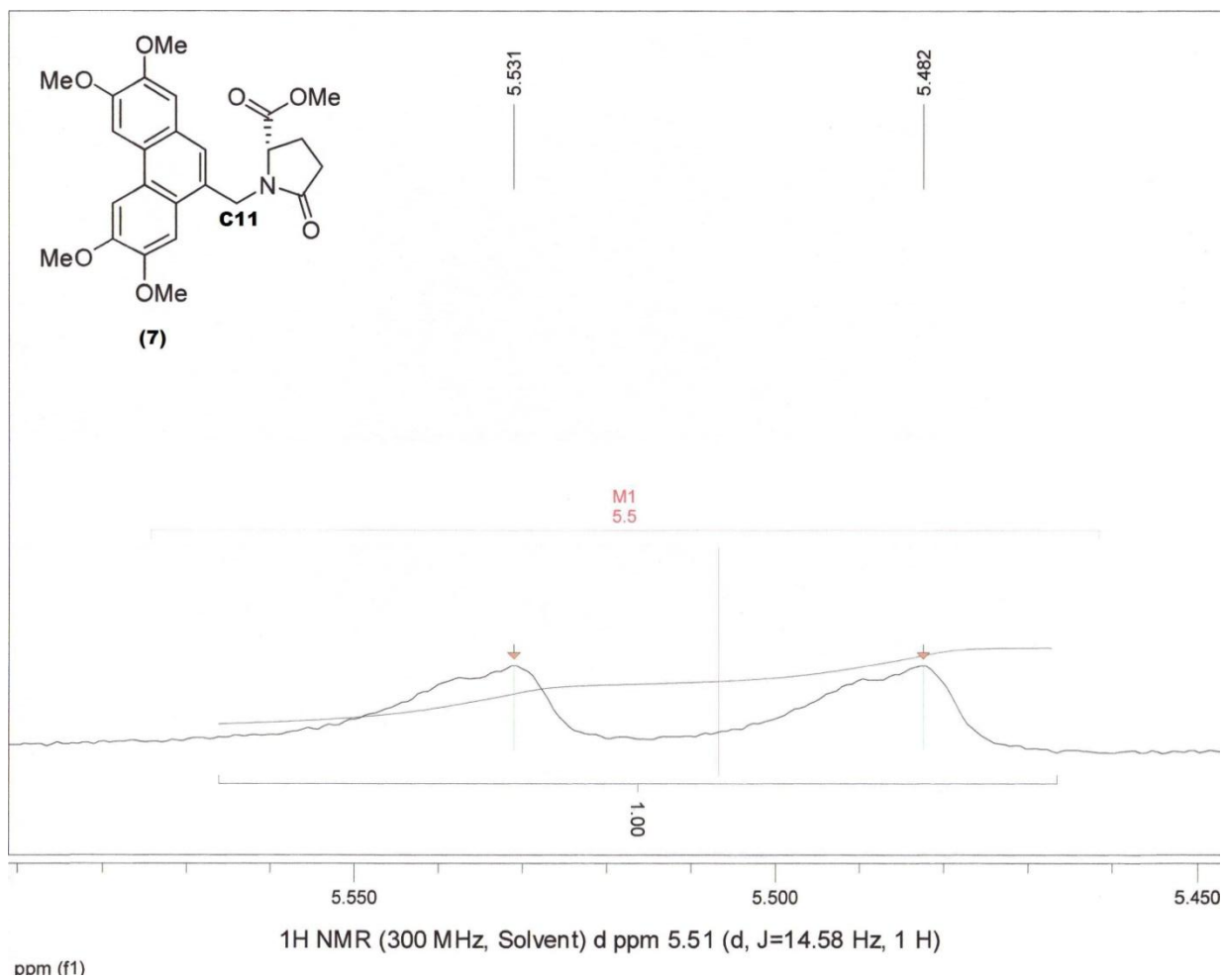


Figure 6: J Coupling of compound 7 at 5.51 ppm.

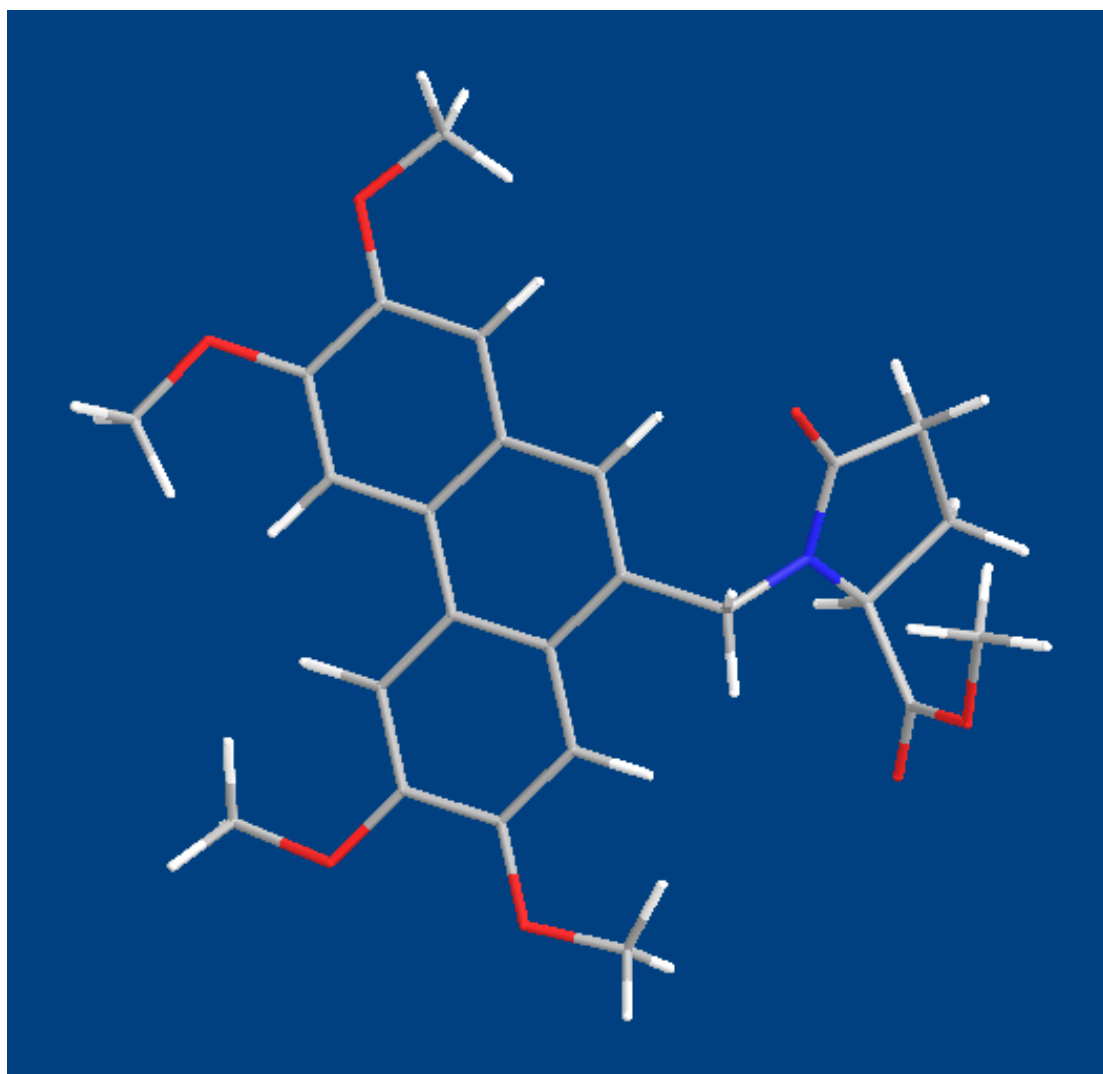


Figure 7: Molecular modeling structure of compound 7.

1.3.6 Synthesis of (S)-5-oxo-1-(2,3,6,7-tetramethoxyphenanthren-9-yl)pyrrolidine-2-carboxylic acid (**8**):

The hydrolysis of the ester **7** was accomplished under basic conditions of 2 N KOH followed by quenching by 2 N HCl. In the past, this reaction was quenched by H₃PO₄ until pH 3 at -10 °C. The product precipitated at low temperatures overnight, so it was left inside the freezer to maximize the yield of product. This saponification method did give a good yield, and it would often form a great excess of white salts that mixed with the product **8** (white crystals). Thus, a mixture of product **8** and salts was unavoidable. In order to remove these salts, we had to add quickly cold water to dissolve the salts, but the water would dissolve the carboxylic acid product **8** as well.

The addition of H₃PO₄ was stopped when pH 3 was reached, but lowering the pH to 1 did not help to avoid the formation of salts. It is important to indicate that any small presence of this salt for the next step would lower the cyclization reaction yield. Therefore, it was decided to add 2 N HCl until pH 1 was reached and extract the organic product with CHCl₃, DCM, and Et₂O. In this way, no salts were formed and nothing precipitated. The carboxylic acid was extracted with CHCl₃, DCM, and Et₂O to obtain a yield of 95%. Product **8** was polar and soluble in water; thus it is essential to point out the necessity to extract the product with CHCl₃ at least five times. The completed extraction was indicated by TLC (one spot seen at $R_f = 0$, since the carboxylic acid does not migrate on silica gel TLC plates). For details, see Experimental section

1.3.7 Synthesis of (**S**)-2,3,6,7-tetramethoxy-13,13a-dihydrodibenzo[*f,h*]pyrrolo[1,2-*b*]isoquinoline-11,14(**9H**,**12H**)-dione (**9**):

Product **9** was obtained using two methods:

1.3.7.1 Method 1: TFAA and BF₃·Et₂O

The carboxylic acid **8** was converted to its mixed trifluoroacetic anhydride by the addition of trifluoroacetic anhydride in 1,2-dichloroethane or dichloromethane at room temperature. The compound was treated with the Lewis acid BF₃·Et₂O and quenched with K₂CO₃, yielding the phenanthrene cyclized amido ketone **9**.²¹ This improved method was perfect for scale-up conditions, contrary to Method 2 that used SnCl₄.

These ketones exhibited a markedly characteristic yellow spot on TLC under ultraviolet absorption using anisaldehyde–H₂SO₄.¹⁹

This Friedel–Crafts cyclization had a higher yield when the solvent 1,2-dichloroethane was used instead of dichloromethane. The choice of solvent was important to obtain higher yield and purity of the ketone. The final yield, after running a silica gel column, using 1,2-dichloroethane was around 70%; on the other hand, using dichloromethane the yield was 20–50%.

A possible explanation for this lower yield could be the formation of rearrangements or by-products as expected by Bourry^{21,22} and Akué-Gédu.¹ These by-products were not detected by mass spectrometry for compound **9**. Therefore, the reaction using BF₃·Et₂O as a Lewis acid apparently did not give a higher yield than 70%.

The main concern was the formation of an alcohol chain by using dichloromethane as solvent at reflux. This by-product **9.1** could be formed that contained a CH₂OH group in the α-position to the newly formed ketone function under reflux conditions.²¹ Therefore, in order to avoid this by-product, the Friedel–Crafts reaction using BF₃·Et₂O as Lewis acid must be run at room temperature. From experience, the expected ketone **9** was not formed when the reaction was heated to reflux overnight in an attempt to increase the yield. The formation of this by-product was explained and presented in Scheme 10.²¹

Scheme 10: Cyclization of compound 8 at reflux.

Scheme 11: Proposed mechanism for formation of 9.1.

A boron enolate **9A** (Scheme 11) could be formed from the reaction of excess $\text{BF}_3 \cdot \text{Et}_2\text{O}$ with the ketone **9** in the presence of trifluoroacetic acid (by-product after cyclization). Then, the remaining dichloromethane can be reacted with the enolate to give the chloromethyl ketone **9B**. Therefore, dichloromethane was evaporated before

addition of K_2CO_3/H_2O to avoid this by-product. The final step was the hydrolysis of the chloromethyl ketone using K_2CO_3/H_2O to form **9.1**, see Scheme 11.

MeQ

Scheme 12: Mechanism for the formation of compound (9) at room temperature.

The characterization of product **9** was fully supported by 1D/2D NMR spectroscopy and MS. After cyclization, the H1 on C1 of each phenanthrene underwent a noticeable downfield shift due to the deshielding of the newly formed ketone. This effect was reversed after reduction with K-selectride for the formation of the secondary alcohol (see Table 3). This downfield shift was also reported in the publication by Buckley and Rapoport.²

Table 3: Comparison of ^1H and ^{13}C NMR shifts for compound 8, 9, and 10

Compound 8

^1H	ppm	^{13}C	ppm
H1	7.16	C1	104.26

Compound 9

^1H	ppm	^{13}C	ppm
H1	7.72	C1	108.14

Compound 10

^1H	ppm	^{13}C	ppm
H1	7.59	C1	104.46

1.3.7.2 Method 2: Oxalyl chloride and SnCl_4

The desired completion skeleton of DCB 3503 was accomplished under Friedel–Crafts conditions using $(\text{COCl})_2$ to obtain an acid chloride to activate the carboxylic acid with SnCl_4 as the Lewis acid. (see Scheme 16). This intramolecular Friedel–Crafts reaction consistently gave a yield (60–70%) of product **9**.

Tin(IV)chloride is hygroscopic, toxic, and expensive; therefore, this reagent had to be replaced by an easier-to-handle, less toxic, and inexpensive Lewis acid in order to be applied for a scale-up process (see Table 4).

In order to quench the excess of SnCl_4 , addition of 20 mL of water in 1 mL increments was useful before addition of 2 N HCl. Water quenched the SnCl_4 slowly and gave a higher yield of a cleaner product. This mixture of water and 2 N HCl could not stay for more than 1 hour; otherwise, the compound **9** would decompose.

Table 4: SnCl_4 and $\text{BF}_3 \cdot \text{Et}_2\text{O}$ reaction time, toxicity, and price

Reagent	Reaction time (1 gram scale)	Yield %	Toxicity	Price (Fisher)
SnCl_4	6 h	70	toxic	\$37 (100 mL)
$\text{BF}_3 \cdot \text{Et}_2\text{O}$	5 h	70	Low toxicity	\$66 (1 kg)



Scheme 13: Proposed mechanism for the SnCl₄-mediated synthesis of 9.

Scheme 13, cont'd

1.3.8 Synthesis of (13a*S*, 14*S*)-2,3,6,7-tetramethoxy-9,11,12,13,13a,14-hexahydrodibenzo[*f,h*]pyrrolo[1,2-*b*]isoquinolin-14-ol (11)

The final product was achieved by reduction of the amide group using 1 molecular equivalent of LiAlH₄. Unfortunately, this reaction did not give as high a yield as the previous reactions. This can be attributed to the sensitivity of the final compound

to harsh conditions such as the strong reducing agent. The final yield varied from 60–80% depending on the quenching method. Two quenching methods were applied:

1. Ethyl acetate and 2 N HCl for 30 minutes.
2. Ethyl acetate and Na₂SO₄·10H₂O for 2 h or overnight.

The best conditions were adding ethyl acetate at -10 °C and then stirring with Na₂SO₄·10H₂O for 3 h. Any other quenching method proved to lower the yield of product.

In order to purify the crude product, column chromatography was used. The solvent system was 2:1:0.2 CHCl₃:EtOAc:MeOH. Even though **11** was a highly polar compound, there was an unwanted side-product with $m/z = 411.19$ and $[M+1]^+ = 412.20$ that was detected using the DART mass spectrometer in positive-ion mode and by HPLC. The detection and separation of this side-product was difficult due to its similar polarity with that of **11**, no coloration with anisaldehyde–H₂SO₄, and a close molecular weight to that of **11** (DCB 3503 = 409.19, $[M+1]^+ = 410.19$). The only solvent method found to completely separate this side-product was 2:1:0.2 CHCl₃:EtOAc:MeOH .

An alternative synthetic route and biological analysis of this side-product is described in Chapter 3.

1.3.8.1 Molecular modeling and dihedral angle between H14 and H13a:

Tripes: Sybyl 8.0 with MM4 was used to calculate the dihedral angle between H14 and H13a for product **11**. This program was highly useful to determine the lowest energy conformation and predict the dihedral angle.

The direct drawing using molecular modeling SYBYL 8.0:Tripes (minimization with MM4 and molecular dynamics). Figure 8.

The predictions for dihedral angle and final energy can be seen in Table 5.

Table 5: DCB 3503 dihedral angle molecular modeling results

Structure	Dihedral angle	Final steric energy (kcal/mol)
DCB 3503 from drawing	51.1	12.5425

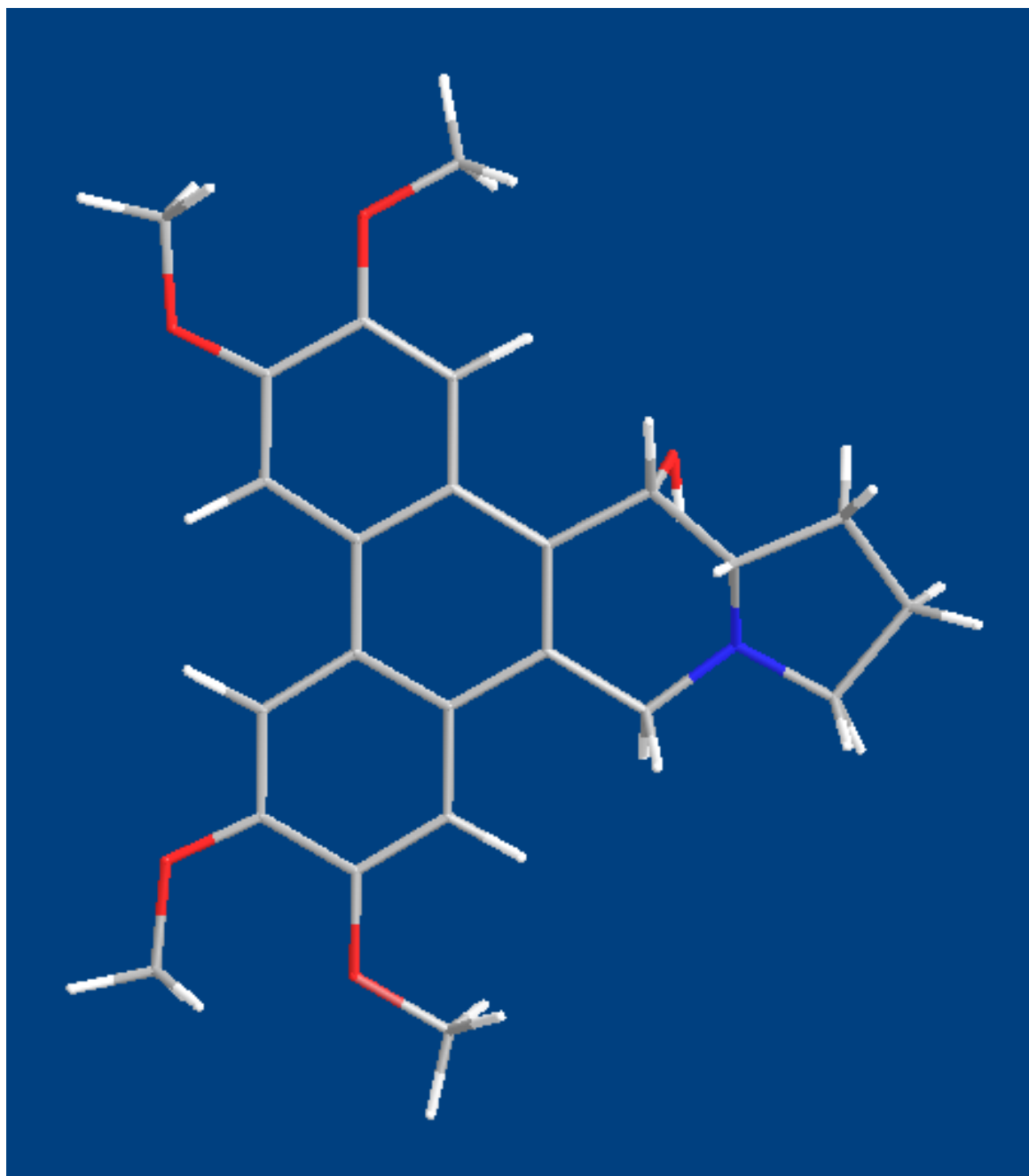
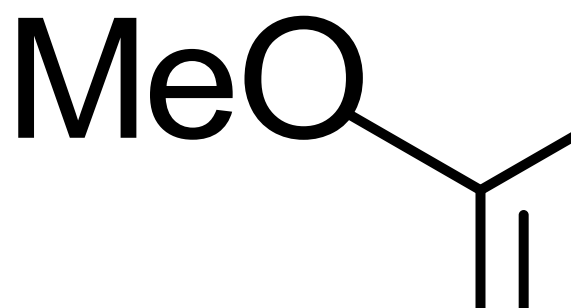


Figure 8: Compound 11 direct drawing and minimization molecular modeling.

1.3.9 Attempted cyclization of **28** with (S)-2-(methoxycarbonyl)pyrrolidinium chloride to obtain **29**.

A tentative pathway for the cyclization of **28** (Scheme 15) was unsuccessful. Similar Lewis acids, such as AlCl_3 ²³, $\text{BF}_3 \cdot \text{Et}_2\text{O}$, SnCl_4 , and $\text{Sm}(\text{OTf})_3$, were tried to obtain the intramolecular cyclization, but these reagents were not suitable for the reaction. The coupling of the brominated intermediate **6.1** with the closed amino acid (S)-2-(methoxycarbonyl)pyrrolidinium chloride was highly successful giving excellent yield, see Scheme 18. The hydrolysis of **24** was a success giving **28** in high yields using 2 N KOH or NaOH.²⁴ The next step was a failure, a different Lewis acids, molecular equivalents, variable temperatures, extended reaction times, different chlorination of carboxylic acids, and quenching methods failed to yield the ketone **29**. Due to this failure of Friedel–Crafts cyclization, further efforts in this area were abandoned. Later on, it was found that Buckley and Rapoport² also tried to these reagents with the free amido compound **28**, and the results were unsuccessful as well.

Chauncy attempted the cyclization of this free amide to also obtain negative results.⁷ Cycloalkylation of using AlCl_3 , $\text{BF}_3 \cdot \text{Et}_2\text{O}$, $\text{Sm}(\text{OTf})_3$ ²⁵, SnCl_4 (at reflux)²⁶ proved unsuccessful as well. According to his paper,⁷ he was successful to obtain the cyclization by using phosphoric acid at 90 °C with yields of 20–35%. These conditions were tried on **28**, but it did not dissolve in phosphoric acid, even at high temperature around 200 °C. The procedure was abandoned. This reaction would have been highly useful because it would have eliminated two steps, and the necessity to reduce the amide, which gives a lower yield due to the sensitivity of the final compound **11** under strong reducing agents.



A = CO ₂ Cl ₂	SOCl ₂	CO ₂ Cl ₂	TFAA	SOCl ₂	CO ₂ Cl ₂
B = SnCl ₄	AlCl ₃	Sm(OTf) ₃	BF ₃ ·Et ₂ O	SnCl ₄	AlCl ₃

Scheme 14: Attempted cyclization of 28.

Chapter Two: Synthesis of DCB 3507

2.1 Statement of Problem

The objective was to effect the synthesis of an analog of DCB 3503 that lacked the MeO groups in the 6, 7 –position of the phenanthrene ring (see Figure 9).

The anticancer activities are to be examined to add to structure–activity relationship development among these compounds.

Figure 9: Structure of DCB 3507.
DCB 3507: $R^1, R^2 = H, R^3 = OH$
Antofine: $R^1 = OMe, R^2, R^3 = H, (S) 13aH$

2.2 Introduction

The synthesis of DCB 3507 started in an undergraduate summer program sponsored by UT Science Alliance for two consecutive summers. This project was under the direct supervision of Dr. David C. Baker and Mr. Conrad Kaczmarek.

The main objective to synthesize DCB 3507 was to find whether there was any difference in biological activity compared to DCB 3503, since it was a similar analog. In this way, it could give valuable information about structure–activity relationships and prove if four methoxy groups were absolutely necessary for biological activity against cancer cells.

A number of examples of Tylophorine analogues are known that lack 6, 7 methoxy groups. One example is the antofine analogues. Their antitumor activity with different substituents on the phenanthrene ring has a variety of cytotoxic activity against various cancer cells with lower potency than DCB 3503. However, no 6,7–desmethoxy derivative of DCB 3503 is known.

2.3 Results and discussion: Total synthesis of DCB 3507

Scheme 15: The synthetic route to DCB 3507.

Scheme 16, cont'd

2.3.1 Synthesis of (*E*)-3-(3,4-dimethoxyphenyl)-2-phenylacrylic acid (13)

2.3.1.1 Condensation reaction to give C.

The synthesis of C was first attempted in order to obtain a tylophorine analog with two methoxy groups in the phenanthrene ring moiety, as seen on Scheme 16.

Scheme 16: Condensation reaction to obtain C

This condensation reaction of C started with commercially available reagents. The synthesis required 3,4-dimethoxyphenylacetic acid (**A**, 30 g), benzaldehyde (**B**, 30 g), TEA (46 mL), and Ac₂O (80 mL). This reaction was left running overnight at 100 °C. The detailed experimental observations can be found in the Appendix section.

2.3.1.2 Condensation reaction to give 13.

Scheme 17: Condensation reaction to obtain 13.

The starting material was changed to synthesize DCB 3507 using two methoxy groups in positions 2 and 3 of the phenanthrene ring, as seen in Scheme 17. The starting commercial materials were 3,4-dimethoxybenzaldehyde (veratraldehyde **1**), and

phenylacetic acid **12**. The detailed experimental observations can be found in the Appendix section.

The product **13** was characterized and verified by using NMR and mass spectrometry. The theoretical exact m/z was 284.105, and the experimental m/z was found 285.111 using AccuTOF–DART in positive-ion mode. The key hydrogen resonance that verified the condensation reaction and stereochemistry product **13** was the characteristic singlet resonance ~7.8 ppm in the vinylic β hydrogen (H_β) for the (*E*) isomer. The undesired (*Z*) isomer would show H_β ~7.1 ppm although the (*Z*) isomer was present in a ratio of 10:1, the (*Z*) isomer was not detected after recrystallization (See Figure 12).

Figure 10: Compound 13 (*E*) and (*Z*) isomers.

The H_β in **13**, which was originally the aldehydic H in the starting material **1**, is more shielded in the (*E*) alkene (See mechanism in Scheme 19)

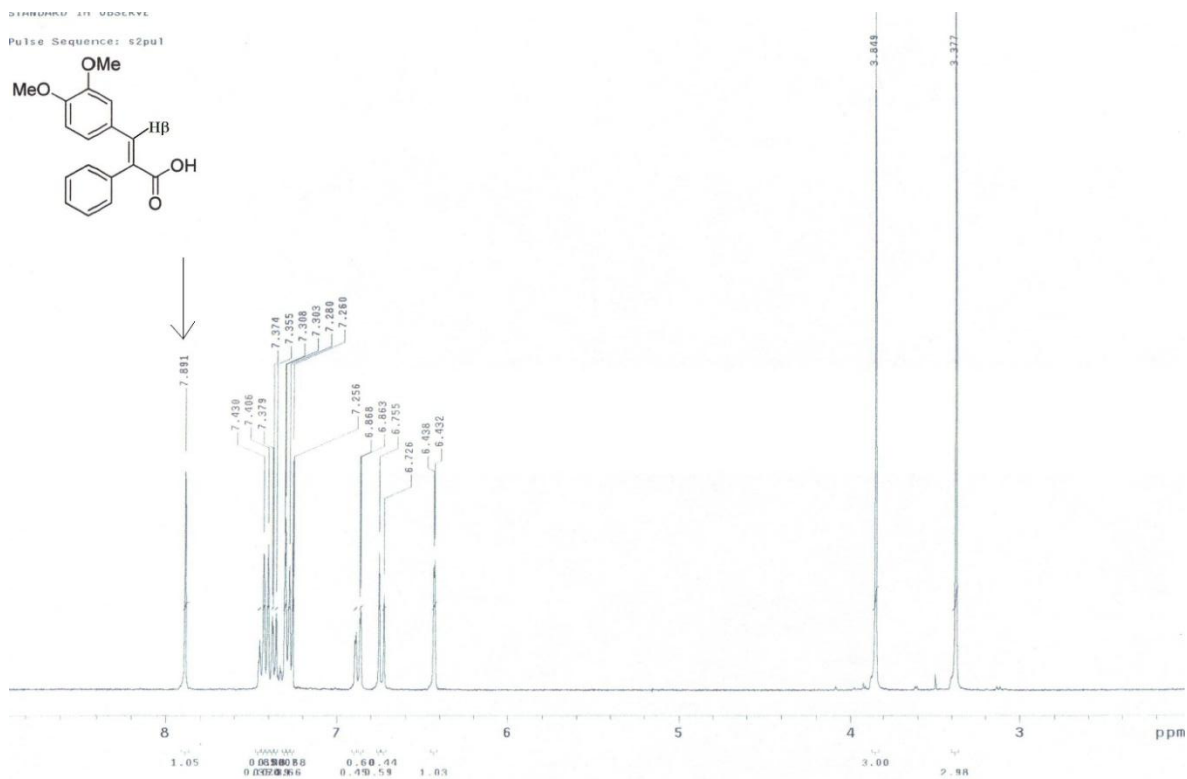
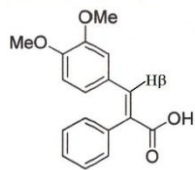
It is known that hydrogen from aldehyde groups is shifted around 9.5–10 ppm, and alkene protons range from 4–5 ppm (without substituents), but this newly formed alkene H_β was found at 7.891 ppm. This shift was expected due a large deshielding effect from to the benzene ring. In Figure 11 the benzene and the alkene are coplanar, so the H_β is further deshielded because of the additional deshielding effect from the double bond of the ketone.

Figure 11: Ring current effect in arenes and compound 13 in plane view.

The H_β indicated the stereochemistry for the desired (*E*) isomer over the undesired (*Z*) isomer. The desired (*E*) isomer showed the predicted H_β singlet at 7.891 ppm, and the undesired singlet at 7.1 ppm was not found in the proton spectrum¹⁸ see Figure 12.

SIEMENS AT 400 MHz

Pulse Sequence: e2pu1



(E)-3-(3,4-dimethoxyphenyl)-2-phenylacrylic acid

Figure 12: ^1H NMR spectrum for compound 13.

Scheme 18: Proposed mechanism for the formation of (*E*)-3-(3,4-dimethoxyphenyl)-2-phenylacrylic acid (13)

2.3.2 Synthesis of methyl 2,3-dimethoxyphenanthrene-9-carboxylate (15)

2.3.2.1 Method 1: VOF₃

Scheme 19: VOF₃ reaction to obtain 15.

Vanadium(V) oxytrifluoride was used to form the phenanthrene system (Scheme 19).² This reaction was applied according to H. Pearson's²⁷ procedure. These reaction conditions were later successfully applied to DCB 3503, and a high yield of product was obtained. The newly formed phenanthrene ring showed a bright blue spot on TLC under anisaldehyde–H₂SO₄ stain.

This oxidative coupling reaction required at least 4.4 equivalents of VOF₃ to close the ring.⁵ A low yield was obtained as an attempt to lower the amount of VOF₃ needed. A mixture of starting material and product was seen on TLC and mass spectrometry. The separation of the product and starting material was difficult, because these two products had similar polarity; therefore, they could not be separated completely.

The use of VOF₃ gave a high yield, but it had to be replaced by another reagent due to its high cost and limited amounts that were commercially available; therefore, VOF₃ was not suitable to scale-up reactions.

2.3.2.2 Method 2: FeCl₃/SiO₂

It has been proved that silica-bound ferric chloride (FeCl₃/SiO₂) can serve as an oxidant for aromatic coupling (Scheme 20).²⁸ The results indicated that solid-supported FeCl₃ could act as an electron-transfer oxidant²⁹ and it was environmentally better than VOF₃.¹⁶ This reaction provides an effective and less expensive (compared to VOF₃) reagent for coupling of aromatic rings.

Scheme 20: FeCl₃/SiO₂ to obtain **15**.

The use of silica gel/FeCl₃ as a solid-supported oxidant was the key to obtaining a higher yield in the intramolecular coupling reaction of **15**. Anhydrous FeCl₃ and FeCl₃-SiO₂ serve as Lewis acids for oxidative coupling reactions. The use of FeCl₃ in EtOAc showed a very low yield (<15%) due to the lack of methoxy groups as explained for DCB 3503 in intermediate **5** by Halton and co-workers.{Brian Halton, 1984 #8} As an alternative reagent, VOF₃ can be used to form the phenanthrene ring, but this reagent is expensive and toxic. Therefore, it could not be used for scale-up conditions (see Table 6).

Table 6: VOF₃ and FeCl₃/SiO₂ reaction time, toxicity, and price

Reagent	Reaction time (1 gram scale)	Toxicity	Price (Fisher)
VOF ₃	4 hours	corrosive	\$25 (5 g)
FeCl ₃ /SiO ₂	48 hours	Low toxicity	\$22 (500 g)

The formation of **15** was verified and characterized by mass spectrometry and NMR spectroscopy. The exact molecular weight of **15** is 296.105, and ion was found at [M+1]⁺ = 297.106 using the AccuTOF DART in the positive-ion mode. The characterization by NMR spectroscopy was used (¹H, ¹³C, and 2D NMR such as gHSQC and NOESY) to prove the structure.

The most important ¹H NMR spectroscopy characterization of **15** was the formation of the phenanthrene system see Figure 13.

Figure 13: Compound 15, phenanthrene ring in bold.

The phenanthrene ring is a benzene derivative that is categorized as an aromatic compound; therefore, the chemical shifts spin–spin splitting, J coupling for **15** gave the following expected results (see Table 7):

Table 7: Chemical shift, splitting, and J coupling for 15

Hydrogen	Chemical shift (ppm)	Splitting	J coupling (Hz)
H1	7.98	Singlet	0
H4	8.44	Singlet	0
H5	8.99	Doublet	8.39
H6	7.62	Triplet	7.28
H7	7.64	Triplet	7.30
H8	7.25	Doublet	8.23
H10	8.55	Singlet	0

NMR spectroscopic analysis:

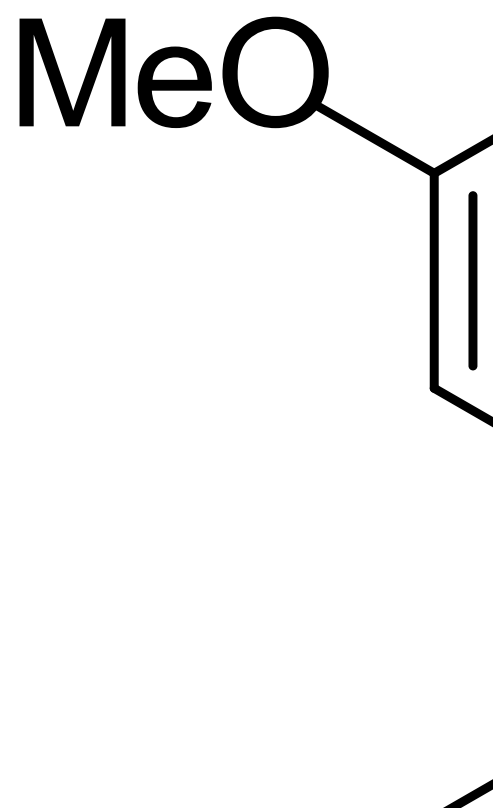
1. Chemical shifts: the seven aromatic protons showed the correct peaks in the aromatic region (6–9 ppm) due to the formation of the phenanthrene system. The chemical shift values for H1, H4, and H10 were expected to be less shielded due to the proximity of the methoxy groups in C2 and C3, and the ester group in C9. The rest of aromatic protons H6, H7, and H8 had to have similar shifts and be more shielded due to a similar environment with only hydrogens as neighbors.

2. Splitting: the splitting of H1, H4, and H10 had to be singlets, because they did not have any hydrogens as neighbors for spin coupling. The H5 and H8 showed the correct doublet as splitting for being only next to H6 and H7 respectively. The H6 and H7, showed the expected triplet for having two hydrogen neighbors in H5, H7, and H6, H8 correspondingly.
3. *J* coupling: The *J* coupling for H1, H4, and H10 were zero because they were singlets. The *J* coupling for H5, H6, H7, and H8 gave interesting results. It was expected very similar *J* coupling values for H5, H6, H7, and H8, but two different *ortho* coupling constants were found: ${}^3J_{5,6} = 8.39$ Hz and ${}^3J_{6,7} = 7.28$ Hz, also ${}^3J_{8,7} = 8.23$ Hz, and ${}^3J_{7,6} = 7.30$ Hz, which can be seen in Figure 14 .

Figure 14: Ortho coupling constants for (15).

The main reason for this *J* coupling difference is due to the different C–C bond lengths in the aromatic system.²⁰ A similar example was found for naphthalene in Friebolin²⁰, which is shown in Figure 15.

Figure 15: Naphthalene *J* coupling according to Friebolin.²⁰



Scheme 21: Proposed mechanism for the synthesis of 15 using VOF_3 or FeCl_3 .

The mixture of SiO₂ in FeCl₃ was made fresh for the intramolecular coupling reaction. A certain amount of SiO₂, preferably 1 equivalent, was left drying overnight at 80 °C in the oven to avoid any moisture present in the silica gel. This dry SiO₂ was poured into a mortar that contained 1 equivalent of FeCl₃. These reagents were ground and mixed using a mortar and pestle. This mixture was poured immediately into a starting material solution of that in dichloromethane to be run for at least 48 hours at room temperature.

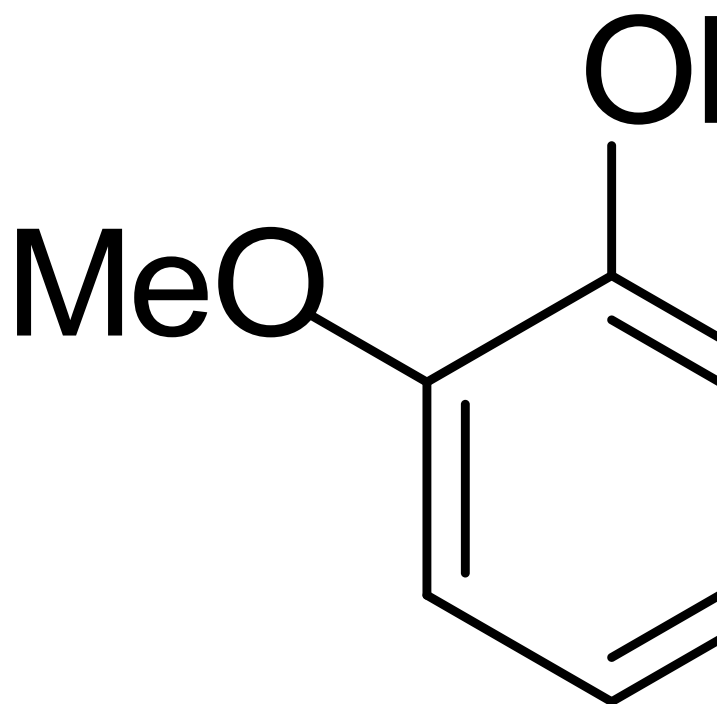
The dryness of SiO₂ was important for the experimental conditions. It was noticed that regular SiO₂, without being dried in the oven overnight, gave low yields, and difficult-to-run columns were necessary to separate the product and starting material.

The formation of the phenanthrene ring must be done prior formation of the alcohol by reduction. This reaction gave almost no product and a tacky solid if any hydroxyl group, including phenols was present in the starting material. See Scheme 22.

Scheme 22: FeCl₃ reaction in the presence of hydroxyl group.

The possible side-product and mechanism was presented by Krishna *et al.*³⁰ There are possibilities that FeCl₃ reacts as a Lewis acid and coordinates with the oxygen of the alcohol, facilitating nucleophilic attack of another alcohol on the electron-deficient primary carbon, which is followed by deprotonation and regeneration of FeCl₃. As a result, the FeCl₃ reagent gives an ether instead of the expected aromatic phenanthrene ring (see Scheme 23).

The formation of the ether could be the answer for the formation of the tacky product. This undesired product did not indicate the presence of any unreacted starting material; therefore, it could not be recycled.



Scheme 23: Proposed mechanism for FeCl₃ reagent in the presence of OH group.

2.3.3 Synthesis of (2,3-dimethoxyphenanthren-9-yl)methanol (16)

The reduction of **15** was accomplished by using one molecular equivalent of LiAlH_4 to reduce the ester carbonyl to methylene hydrogens (see Scheme 24).

Scheme 24: Reduction of compound **15**.

These methylene hydrogens were homotopics and showed only one peak in the ^1H NMR spectrum. It was also noted that the ester peak at 4.05 ppm from compound **15** was not present after the reduction.

2.3.4 Synthesis of (S)-methyl 1-((2,3-dimethoxyphenanthren-9-yl)methyl)-5-oxopurrolidine-2-carboxylate (17)

2.3.4.1 AB Spin system

The synthesis of intermediate 17 required three steps from the alcohol 16. The same steps and conditions were repeated from intermediate 7 to synthesize intermediate 17.

Intermediate **17** was characterized by ^1H , ^{13}C , gCOSY, gHSQC, and NOESY NMR spectroscopy. Some features of the ^1H NMR spectrum are worth mentioning. The C11 protons in the tetracyclic base appeared as an AB spin system in NMR spectroscopy (see Figure 16). It is important to indicate that this effect was not seen in intermediate **7** due to the homotopic methylene protons.

In the ^1H NMR spectrum it can be seen that the four signals for the methylene protons on C11 in the region 5.5 to 4.4 ppm were not homotopic (equal intensities or one signal), because they had different magnetic shieldings. As a consequence, they gave separate signals. This feature is also known as “roof effect” or AB spin system. The inner lines were stronger than the outer lines.

Analysis of the AB spin spectrum:

It started by numbering the resonances frequencies of the four lines of the AB spectrum from left to right as f1, f2, f3, f4. As in the AX spectrum the coupling constants J_{AB} is equal to the frequency interval between lines 1 and 2 or between 3 and 4:

$$|J_{AB}| = |f1 - f2| = |f3 - f4| \text{ [Hz]}$$

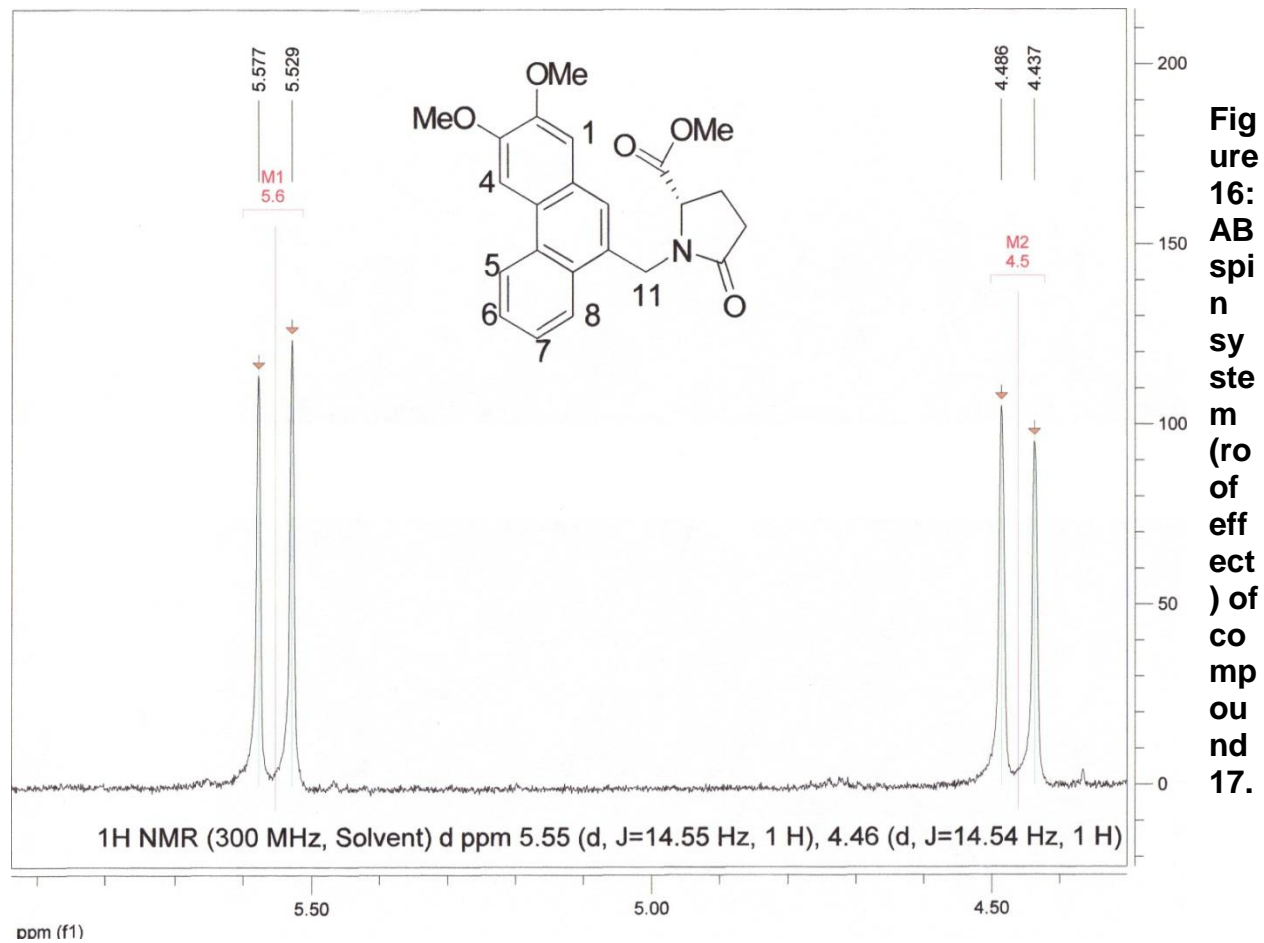
$$|J_{AB}| = |5.577 - 5.529| = |4.486 - 4.437| = 14.55 \text{ Hz}$$

The chemical shifts are given by the centers of gravity of the line pairs 1, 2, 3, and 4. The chemical shifts difference can be determined by the following equation:

$$\Delta\nu = \sqrt{|(f1 - f4) - (f2 - f3)|}$$

$$\sqrt{(5.577 - 4.437) - (5.529 - 4.486)} = 0.314 \text{ ppm} = 0.311 * 300 = 94.48 \text{ Hz}$$

The roof effect is a typical indication of strongly coupled spin systems. In the case $\Delta\nu$ is zero, only a singlet appears in the spectrum. It means the AB system is essentially changed to an A_2 spectrum.



2.3.4.2 Geminal coupling 2J (H,H), bond angle, and effect of neighboring π electrons for methylene protons on C11 of 17.

Geminal coupling 2J (H,H)

The diastereotopic hydrogens on C11 (4.5 and 5.6 ppm) also showed a noticeable difference in chemical shifts, just like its analog intermediate 8. The geminal coupling constant was found to be 2J (H,H) = 14.55 Hz.

Bond angle

The bond angle for the geminal hydrogens on C11 was also calculated drawing the intermediate using molecular modeling: Tripos: SYBYL 8.0 (dynamics, MM4 minimization energy) as shown in Figure 17. The bond angle = 109.5°. It can be observed that 2J (H,H) = 14.55 Hz correlated with the predicted bond angle 109.5° in Figure 17.

The major effect for the difference in the diastereotopic hydrogens in C11 was the presence of the amide group as explained for intermediate 8. This difference was smaller (2.9 and 3.2 ppm) when the amide was reduced to the tertiary amine with LiAlH_4 to obtain 21 (DCB 3507).

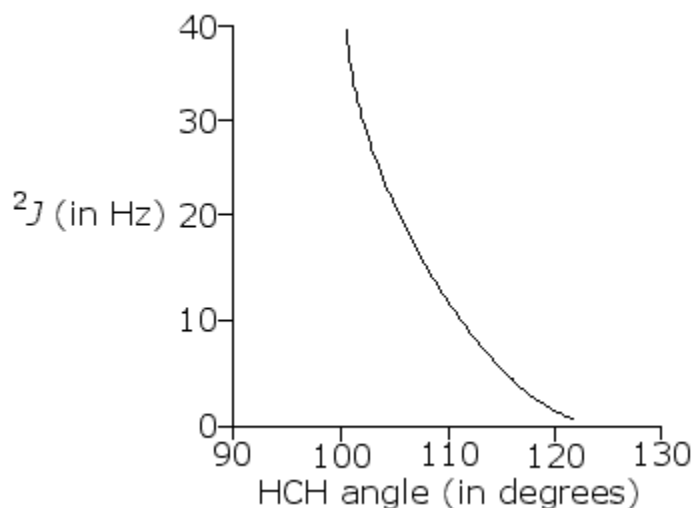


Figure 17: Coupling constant vs bond angle.

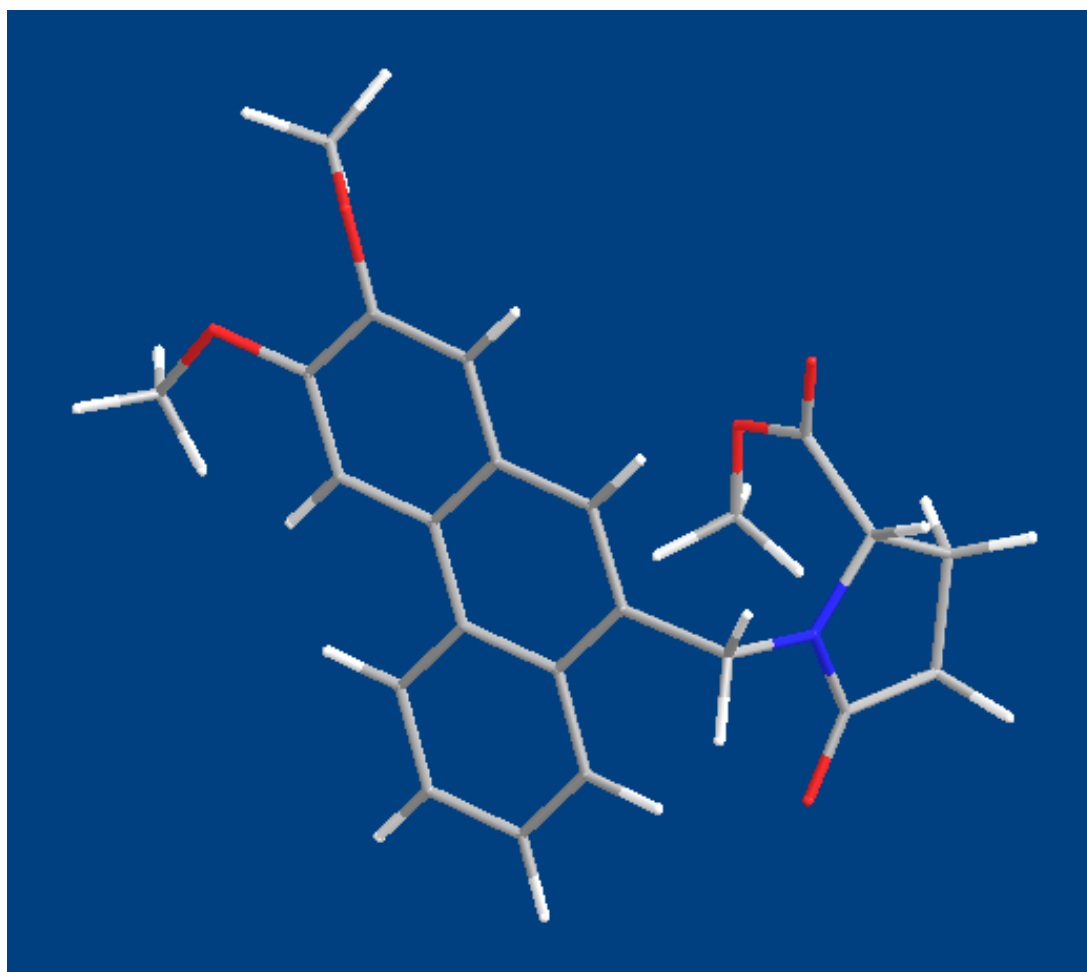


Figure 18: Structure of compound 17 from molecular modeling.

2.3.5 Synthesis of (S)-2,3-dimethoxy-13,13a-dihydrodibenzo[*f,h*]pyrrolo[1,2-*b*]isoquinoline-11,14(9*H*, 12*H*)-dione (19)

Compound **19** was obtained by two methods:

2.3.5.1 Method 1 TFAA and BF₃·Et₂O

The intermolecular Friedel–Crafts cyclization reaction of **18** using TFAA and BF₃·Et₂O was accomplished under the same conditions as used for **9** to obtain the ketone **19**.²¹

2.3.5.2 Method 2 (COCl)₂ and SnCl₄

This cyclization was also obtained using (COCl)₂ and SnCl₄. Oxalyl chloride was added to prepare the carboxylic acid chloride, and tin tetrachloride was used as a strong Lewis acid to promote electrophilic addition to the aromatic system. This reaction required heating at 30 °C prior addition of SnCl₄, but it was noticed that a higher yield was obtained when it was run at room temperature for at least four hours or overnight. In order to quench the reaction, addition of 2 N HCl was needed. This weak acidic solution must be added dropwise. It should be noted that water must be added before 2 N HCl decompose the SnCl₄. The characteristic yellow spot was also observed on TLC under ultraviolet light using anisaldehyde for both methods.

Intermediate **18** was characterized by ¹H, ¹³C, gCOSY, gHSQC, and NOESY NMR spectroscopy. The C9 protons appeared as an AB spin system. The NMR spectrum with the chemical shifts and the coupling constant are shown in Figure 19. It is important to indicate that this effect was also seen in intermediate **8**.

In the ¹H NMR spectrum it can be seen that the four signals for C9 protons in the region 5.9 to 4.8 ppm did not have equal intensities. This feature is also known as “roof effect” or AB spin system. As in the AX spectrum the coupling constants J_{AB} is equal to the frequency interval between lines 1 and 2 or between 3 and 4:

$$|J_{AB}| = |f_1 - f_2| = |f_3 - f_4| \text{ [Hz]}$$

$$|J_{AB}| = |5.873 - 5.812| = |4.806 - 4.745| = 18.3 \text{ Hz}$$

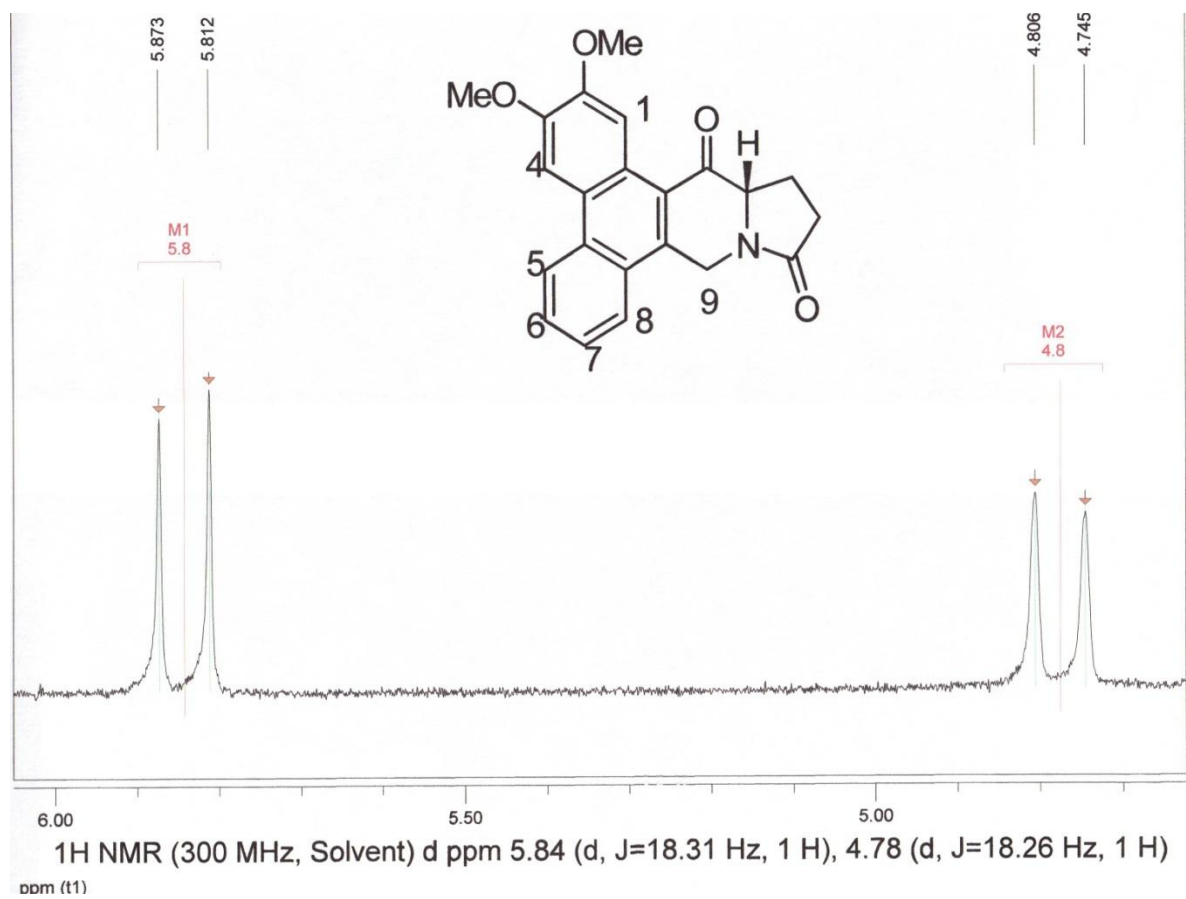


Figure 19: AB spin system (roof effect) of compound 19.

The aromatic H1 chemical shift of phenanthrene **18** undergoes a downfield shift due to the deshielding of the newly formed ketone **19**. This effect was reversed after reduction of **19** with K-Selectride with the formation of the secondary alcohol **20** (see Table 8).

Table 8: Comparison of ^1H and ^{13}C NMR shifts for compound 18, 19, and 20

Compound 18

^1H	ppm	^{13}C	ppm
H1	6.93	C1	119

Compound 19

^1H	ppm	^{13}C	ppm
H1	9.03	C1	125.1

Compound 20

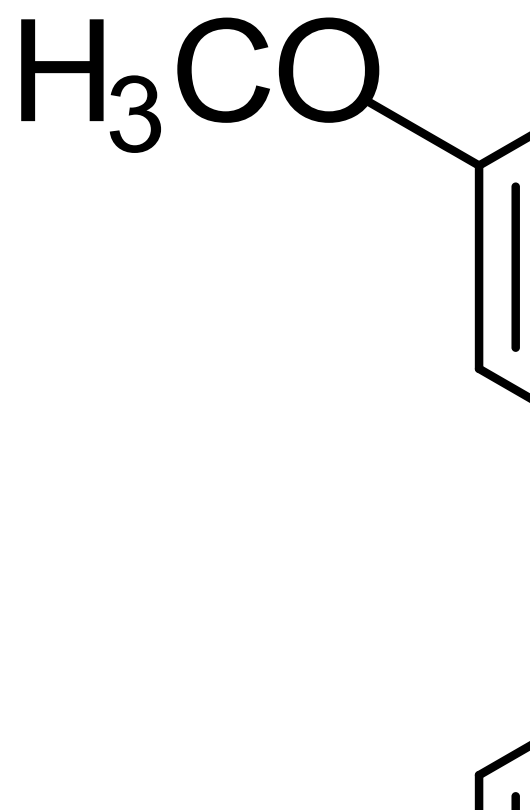
^1H	ppm	^{13}C	ppm
H1	7.6	C1	104.47

Product **19** was always produced in lower yield than **9**. The percent yield ranged from 50–60%. Several conditions were changed, such as temperature, molecular equivalents of TFAA, mol equivalent of $\text{BF}_3\cdot\text{Et}_2\text{O}$, reaction time, and quenching time to improve the yield, but the cyclization could not be improved.

A possible explanation for this lower yield can be explained by Akué-Gédu and co-workers.¹ They postulated that the presence of deactivating functional groups in the aromatic moiety decreased the rate of ketone formation. On the other hand, cyclization of acids with electron-rich aromatic moieties gave better yields. Akué-Gédu *et al* gave the following examples, Scheme 25.¹

Scheme 25: Akué-Gédu's reaction example

Thus, the presence of electron-rich methoxy groups in the phenanthrene ring activated the aromatic moiety to form the Friedel–Crafts cyclization of **18**. In the reaction mechanism, shown in Scheme 26, it can be observed that after the cyclization produced by the π aromatic bond on C9–C10, it formed a carbocation on C9. This positive charge can be delocalized in the phenanthrene due to the aromatic π bonds. This delocalization can be enhanced by the presence of electron-donating groups, in this case methoxy groups (OMe), which donate their lone-pair of electrons localized on the oxygen. These pair of electrons created a resonance to delocalize the positive charge. It is worth mentioning, that the presence of only two methoxy groups vs. four methoxy groups appears to have lowered the yield. The two methoxy groups **9** gave a lower yield than the four methoxy groups **19**; meanwhile, according to the literature, the total absence of electron-donating groups (only hydrogens) or the presence of electron withdrawing groups on the phenanthrene ring produced almost zero percent yield. Such behavior is in line with electrophilic aromatic reactions in general and Friedel-Crafts reactions in particular.



Scheme 26: Reaction mechanism for the synthesis of 19.

2.3.6 Synthesis of (13a*S*, 14*S*)-14-hydroxy-2,3-dimethoxy-12,13,13a,14-tetrahydrodibenzo[*f,h*]pyrrolo[1,2-*b*]isoquinolin-11(9*H*)-one (20)

Stereocontrolled ketone reduction of the intermediate **19** on C14 to the secondary alcohol **20** with (*S*) stereochemistry was achieved by either K-selectride or L-selectride in high yield. The decision to synthesize the secondary alcohol with the (14*S*) stereochemistry was mandated given the higher biological activity of (14*S*) DCB 3503 in contrast to (14*R*) DCB 3501 (see Scheme 27).



Scheme 27: DCB 3503, 3501, and undesired product

The two diastereotopic protons on C9 have noticeably different chemical shifts. This difference is around 1 ppm (4.5 and 5.4 ppm). This chemical shift difference could be due to the oxygen's lone pairs of the amide group that deshielded the hydrogen on the same face of the nitrogen, which is more downfield; meanwhile, the other hydrogen is more upfield because it is more shielded as shown in Figure 20.

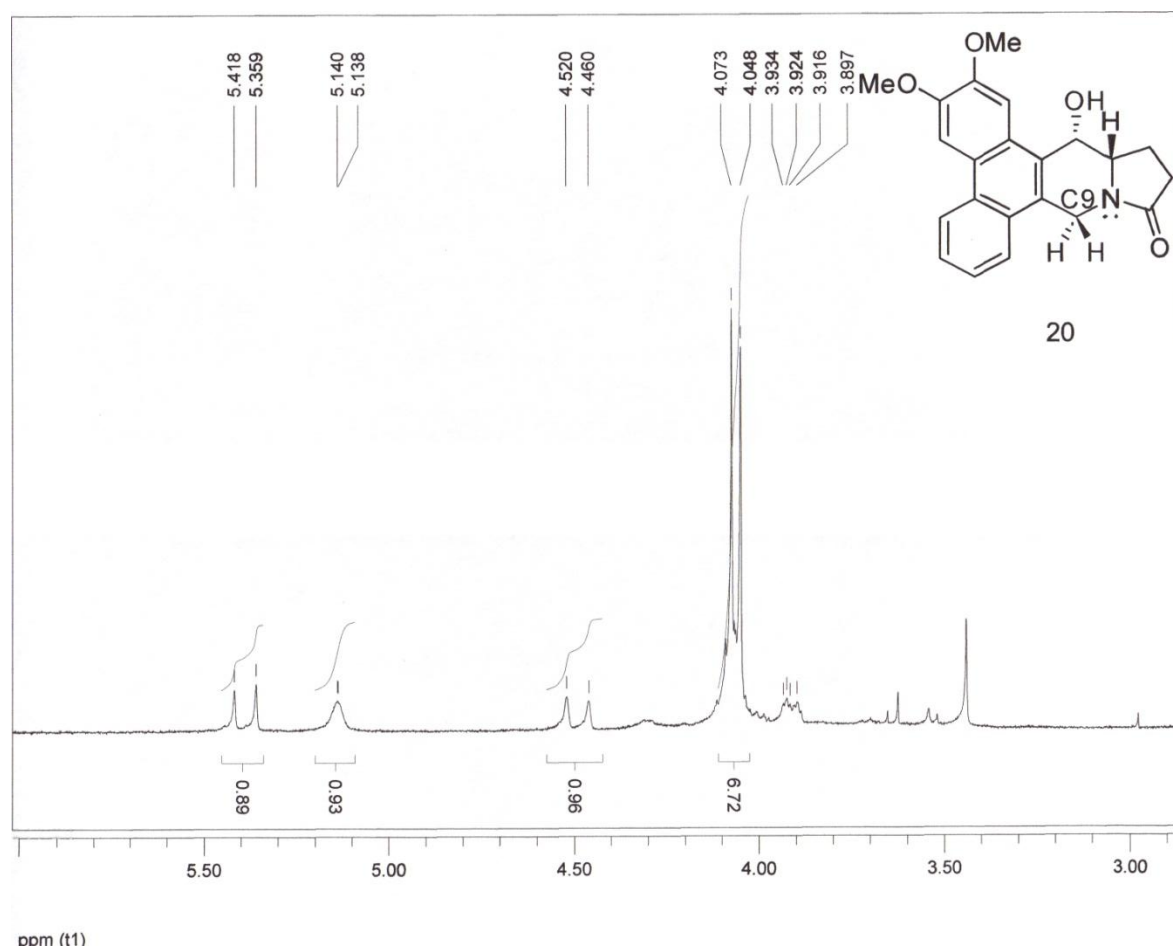
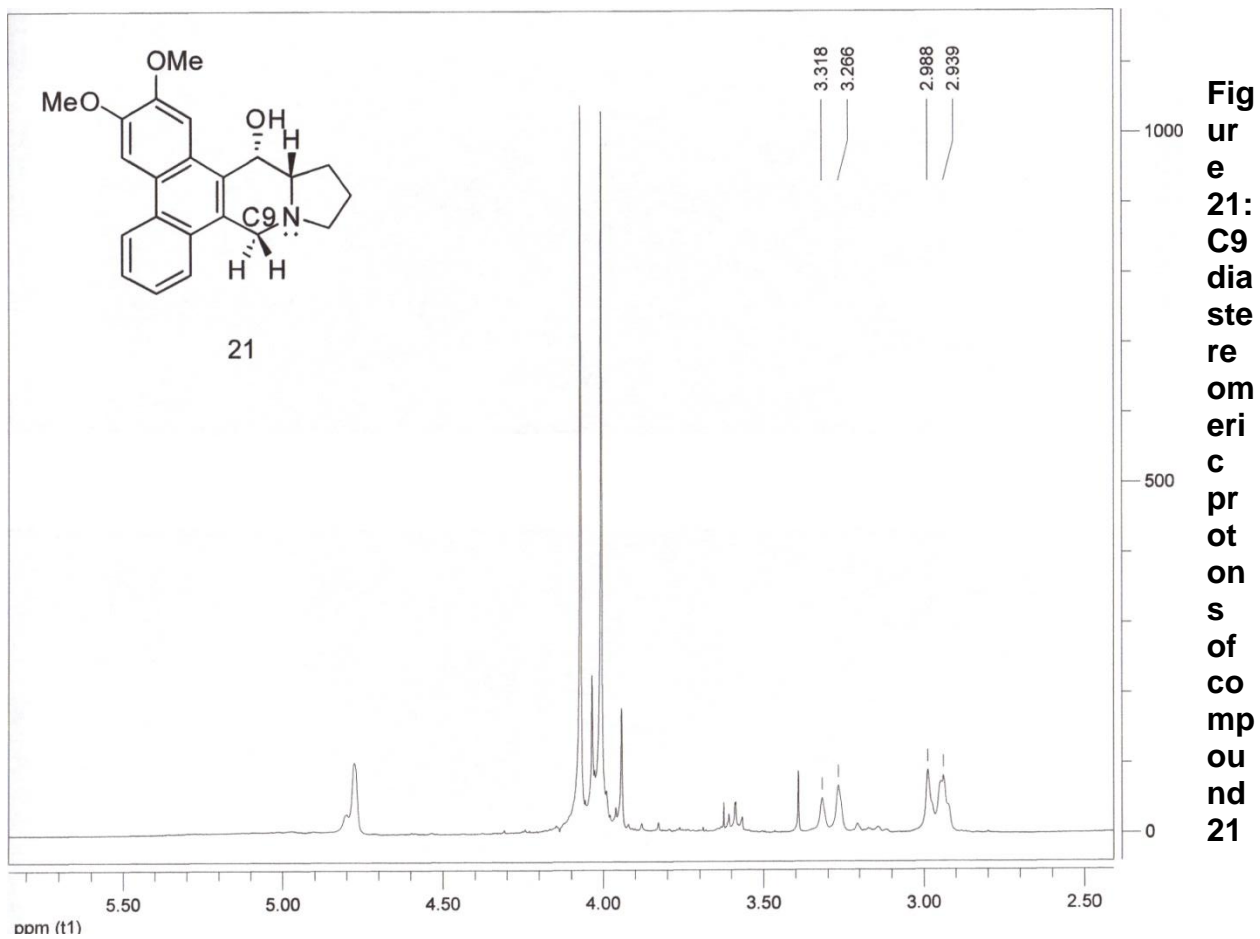


Figure 20: C9 diastereomeric protons of compound 20.

2.3.7 Synthesis of (13a*S*, 14*S*)-2,3-dimethoxy-9,11,12,13a,14-hexahydrodibenzo[*f,g*]pyrrolo[1,2-*b*]isoquinolin-14-ol (**21**)

The reduction of the amide or lactam intermediate **20** to a tertiary amine **21** was achieved by 1 equivalent of LiAlH₄ with high yield. This reduction was quenched by EtOAc and two options: 2 N HCl or Na₂SO₄·10H₂O. It was noted that using the second reagent gave a little higher yield because the final product is more stable under neutral conditions, instead of acidic or basic conditions. Unfortunately, this product was unstable and tended to decompose when exposed to light, air, and solvent.

Final product **20** was characterized by ¹H, ¹³C, gCOSY, gHSQC, and NOESY NMR spectroscopy. The C9 protons did not appear as an AB NMR spin system like the previous intermediates. The C9 proton chemical shifts moved upfield due to the reduction of the amide, from 4.5 to 5.4 ppm and from 2.9 to 3.2 ppm. It is clear that the deshielding effect of the amide kept the C9 protons at downfield. This difference became really shorter when the lactam was reduced with LiAlH₄ to obtain the final product **21** as shown in Figure 21. The effect of neighboring π-electrons from the amide group caused a negative contribution to the geminal coupling.



2.3.8 Karplus equation and molecular modeling applied to DCB 3507

DCB 3507 has a secondary alcohol on C14 with a stereochemistry (S) due to a previous stereoselective reduction using K-Selectride. In order to confirm this configuration, some analysis was done to confirm this chiral carbon that included dihedral angle, 3J coupling constant, Karplus equation, and molecular modeling (Tripos:SYBYL 8.0).

2.3.8.1 Dihedral angle analysis

DCB 3507 has a dihedral angle between hydrogens on H14 and H13a as shown in Figure 22.



Figure 22: Dihedral angle case A and case B

The chirality is defined as 13aS by synthesis from the precursor amino acid **17**. There was no evidence of racemization during synthesis which would have produced a diastereomeric mixture that would have been seen in the NMR spectrum. The dihedral

angle for DCB 3507 (CASE A) should be small if hydrogens on C14 and C13a have chiral carbons (13a*S*,14*S*); in other words, both hydrogens are “up” as shown in Figure 20, probably less than 60°. If the stereochemistry on C14 and C13a would have a configuration (13a*R*,14*S*) (CASE B); then, the dihedral angle should be much larger than 60°. The dihedral angle could be properly measured by a combination of several methods, such as vicinal coupling constant ^1H NMR (3J , H–C–C–H), the Karplus equation, and molecular modeling.

2.3.8.2 Vicinal coupling constant analysis

The 3J coupling constant between the vicinal protons H14C and CH13a was measured from ^1H NMR spectroscopy at 300 MHz. The hydrogen on C14 appeared at 4.75 ppm as a doublet with a coupling constant $J = 1.78$ Hz, as shown in Figure 24. The coupling constant for C13a could not be measured because it was highly overlapped by other methylene hydrogens.

2.3.8.3 Karplus equation analysis

Vicinal coupling or 3J coupling is dependent upon the dihedral angle between the nuclei. The magnitude of these couplings is generally the smallest when the torsion angle is close to 90°, and largest (around $J = 12$ Hz) at angles of 0 and 180°. The relationship between dihedral angle and coupling constant is known as the **Karplus relationship**,²⁰ and the following Figure 23 depicts a typical **Karplus curve**. For a small, relatively rigid molecule, where a small coupling constant (1.78 Hz) is observed, the small gauche angle as in Case A (Figure 22) is supported. This together with the known configuration of C13a, leads one to assign the (*S*) configuration to C14.

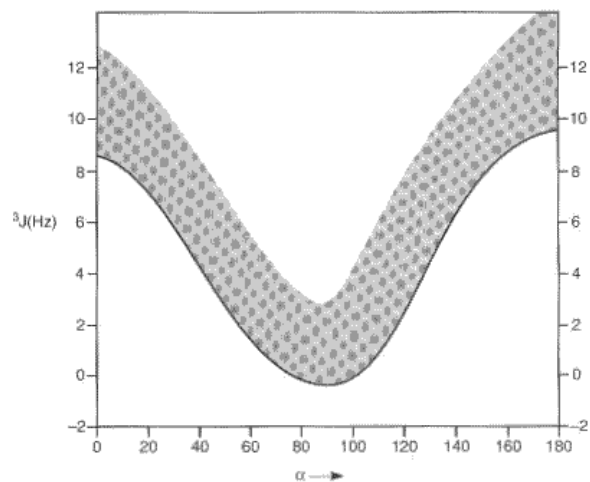


Figure 23: Karplus curve.

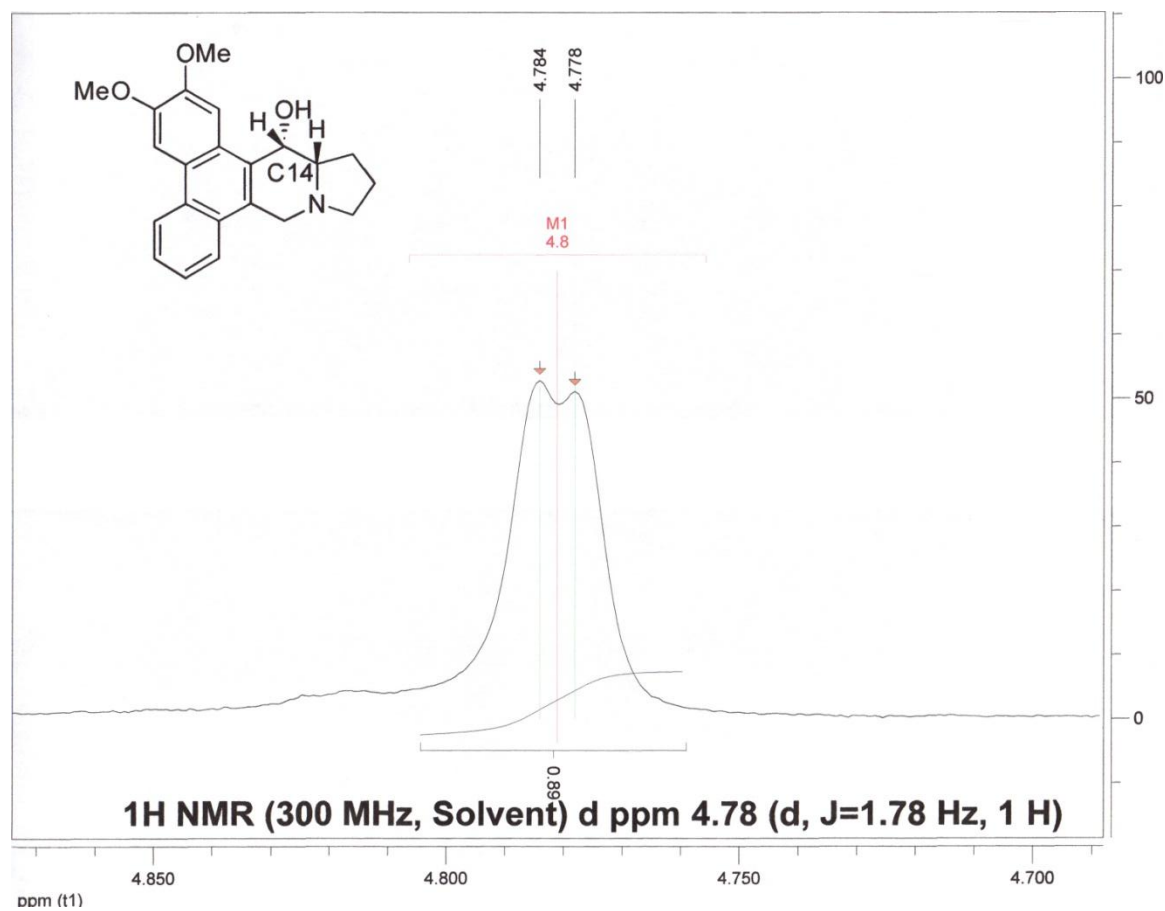


Figure 24:
J
coupling of compound 21 at 4.78 ppm

The coupling constant $J = 1.78$ Hz was inserted into the Karplus equation, and it gave a theoretical dihedral angle = 60.5° .

2.3.8.4 Molecular modeling (Tripos:Sybyl 8.0)

The application of molecular modeling using the program Tripos: SYBYL 8.0 (dynamic and MM4 minimization) was used to calculate the dihedral angles.

The drawing of the structure and use of molecular dynamics and MM4 to minimize energy was the best approach. See Figure 25.

Table 9 resumes the predicted calculations from molecular modeling for DCB 3507.

Table 9: DC 3507 dihedral angle molecular modeling results

Structure	Dihedral angle (\AA)	Final steric energy (kcal/mol)
DCB 3507 from drawing	52.2	11.3392

A similar analysis to calculate dihedral angles was applied to DCB 3503 in Chapter 1. Moreover, two additional structures were built using molecular modeling for DCB 3507 with dihedral angles higher than 60° by increasing theoretical dynamics and MM4 in SYBYL. These structures can be seen in Figures 23 and 26. Table 10 includes data from DCB 3503, DCB 3507 and the two additional structures which were arranged according to steric energy (from low to high).

Table 10: DCB 3507 and DCB 3503 dihedral angle molecular modeling results

Structure	Dihedral angle (\AA)	Final steric energy (kcal/mol)	Figure
1.DCB 3507	52.2	11.3392	25
2.DCB 3503	51.1	12.5425	8
5.DCB3507	69	25.408	26

The above table 10 gave us an important conclusion for the dihedral angle approximation for either DCB 3503 or DCB 3507. It can be concluded that the dihedral angle should be more than at 50.4° and less than 60° , because at 50° the steric energy is almost double that 52.2° , and the dihedral angle should be no higher than 60° , because the steric energy increases and the molecule starts to bend in the pyrrolidine moiety as seen in Figures 25 and 26.

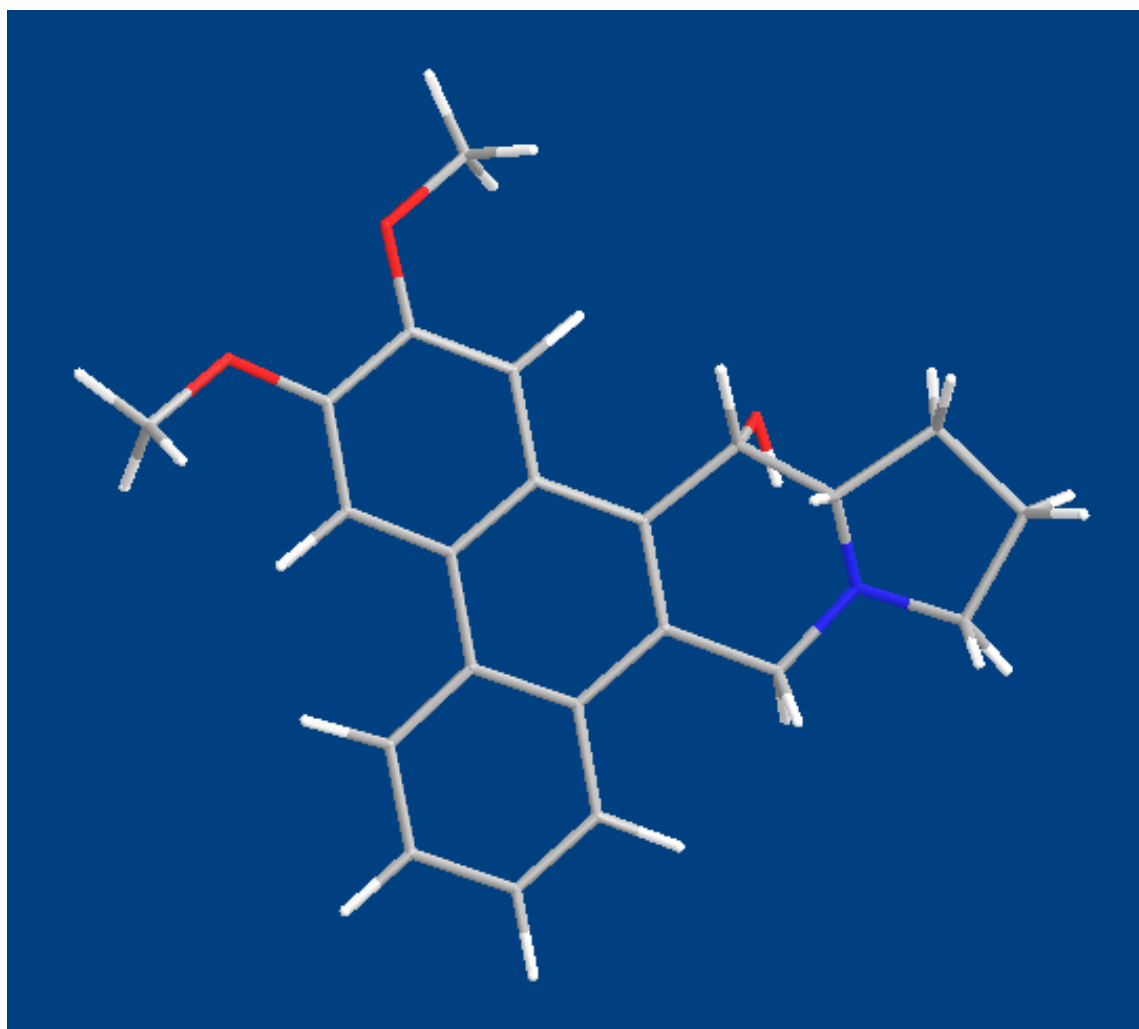


Figure 25: Direct drawing and minimization molecular modeling of compound 21.

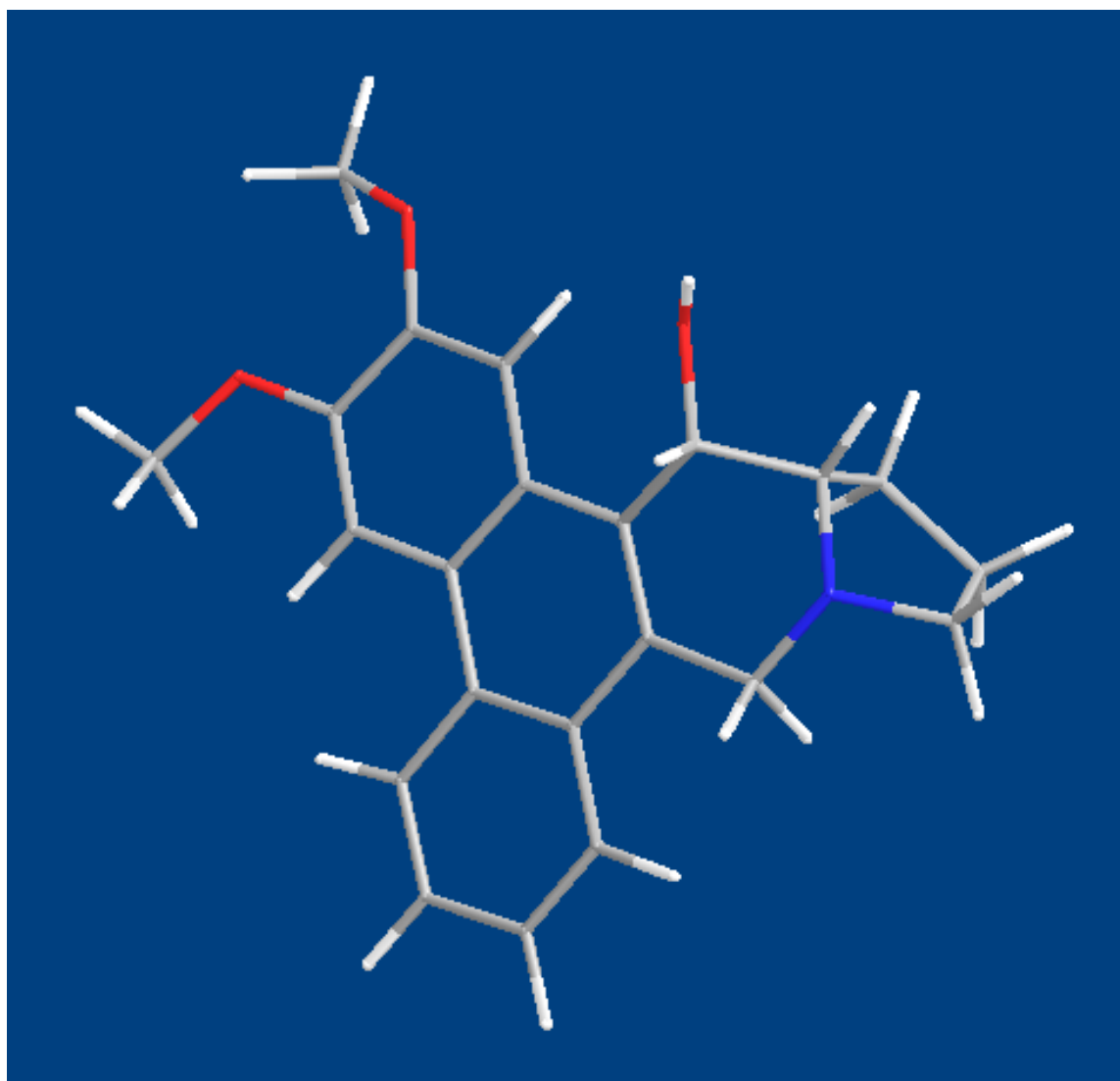


Figure 26: Direct drawing non planar $DH = 69^\circ$ molecular modeling compound 21.

Chapter Three: Synthesis of DCB 3508

3.1. Statement of Problem

The synthesis of DCB 3508 was carried out to compare its activity with that of DCB 3503 and DCB 3507. DCB 3508 is an analog of DCB 3503 in which the compound is open at C10 of the phenanthrene system. See Figure 27.

Figure 27: Structure of DCB 3508

3.2 Introduction

The idea of synthesizing DCB 3508 (Figure 27) came as a result of an unexpected impurity found in the mass of DCB 3503 and an interest to find the biological activity for an open-ring analog to DCB 3503. Compound **11** (DCB 3503) had an exact mass of 409.19. When it was run using DART in positive-ion mode, it showed the expected fragment $[M+1]^+$ 410.197, but it also showed a peak at 412.213. It came to my attention that it might be a side-product with higher polarity than **11**, because the development of TLC (2:0.5 CHCl₃:CH₃OH) showed an almost colorless spot at the baseline of the TLC when it was stained with anisaldehyde-H₂SO₄. Also, when running the impure **11** on HPLC, it showed a small peak that was very close to the peak for DCB 3503.

3.3 Results and discussion: Total synthesis of DCB 3508

Scheme 28: The synthetic route to DCB 3508.

3.3.1 Synthesis of (S)-methyl-1-(2,3,6,7-tetramethoxyphenanthren-9-yl) methylpyrrolidine-2-carboxylate (24)

The idea of coupling (S)-2-(methoxycarbonyl)pyrrolidinium chloride **23** directly to **6.1** to obtain **24** has been tried before without success using K_2CO_3 in DMF but according to Fülep and co-workers,²⁴ it could be accomplished using K_2CO_3 in acetone with NaI at room temperature, and for my reaction it gave a 40-50% yield. A similar alkylation was reported by Akué-Gédu¹, and Vanecko and West³² suggested an increase in temperature. This N-alkylation was a complete success only after heating the solution at reflux for 48 hours; the product was produced in high yield and almost no by-products were found.

It was interesting to indicate that Govindachari and co-workers³³ tried a similar alkylation without success under Marchini and Belleau's conditions. Govindachari used 2,3,6,7-tetramethoxy-9-chloromethylphenanthrene with proline ester, dissolved them in dry toluene, and refluxed with stirring for 20 h. However, he was successful in obtaining the alkylation under the same conditions using prolinol, instead of proline ester. Therefore, the following are conclusions.

1. The presence of Br or I as a leaving group in the starting material **6.1** determined the successful reaction. It seemed that this alkylation could not be completed if Cl was the as leaving group.
2. According to Govindachari *et al*,³³ the alkylation of 2,3,6,7-tetramethoxy-9-chloromethylphenanthrene and proline ester undergoes a self-condensation of proline ester much faster than reaction with the halide. This could have been avoided using a better leaving group (Br or I)
3. The choice of solvent is important for the alkylation. Although DMF is a well-known solvent for alkylations, it did not work for this case; however, acetone and dry toluene was found to be useful.
4. The strength of the base had an important role for this alkylation. Potassium carbonate is a weak base that is used for easy alkylations (good leaving groups and strong nucleophiles). The use of strong bases, such as NaH, was not used to avoid self alkylation of proline or elimination reaction of the halides.

The structure of **24** was confirmed and characterized by mass spectrometry and NMR spectroscopy. The exact molecular weight of **24** was 439.199, and it was found as m/z 440.205 by AccuTOF-DART in the positive-ion mode. NMR spectroscopy supported the structure. The most important prove of that the coupling reaction between **6.1** and proline ester **23** was successful was the formation of the diastereotopic geminal hydrogens (4.48, 3.53 ppm) at C1 for **24**. It is also important to indicate that the starting material **6.1** did not have diastereotopic hydrogens on C1; they were homotopic protons giving one signal (4.99 ppm) (see Figure 28).

These geminal diasterotopic protons in **23** were also proved by 2D NMR spectroscopy. The gCOSY spectrum showed a strong correlation between 4.48 and 3.53 ppm, which could indicate either geminal or vicinal hydrogens. The gHSQC spetrum confirmed that they were geminal hydrogens, because these two hydrogens (4.48, 3.53 ppm) were on the same F2 axis that correlated to only one carbon. The NOESY spectrum also indicated a strong proximity through space.

The diastereotopic hydrogens on C1 in product **23** were also proved by J coupling measurements. The diasterotopic hydrogens on C1 showed two distinct chemicals shifts, but the same geminal coupling 2J (H,H) = 12.13 Hz (see Figure 29 and 30).

Figure 28: Diastereotopic hydrogens of 24.

Figure 29: *J* coupling of compound 24 at 3.53 ppm.

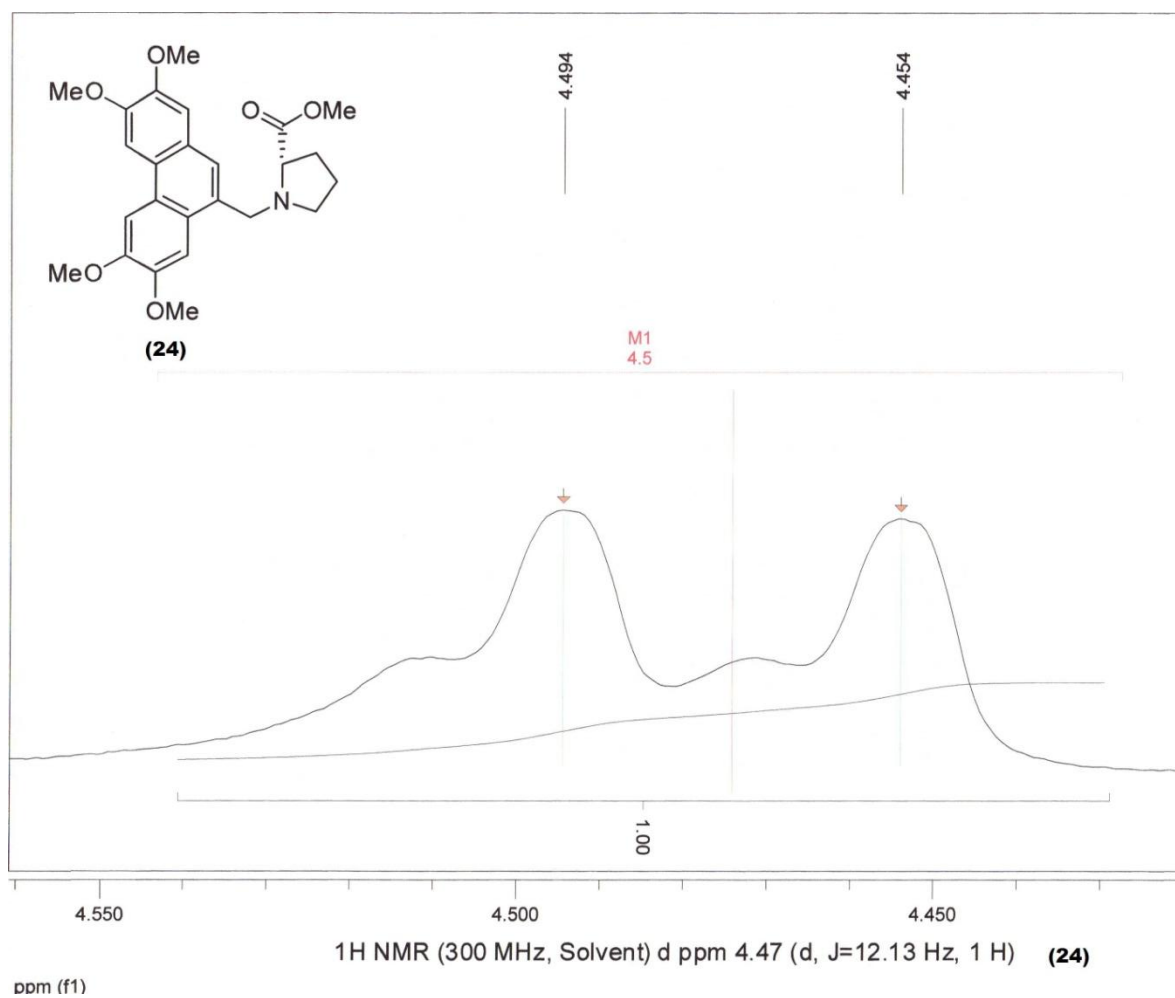


Figure 30: *J* coupling of compound 24 at 4.48 ppm.

3.3.2 Synthesis of (S)-1-((2,3,6,7-tetramethoxyphenanthren-9-yl)methylpyrrolidin-2-yl)methanol (**25**)

DCB 3508 was synthesized in two easy ways. Both pathways require reduction (see Scheme 29).

First pathway: Product **25** was accomplished by reduction of **7** with 2 equivalents of LiAlH₄ to reduce both the ester and lactam. This product **25** was obtained in high yield without any side products.

Second pathway: Product **25** was accomplished by using 1 equivalent of LiAlH₄ with **24** to obtain **25**. This reaction also gave a high yield of product, and TLC showed the same $R_f = 0.06$ value as the impurity seen on the impure DCB 3503.

First reaction pathway:

Second reaction pathway:

Scheme 29: Synthesis of 25 by two routes.

The structure of the impurity **25** was found using TLC, HPLC, MS, and NMR spectroscopy. The total mass of the uncharged impurity had to be [M]: 411.20. The TLC showed a spot almost on the TLC baseline that indicated a higher polarity than that for **11** ($R_f = 0.13$) (see Figure 31). Using this information, several possible structures were formulated that contained a [M] of 411.20 and had higher polarity than **11**. The structure of **25** was the best candidate due to the perfect mass match and the free alcohol that increased the polarity. The use of 1D and 2D NMR spectroscopy (gCOSY, gHSQC, and NOESY) proved the structure.

The possibility to obtain chemically **25** as a by-product from the reduction of **11** using LiAlH_4 could not be reasonable. It was possible that unreacted compound **8** was carried along with the product during the last two steps of the synthetic path, finally being reduced with LiAlH_4 . It is important to indicate that compound **8** was observed on TLC in very small quantities at $R_f = 0$. HPLC was then used to find any possible by-product that might not be seen on TLC. The possible reaction route for this by-product is proposed in the Scheme 30.

Figure 31: R_f values for compound 11 and 25.

Scheme 30: Reaction route for by-product 25.

Compound 25 was synthesized in order to be assayed in the 60-cell screen for antitumor activity at the National Cancer Institute. This compound was an analog of DCB 3503 with potential anti-cancer properties. Unfortunately, this compound **25** was not as potent as DCB 3503.

Similar polar phenanthrene-based tylophorine derivatives containing a prolinol were synthesized and evaluated as potential antitumor agent by Wei and co-workers.³⁴(Figure 32). These structures (B and D) are shown below.

These compounds were evaluated for cytotoxic activity against the A549 human cell cancer line as described in the paper by Wei and co-workers.³⁴ It is important to indicate that compound A and D showed the highest potency with IC₅₀ values of 0.27 and 0.16 μ M, respectively, which are currently used as anticancer drugs.

These compounds contained structural similarities to DCB 3508. A core phenanthrene structure with an open chain at C10, a hydroxyl terminal group in the pyrrolidine structure, a methoxy group on C6, and 1,3-dioxolane moiety groups compared to methoxy substituents in the DCB 3508

Figure 32: Tylophorine derivatives containing prolinol.

Table 11: Partial table from the paper of Wei *et al*²⁹

Compound	IC ₅₀ (μM)
A	0.27
B	0.7
C	0.5
D	0.16

Chapter Four: Synthesis of DCB 3509

4.1 Statement of Problem

We obtained the biological results from DCB 3503, 3507, and 3508 conducted at the NCI. These data were plotted in the molecular modeling program, CoMFA, to predict biological activity for a range of analogs. CoMFA predicted high biological activity for DCB 3509 (see Figure 33); therefore, it was synthesized.

Figure 33: Structure of DCB 3509.

4.2 Introduction

Synthesis of DCB 3509 came from an interest to explore the biological activity of a DCB 3503 analogs with a short aliphatic chain with a hydroxyl group at the end on the aromatic C3 position. DCB 3509 will be submitted soon for biological analysis at the National Cancer Institute. Meanwhile, CoMFA, a molecular modeling program, predicted that DCB 3509 could be highly potent.

4.2 Results and discussion: Total synthesis of 3509

Scheme 31: The synthetic route to DCB 3509.

Scheme 34, cont'd.

Scheme 34, cont'd

The total synthesis of DCB 3506 or **36**, as described in Scheme 34, has been previously accomplished by Mr. Conrad Kaczmarek in the laboratory of Dr. David Baker in 2004. The discussion of DCB 3506 can be found in his MS Thesis. Therefore, since it was not an original work by this author, I did not include any chemical discussion in this dissertation. However, the synthesis of **36** is covered in the experimental section in this dissertation.

4.3.1 Synthesis of Preparation of (13a*S*, 14*S*)-3-(3-hydroxypropoxy)-2,6,7-trimethoxy-9,11,12,13,13a,14-hexahydrodibenzo[*f,h*]pyrrolo[1,2-*b*]isoquinolin-14-ol (37)

The synthesis of **37** was accomplished by an alkylation of **36** by 3-bromopropanol using K_2CO_3 as base. The alkylation was run at 70 °C for 48 hours, because after only 24 hours the alkylation was incomplete, and some starting material was detected by mass spectroscopy. If this was the case, 0.5 molecular equivalents of 3-bromopropanol linker arm and K_2CO_3 was added which reflux overnight to complete the reaction, which solved the problem.

This alkylation gave an exclusive substitution at the phenolic oxygen on C3 as shown in Scheme 32. Because the phenol is a stronger acid than the secondary OH on C14 a mild base (K_2CO_3) was used to achieve stereoselectivity; therefore, strong bases such as NaH and hydroxides of alkali metals and alkaline earth metals like NaOH and $Ca(OH)_2$ were avoided.

Scheme 32: Alkylation of 36 to obtain 37.

The exclusive substitution on the phenol instead of the secondary alcohol was proved by mass spectrometry and NMR spectroscopy (Figure 34).

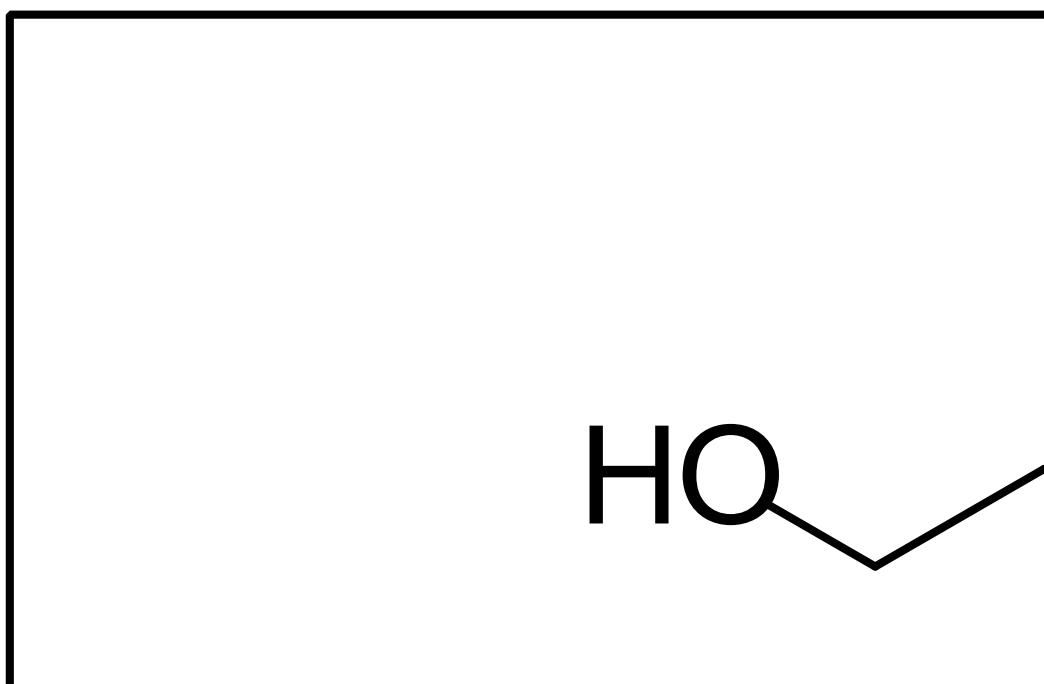


Figure 34: Possible substitutions for compound 37.

Mass spectrometry (AccuTOF-DART in the positive-ion mode) of **37** indicated an exact mass of $[M+1]^+ = 454.215$ and molecular fragment $[M-OH]^+ = 436.211$ that corresponded to the ionization of the secondary alcohol. In the event that the secondary alcohol was alkylated by the 3-bromopropanol, the exact mass would be 453.215, that is the same as **37**, but it would leave a free phenol that is easier to fragment due to the aromatic ring, and be detected than a primary alcohol; therefore, its expected fragment $[M-OH]^+ = 437.220$, was not found. The molecular ion of the fragmented phenol was stabilized by the ring, thus increasing the probability of its appearance than a primary alcohol.³⁵ This ion fragment 437.220 was not detected by mass spectrometry; therefore, there is a high probability that alkylation went exclusively to the phenol.

There was another product that could be produced. A potential quaternary amine could be formed if the tertiary amine alkylated the 3-bromopropanol, as shown in Scheme 36.

Scheme 33: Alkylation of 36 at the tertiary amine.

The possibility of forming a quaternary amine over alkylation in the phenol is low. This cationic compound would be unstable and undetectable by mass spectrometry, because DART-ESI in positive/negative mode does not detect cationic/anionic compounds. In order to easily rule out possible this side-product, we turned to NMR spectroscopy. The ^1H NMR spectrum clearly showed the methylene triplet at 4.22 ppm with an integration of 2H that corresponded to C1 on **37** (Figure 35). The downfield chemical shift of C1 at 4.22 ppm was predicted due to the deshielding effect of the oxygen's lone pair electrons. On the other hand, if the formation of a quaternary amine would exist, it would give a methylene multiplet for C1 with an expected chemical shift at 3.22 ppm with an integration of 2. This chemical shift or multiplet was not seen in the ^1H NMR spectrum; moreover, the phenolic proton chemical shift around 5.35 ppm was not present either.

Figure 35: Chemical shifts for alkylation of 37.

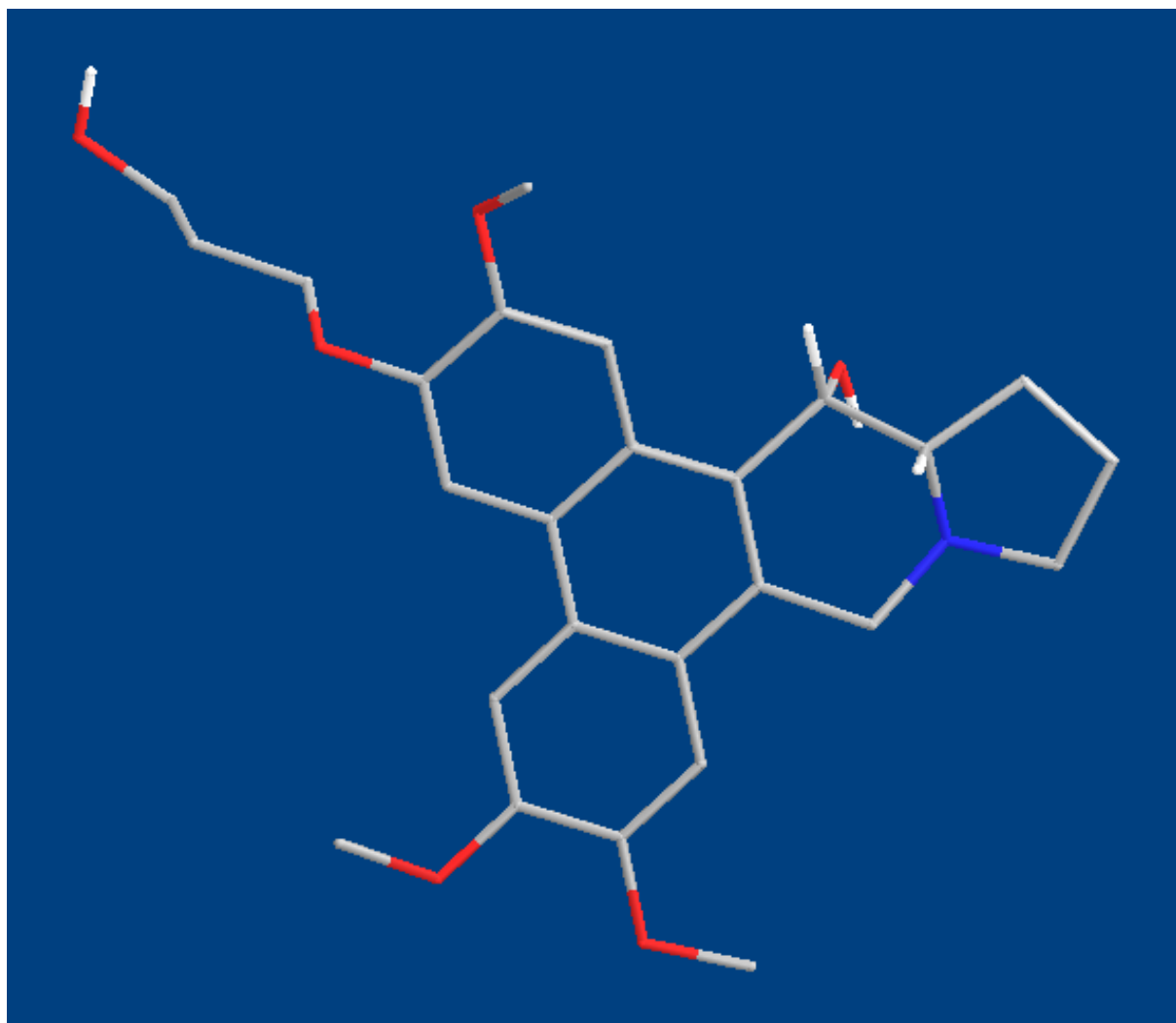


Figure 36: Molecular modeling structure for compound 37.

Chapter Five: Synthesis of Biotinylated Tylophorine Analog

5.1 Statement of Problem

Another project was the synthesis of a tylophorine attached to an aliphatic chain of 6 carbons with a biotin **41**, to help identify the protein receptor(s) in the cancer cell. Biotin is a naturally occurring compound that binds with high affinity and specificity to avidin and streptavidin proteins. The bond formation between biotin and avidin is rapid and unaffected by most extremes of pH, organic solvents, and denaturing agents. These conditions are ideal for the construction of a robust biological probe.

We were aware of the strength and specificity of the avidin–biotin complex; therefore, these biotin and linker arms are the best tools that will help us to understand the reaction mechanism of our tylophorine (DCB-3503) in the cell. This biological research will be done by our collaborator, Dr. Y.-C. Cheng at Yale University School of Medicine.

One of the main problems would be the attachment of biotin through a peptide bond. The attachment was considered through different intermediates in the synthetic route.

Another important problem would be the nucleophile at the end of the aliphatic chain. The nucleophile will have to be an amino group, but other groups were also analyzed.

Figure 37: Biotinylated tylophorine analog structure.

5.2 Introduction

The biotinylation of DCB 3503 via a tether was made to do studies of the molecular mechanism of DCB 3503 in cancer cells at the laboratory of Dr. Y. C. Cheng at Yale University.

The remarkably high affinity ($K_d = 10^{-5} \text{ M}^{-1}$) of the vitamin biotin for the glycoprotein avidin has been used as a powerful tool in a wide variety of bioanalytical applications. In the past, researches have routinely employed a six-atom (amino caproyl) linker chain between the biotin and active compounds in various chemical application with great success. Following this idea, our lab decided to link our DCB 3503 with a tether, in this case a saturated chain of 6 carbons to biotin.

The author decided to attach a linker not higher than 6 carbons, because of possible lipophilicity problems inside the cell. Also a linker with less than 4 carbons has been reported as unsuccessful on experiments. Therefore, a 6 carbon member link was considered ideal.

This synthesis turned out to be challenging due to the functional groups in DCB 3506 and tendency of DCB 3506 to undergo further reactions. Several synthetic routes have been tried; two routes reached the final step to obtain the final compound, but unfortunately failed in the last step.

5.3 Results and discussion: Total synthesis of a biotinylated tylophorine analog.

Scheme 34: The synthetic route to synthesis of biotinylated tylophirine analog.

5.3.1 Synthesis of (13aS, 14S)-3-(6-bromohexyloxy)-14-hydroxy-2,6,7-trimethoxy-12,13,13a,14-tetrahydrodibenzo[f,h]pyrrolo[1,2-b]isoquinolin-11(9H)-one (**38**)

The synthesis of **38** was achieved under the same conditions as those for **37**. The alkylation required a commercially available 1,6-dibromohexane to be used as linker arm, the intermediate **35** tylophorine analog, and K_2CO_3 as a weak base.

This reaction was run at 75 °C for 48 hours. It was also noticed that for only 24 hours the reaction was incomplete, because mass spectrometry indicated presence of starting material. In order to solve this problem, 0.5 equivalents of 1,6-dibromohexane and K_2CO_3 were added to the solution with reflux overnight. At room temperature, the solvent was vacuum evaporated at 35 °C until it turned into a mixed solid/liquid phase. Then 1:2:1 EtOAc:hexanes:Et₂O was added, and the solution was left stirring for 30 minutes at room temperature, and product **38** precipitated as yellow powder in high yield.

The presence of the terminal Br gave the characteristic mass peaks for halogen compounds. It is known, that a compound that contain one bromine atom would have an M+2 peak almost equal in intensity to the molecular ion because of the presence of a molecular ion containing the two isotopes ⁷⁹Br and ⁸¹Br in an approximately ratio 1:1 (50.5:49.5). This means that a compound containing 1 bromine atom will have two peaks in the molecular ion region as shown in Figure 38.

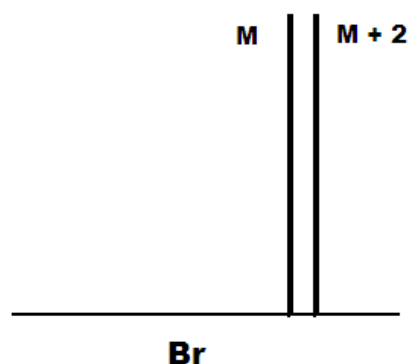


Figure 38: Characteristic peak intensities for a monobrominated compound

In compound **38**, the exact molecular mass was $[M] = 571.157$. The protonated (including a hydrogen) ion **38** $[M+1]^+ = 572.167$ and $[M+2]^+ = 574.167$ with almost two high-intensity peaks were found in the mass spectrum. The ion fragment $[M-OH]^+ =$

554.171, for which the theoretical exact mass is $[M-OH]^+ = 554.154$ was also present. Therefore, mass spectrometry of **38** proved the presence of the alkylated compound. (See Figure 40).

The NMR characterization of **38** also corresponded to the predicted chemical shifts. The most important peak found in this structure was the aliphatic methylene hydrogens on C1, see Figure 36, because these two hydrogens would have a unique chemical shift around 4.24 ppm due to the presence of oxygen, a triplet multiplicity, and an integration of 2H. On the other hand, the methylene hydrogens on C6 had a chemical shift around 3.50 ppm as expected due to the presence of bromine.

There are two other possibilities for alkylation, but these were discarded. The first possibility would be the alkylation of the secondary alcohol, but primary alcohols are weak nucleophiles and could not compete with phenol anion which is a stronger nucleophile. The second possibility would be the alkylation of the nitrogen in the amide group. This possibility was immediately discarded, because the amide group is of very low nucleophilicity.

Figure 39: Compound 38.

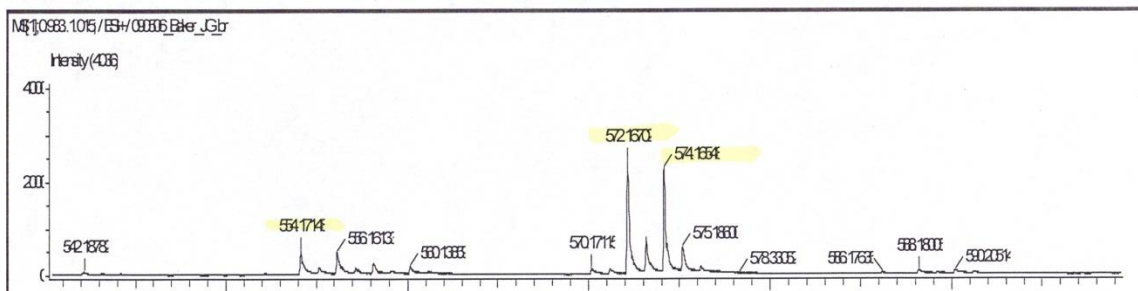
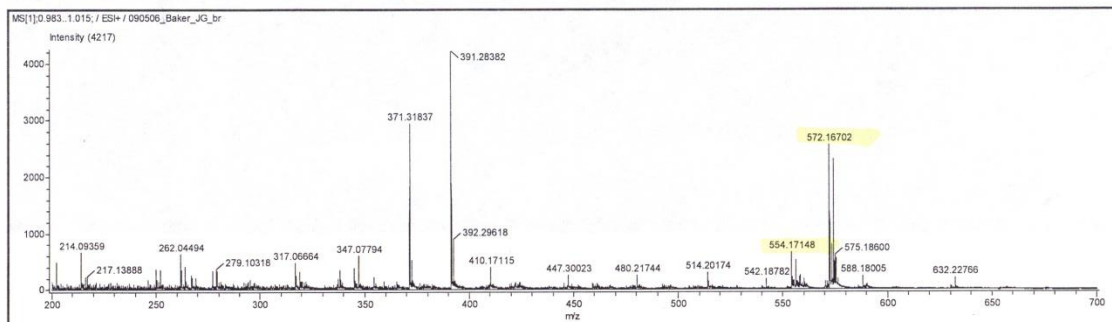
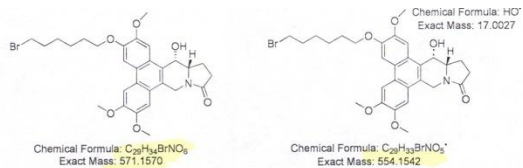


Figure 40: Mass spectrum of compound 38

5.3.2 Synthesis of (13a*S*,14*S*)-3-(6-azidohexyloxy)-14-hydroxy-2,6,7-trimethoxy-12,13,13a,14-tetrahydrobenzo[*f,h*]pyrrolo[1,2-*b*]isoquinolin-11(9*H*)-one (39)

The synthesis of product **39** was achieved by a displacement of the bromo group of **38** by an azido group. This simple transformation was a successful reaction that gave **39** in high yield and as a stable product.

The exact molecular weight of **39** was proved by AccuTOF–DART position-ion mode mass spectrometry. The exact mass was $[M] = 534.248$, and its experimental mass was found $[M+1]^+ = 535.253$, with an ion fragment $[M-OH]^+ = 517.237$, for which the theoretical fragment mass is $[M-OH]^+ = 517.245$. Neither the starting material **38** nor its ion fragments were present in the mass spectrum. The mass spectrum is shown in Figure 42.

The TLC plate of **39** had a smaller R_f than **38**. This smaller R_f was expected, since the brominated **38** is a little less polar than the azide **39** as seen on Figure 41.

Figure 41: R_f values for compound **38** and **39**.

The complete characterization was done by NMR spectroscopy. The product **39** was proved by using 1D, 2D (gCOSY, gHSQC, and NOESY). All the correlations and chemical shifts were found in the expected chemical shifts.

It was noticed that product **39** was highly stable under light, heat (40–50 °C), solvents, and air. It was easy to be detected under UV light and could be purified by silica gel column chromatography, with the solvent system 2:1:0.5 CHCl₃:EtOAc:MeOH. The solvent system needed EtOAc to slow the column to separate any small traces of DMF solvent that high vacuum could not evaporate.

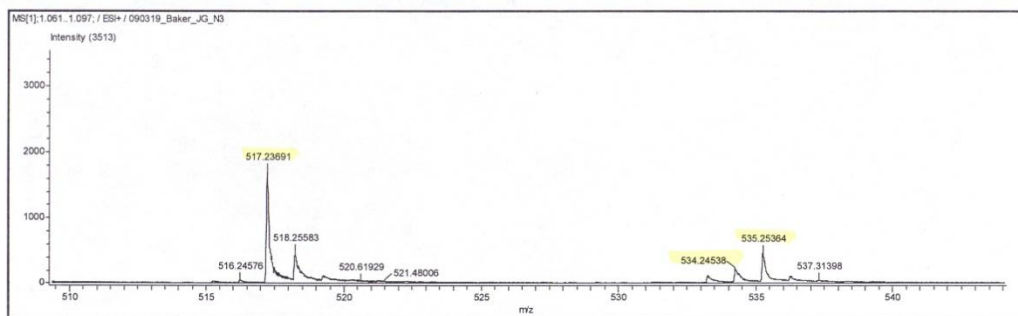
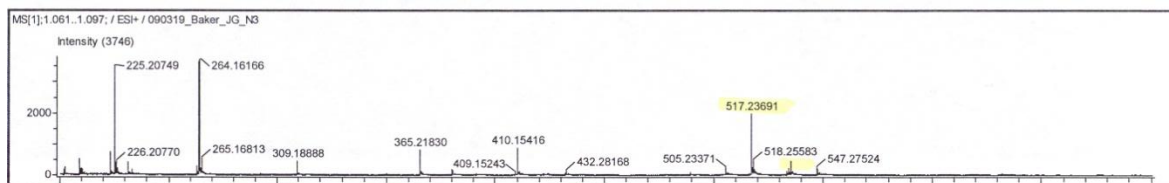
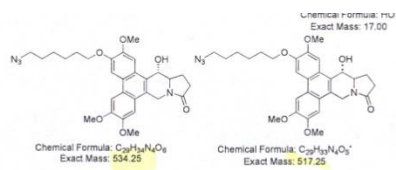


Figure 42: Mass spectrum of compound 39.

5.3.3 Synthesis of (13a*S*,14*S*)-3-(6-aminohexyloxy)-2,6,7-trimethoxy-9,11,12,13,13a,14-hexahydrodibenzo[*f,h*]pyrrolo[1,2-*b*]isoquinolin-14-ol (**40**)

The synthesis of **40** was performed by reduction of the azide and lactam group from the intermediate **39** with 2 equivalents of LiAlH₄. The double reduction reaction transformed the azide into a primary amine and reduced the cyclic amide group or lactam into a tertiary amine. In order to verify the product **40**, the following tests were done:

1. Ninhydrin stain test: This functional group-selective ninhydrin was used to detect the presence of a primary amine on TLC chromatography, which showed a positive result with a big and strong purple-blue spot that stained almost immediately at the bottom of the TLC plate (after heating with a heat gun). A separate TLC plate was stained with anisaldehyde–H₂SO₄ to detect any presence of starting material **39**. No starting material or side-product was found on TLC. Primary aliphatic amines bind strongly to silica gel, so primary amines would not be expected to migrate on silica gel TLC; therefore, the primary amine compound stayed at the bottom. This test also showed positive, because the purple stain spot was at the base of the silica gel plate. A representative picture of TLC plate of starting material **39** with $R_f = 0.25$ on anisaldehyde, and product **40** with $R_f = 0$ on ninhydrin is shown in Figure 43.

Figure 43: R_f values for **39 and **40**.**

2. Mass spectrometry: The molecular weight was determined using AccuTOF–DART in the positive-ion mode. The exact mass of **40** with addition of H⁺ was

$[M+1]^+ = 494.278$. This protonated product and ion fragment $[M-OH]^+ = 477.275$ were detected as high-intensity peaks on mass spectrometry, as shown in Figure 45.

The following Table 12 shows the theoretical mass calculation and experimental mass detected on AccuTOF DART positive-ion mode for the $[M+1]^+$ and $[M-OH]^+$.

Table 12: Compound 40 theoretical and experimental mass

Product/fragment	Theoretical mass	Experimental mass
$[M+1]^+$	495.278	495.279
$[M-OH]^+$	477.275	477.271

The following structures, Figure 44, represent **40** as product $[M]$, and its ion fragment $[M-OH]^+$ found on mass spectroscopy.

Figure 44: Molecular weight and fragment ion for compound 40.

It is important to indicate that no starting material **39** $[M+1]^+ = 535.248$ or its ion fragment $[M-OH]^+ = 517.25$ were detected on mass spectrometry.

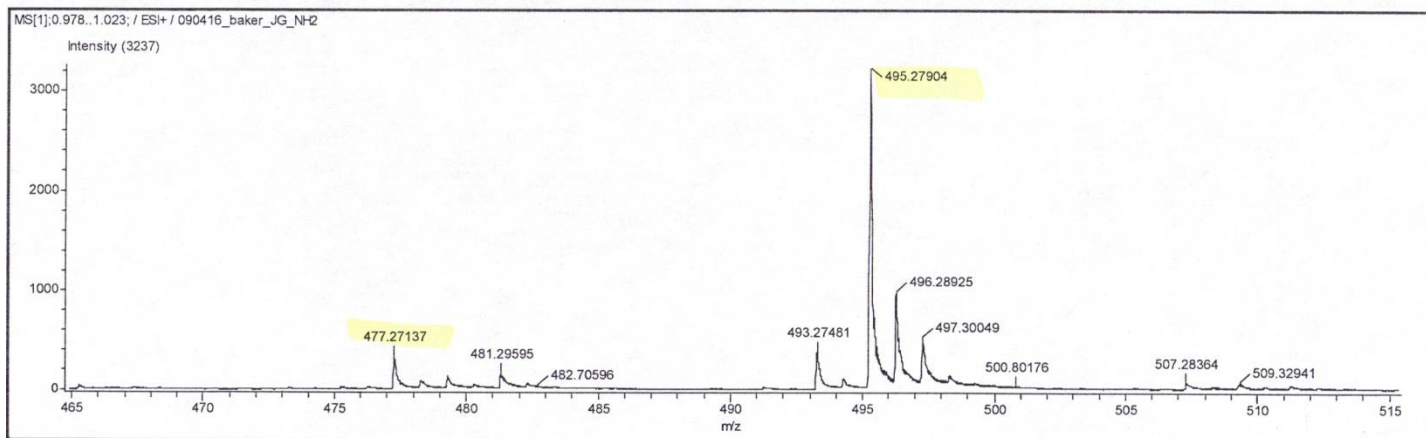
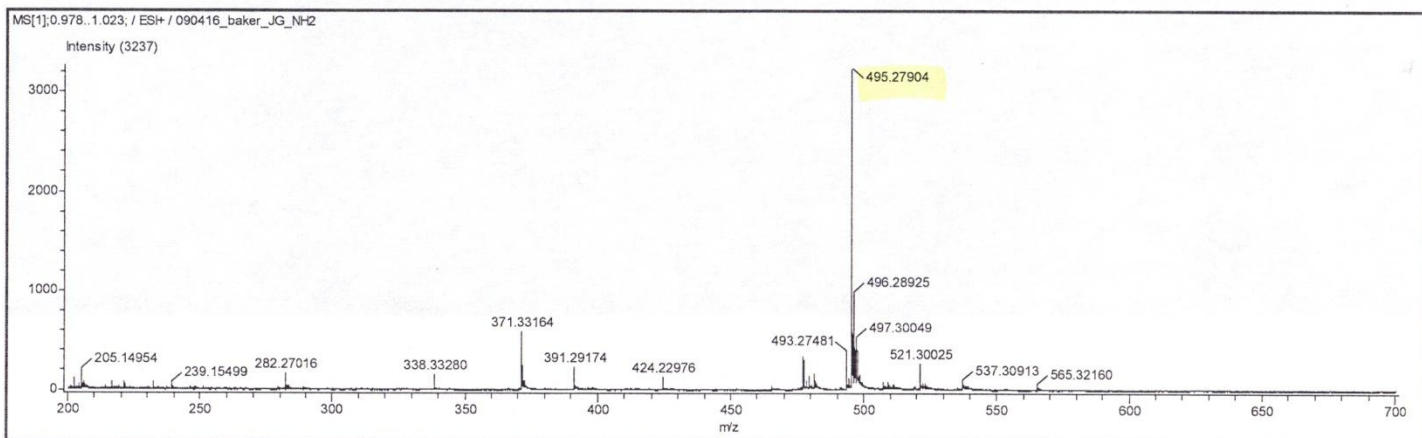
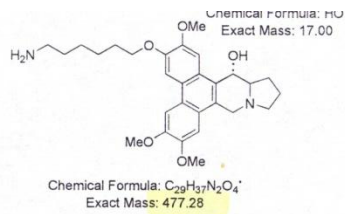
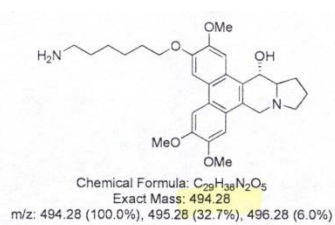


Figure 45: Mass spectrum of compound 40.

3. HPLC: The HPLC showed a fairly clean crude product with a major peak with high intensity that represented the product.

Unfortunately, this product was highly sensitive to heat and unstable. It was noticed that during vacuum evaporation the product decomposed at 35 °C, turning from a yellowish solution to a brownish oily product. Therefore, the solvent had to be removed using vacuum evaporation at room temperature. This product seemed to decompose after few hours of being made. It is known by experience that after overnight in the vacuum pump the product would not show the same high intensity peaks on the Accutof-DART positive-ion mode, and the intensity of the ninhydrin spot did not have the same strong purple stain. Under these circumstances, this amine had to be directly used for the next reaction without any purification.

Changing the conditions for the reduction reaction were tried in order to improve the yield and quality of product.

1. The molecular equivalents of LiAlH_4 were reduced, since the reduction required only two molecular equivalents of LiAlH_4 to reduce the azide and lactam group, only 25% of the LiAlH_4 was taken out to reduce the azide and lactam group, but the reaction still showed presence of starting material.

2. The duration of the reaction was reduced from overnight to six and three hours respectively, in different reactions, but the same sensitive product always resulted.

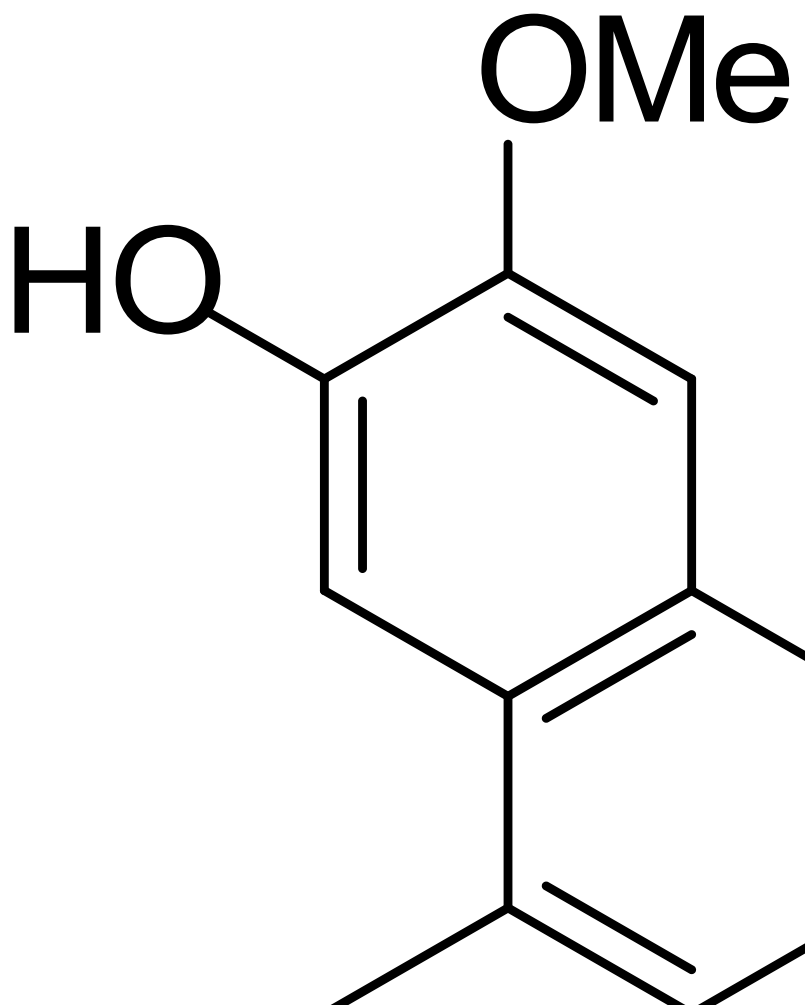
Then, three different quenching methods were used to improve the stability of the product:

1. EtOAc and 2 N HCl: Ethyl acetate is known to quench LiAlH_4 at -10 °C, but addition of 2 N HCl gave lower yield, because it probably protonated the primary amine transforming into an aminium group (), which during organic/aqueous extraction went to the aqueous phase.

2. EtOAc and $\text{Na}_2\text{SO}_4 \cdot 10\text{H}_2\text{O}$: Addition of $\text{Na}_2\text{SO}_4 \cdot 10\text{H}_2\text{O}$ gave a better yield than the previous method (EtOAc and 2 N HCl), but four hours were required to decompose the LiAlH_4 , because with any extended time in EtOAc the solution and product would decompose. An overnight quenching was expected to lower the yield.

3. EtOAc and 3 M NaOH: Addition of 3 M NaOH gave the highest yield, but the amine was still sensitive to heat and decomposed upon standing in solution.

Under these circumstances, the possibility to eliminate a reduction reaction using LiAlH_4 in the reaction pathway was analyzed. Therefore, the following route was applied (see Scheme 35).



Scheme 35: Alternative route to obtain 44.

In order to eliminate the reduction reaction of the azide group using LiAlH_4 , product **36** (DCB 3506) was used to successfully obtain **42** in an alkylation reaction. Then, a transformation reaction from Br to N_3 was also carried out in high yield. The reduction of the azido group was achieved using hydrogenation under pressure (50 psi) using two different catalysts: Pd-C or PtO_2 (Adams' catalyst). Unfortunately, product **44**

was still as sensitive and unstable as **40**. Therefore, the next step had to be carried out without purification.

5.3.4 Synthesis of *N*-(6-((13a*S*,14*S*-14-hydroxy-2,6,7-trimethoxy-9,11,12,13,13a,14-hexahydrodibenzo[*f,h*]pyrrolo[1,2-*b*]isoquinolin-3-yloxy)hexyl)-5-((3a*S*,4a*S*,6a*R*)-2-oxohexahydro-1*H*-thieno[3,4-*c*]imidazol-4-yl)pentanamide (41)

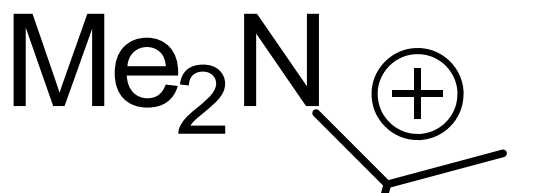
In order to link biotin via a peptide bond to the primary amine **40**, (HATU) or (HBTU) (see Figure 46) was used as a coupling reagent. Both of these coupling reagents were chosen because either was successful for generating the peptide bond. Other coupling reagents were tried, such as DCC (1,3-dicyclohexylcarbodiimide), DIC (diisopropylcarbodiimide), and EDC (ethyl(dimethylamino)propylcarbodiimide), but these were either unsuccessful or gave the product in low yield.

Figure 46: Chemical structure for HBTU, DCC, DIC, and EDC.

The carbodiimide activated ester is very reactive. In the case of slowly reacting nucleophiles, rearrangement is a common side reaction, which might have formed the stable acyl urea (see Scheme 36). Since the coupling reagent was left stirring overnight with biotin, this could be the reason for the unsuccessful reactions using DCC, DIC, and EDC. Later it was found that this problem could be avoided by adding HOBt.

Scheme 36: The carbodiimide activated ester rearrangement.

There exists a large number of coupling reagents, but two are more popular, HBTU and HATU. These analogous compound HATU and HBTU were used to form the peptide bond. The following reactions represent the mechanism reaction to obtain **41** in either case (see Scheme 37 and 38)



Scheme 37: Mechanism using HATU.



Scheme 38: Mechanism using HBTU.

Mass spectrometry:

1. AccuTOF-DART in either the positive- or negative-ion mode did not detect **41**. This is expected due to the high molecular mass $M = 720.356$ and the presence of biotin. Starting material **40** was not detected either.
2. Quatro II spectrometer: The Waters Quattro II is a triple quadrupole mass spectrometer. The Quattro II is equipped with an electrospray-ionization (ESI) source and an atmospheric pressure chemical ionization (APCI) source. It is integrated with an Agilent 1050 HPLC system. The Quattro II detected the **41** mass $[M+1]^+ = 721.214$ and its ion fragment $[M-OH]^+ = 703.191$ with high intensity, as seen in Figure 47. Although, it is known that the Quattro II does not provide high-resolution MS, it showed the expected $[M+1]$ ion.
3. MALDI-TOF MS: This instrument provided high-resolution, and the peaks could be calibrated with an internal calibration standard. MALDI detected the $[M] = 720.3385$ and sodium adduct $[M + Na]^+ = 743.3406$ with a ppm error of 6.7 ppm (see Figure 48), and 2.6 ppm (see Figure 49) on different occasions. According to our instrument specifications; the limit of error for the MALDI-TOF MS should not be higher than 10 ppm.

It is important to indicate that these spectra show higher peaks at 795.5387, 853.5866, 911.6284, 969.6696 that belonged to the internal calibration standard that was mixed with **41** in order to calibrate the peaks.

Table 13 shows the summary of molecular masses for the theoretical and experimental results.

The ppm error was calculated with the following formula given by the mass spectroscopy center.

Mass Accuracy

$$\Delta m = m_{\text{theoretical}} - m_{\text{measured}}$$

$$\text{ppm Error} = (\Delta m / m_{\text{theoretical}}) \times 10^6$$

Example:

$$\Delta m = 743.345 - 743.347 = 0.002$$

$$\text{ppm Error} = (0.002 / 743.345) \times 10^6 = 2.690$$

Table 13: Theoretical and experimental mass for compound 40

Product 41	Theoretical mass (<i>m/z</i>)	Experimental mass (<i>m/z</i>)
[M]	720.356	720.338
[M – OH] ⁺	703.353	703.343
[M + Na] ⁺	743.345	743.347

The crude product **41** was run on the HPLC using a reversed-phase column (C18). This separation indicated the number byproducts and starting materials in the crude product. Since the HPLC spectrum indicated at least 7 peaks, a precipitation of the pure product was tried using MeOH:Et₂O (10:1). A yellowish solid precipitated overnight in the freezer. This solid was run in the HPLC using the method Tylo 79:21 (79% MeOH and 21% H₂O) that demonstrated the best separation of peaks. The HPLC results showed 6 peaks (see Figure 50). Since it is a novel compound, the author did not know which peak belonged to product **41**. In order to solve this problem, a HPLC–MS separation was used (using the same separation method Tylo 79:21 and reversed-phase column (C18) to find which peak belonged to product **41**. Product **41** was the fifth peak that came out from 4.06 to 5.08 minutes (see Figure 51), with molecular weight $[M+1]^+ = 721.13$. Using these important results, the next step will be used a Biotage instrument with reversed-phase column to separate the product **41**.

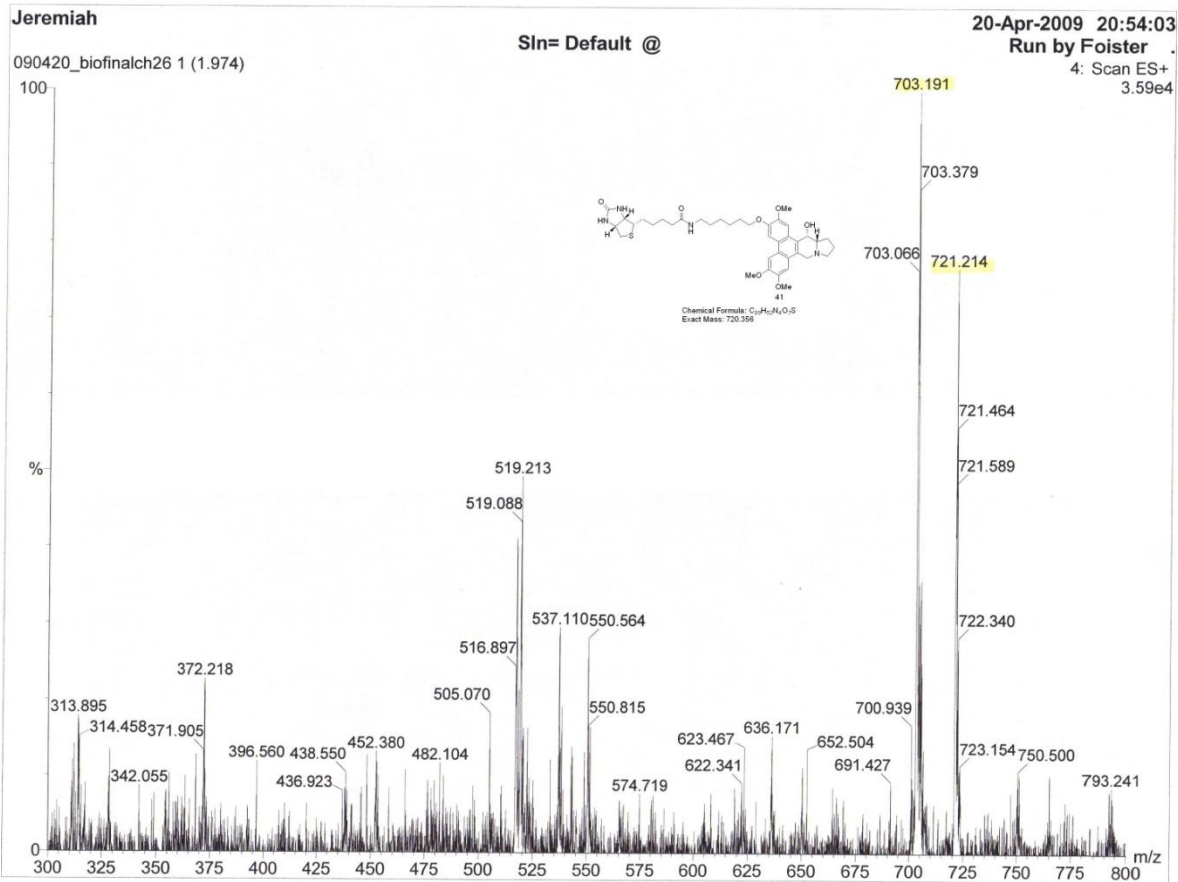


Figure 47: QUATRO II mass spectrum for compound 41.

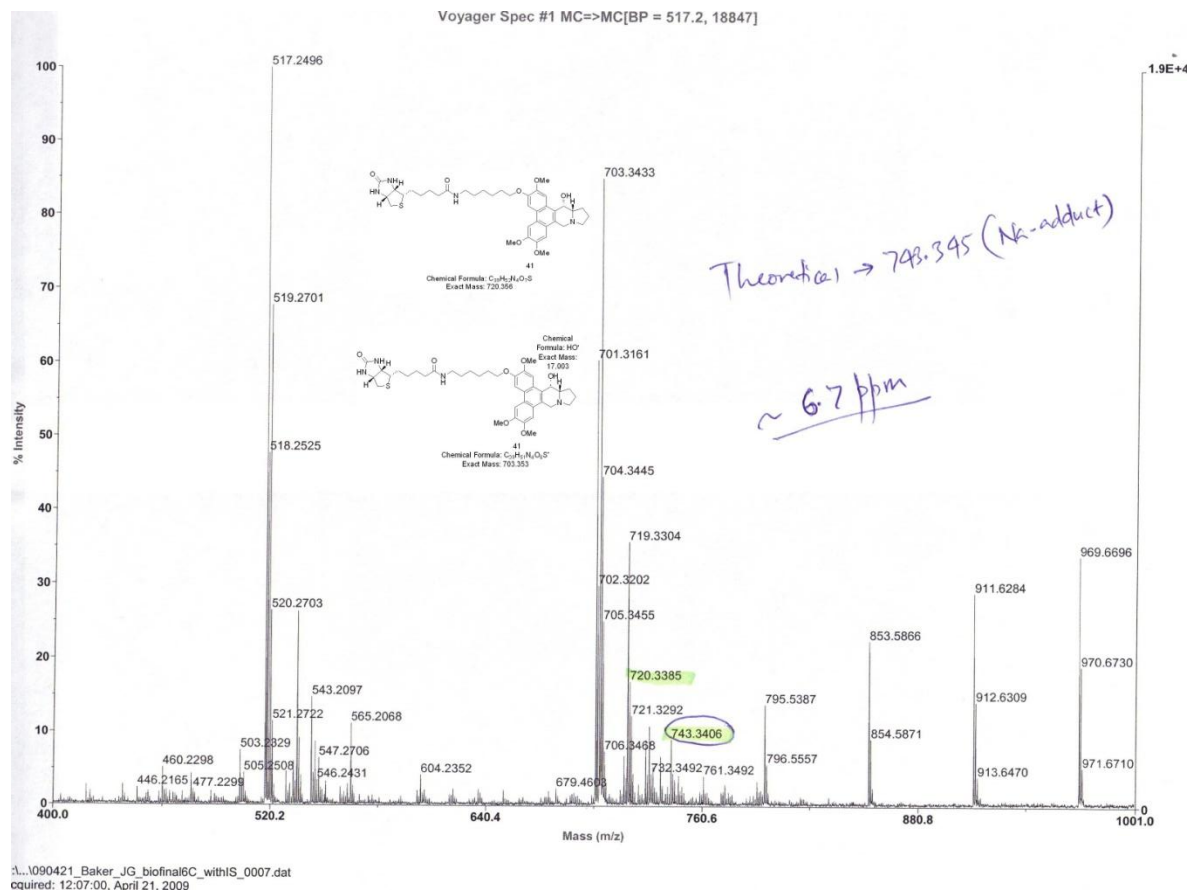
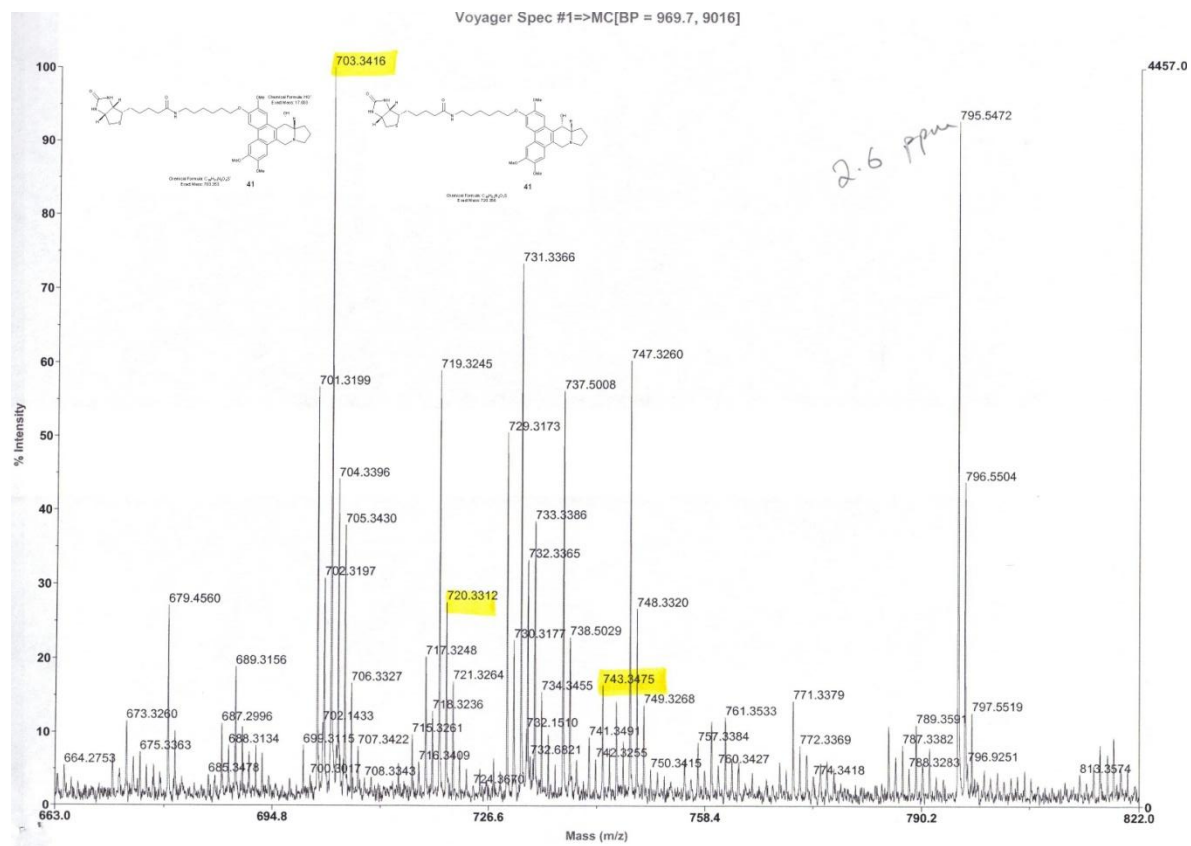
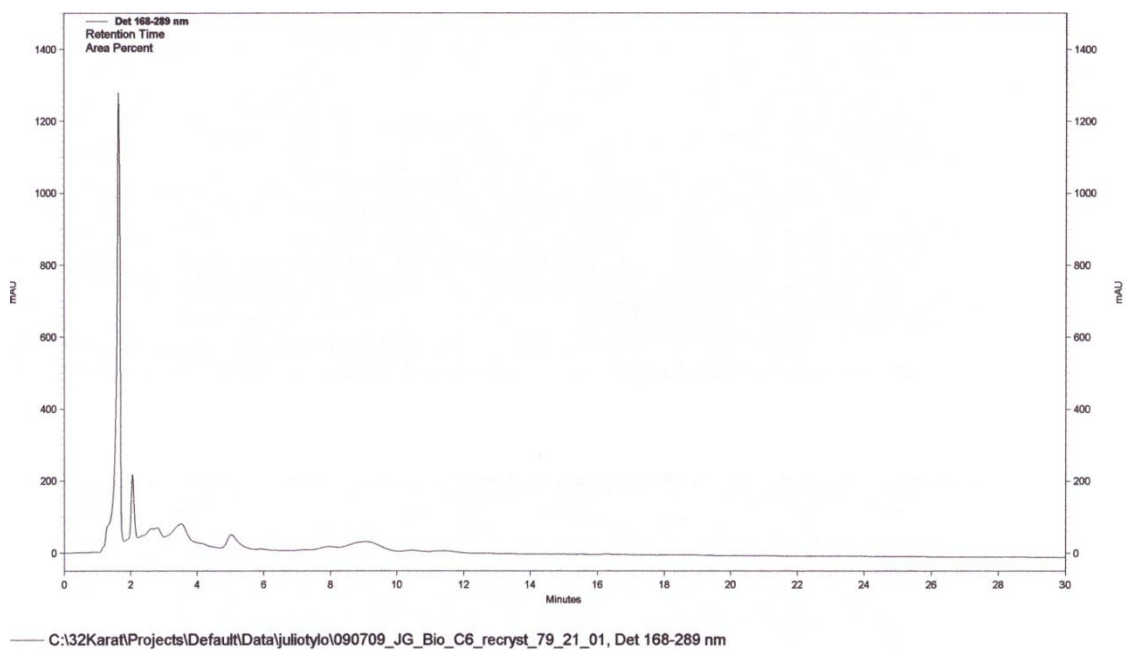


Figure 48: MALDI mass spectrum with 6.7 ppm error for compound 41.



H:_090423_JG_BIOfinal6C_SM_2_andmatrixandISTD_0001.dat
 acquired: 11:25:00, April 23, 2009

Figure 49: MALDI mass spectrum with 2.6 ppm error for compound 41.



*Vial 1
(MeOH)
w compound*

Figure 50: HPLC results for compound 41 with method 79:21 (MeOH:H₂O).

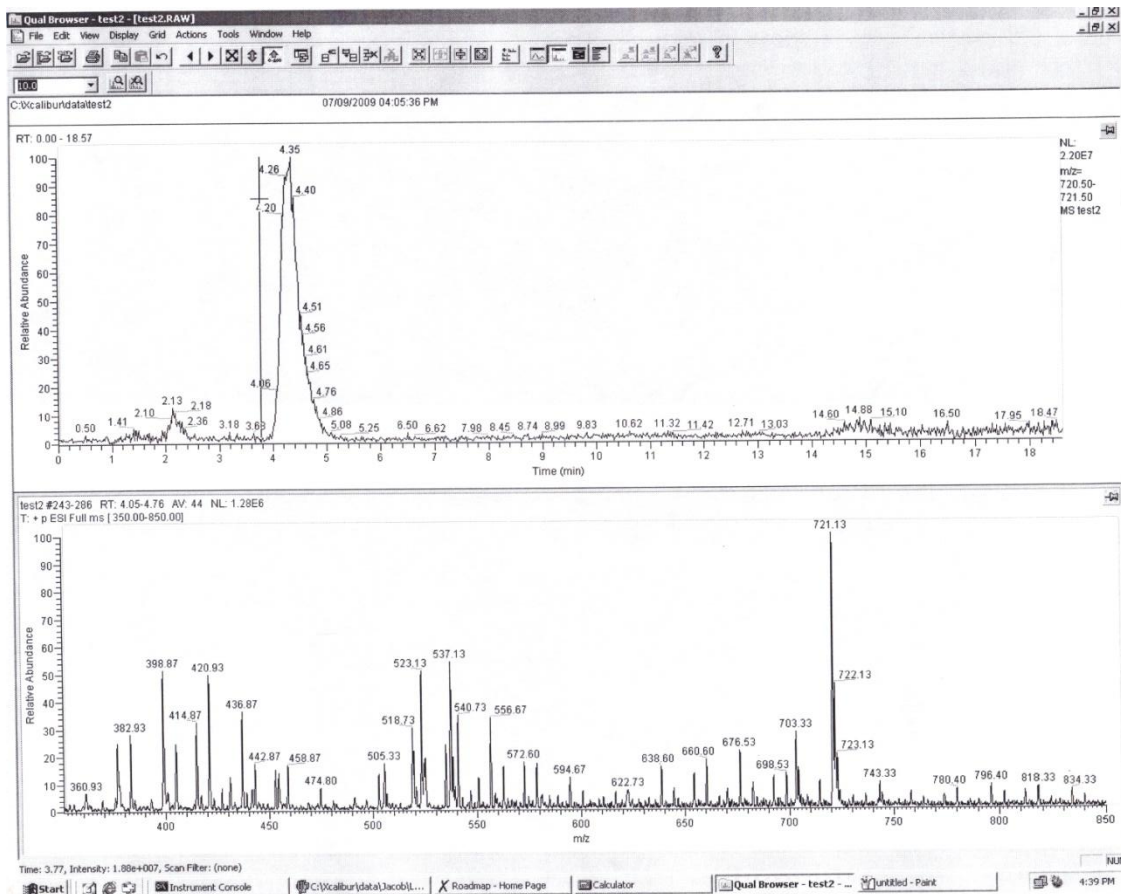


Figure 51: HPLC–mass spectrometer results for compound 41.

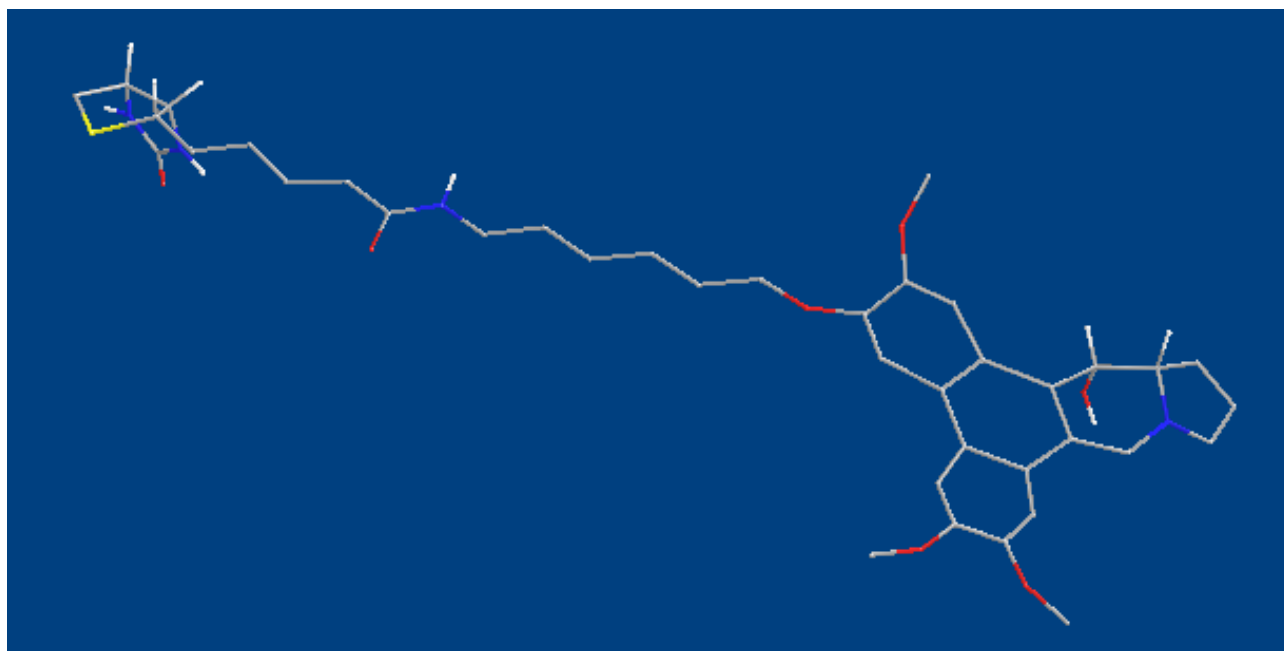


Figure 52: Molecular modeling of the structure for compound 41.

CHAPTER 6: Evaluation of the Tylophorine Analogs in the National Cancer Institute's screen.

6.1 Statement of Problem

The goal was to have the National Cancer Institute evaluate synthetic analogs to DCB 3503 in their 60-cell line panel of human-derived cancer cells. Structure–activity relationships, which are important in rational design of analogs, are expected to emerge.

6.2. Background.

6.2.1. Screening

The Developmental Therapeutics Program (DTP) of the National Cancer Institute (NCI) conducts a screening program *in vitro* and *in vivo* for potential anti-cancer compounds. The main purpose of this project is to identify and evaluate novel chemical compounds and to define, to a limited extent, their mechanism of action.

6.2.2. In Vitro testing cells

The In Vitro Cell Line Screening Project (IVCLSP) was developed in 1990 at the NCI. This project routinely screens 60 different human tumor cell lines with subpanels that include the following: lung cancer, colon cancer, breast cancer, ovarian cancer, leukemia, renal cancer, melanoma, prostate cancer, and CNS cancer (central nervous system). The goal was to evaluate synthetic compounds or natural product samples to observe any selective growth inhibition or cell killing for any tumor cell indicated above.

The biological results are represented by algorithms, which can be indicative of certain mechanisms of action from a test compound. These algorithms could indicate a range of compounds that might interact with specific molecular targets. Analysis of this data can be performed by a program called COMPARE.

6.2.3. Concentrations parameters

The NCI used these parameters: GI_{50} , TGI, and LC_{50} mainly as algorithms to represent the results from each cancer cell screened.

GI_{50} : These data represent the drug sensitivity. In other words, GI_{50} indicates the concentrations required to inhibit cancer cell growth by 50%. The GI_{50} is a measure of the growth inhibitory power of the test agent.

TGI: These data signify the cytostatic effect. In other words, TGI is a measure of the suppression of cellular growth or multiplication.

LC50: These data indicate the lethal concentration that kills cancer cells by 50%.

6.2.4 The Mean Graph

The mean graph represents the *in vitro* results that emphasize differential results on various tumor cell lines.

The mean graph plots the positive and negative results from a set of GI₅₀, TGI, and LC₅₀ values. The vertical line represents the mean response of the cell lines. Positive and negative results are plotted along the vertical line. Results on the right represent cellular sensitivities of the cell that exceed the mean. Results on the left represent cell line sensitivities of the cell less than the average value.

6.3 DCB 3503 cytotoxic analysis and structure–activity relationships

Evaluation of DCB 3503 in the National Cancer Institute’s tumor screen showed a uniform and potent inhibition of cell growth in all 60 cell lines (GI₅₀ ~ 10⁻⁸ M) as seen in Figures 51 and 53, with notable selectivity toward several refractory cell lines, including melanoma and colon cancer cell lines based on GI₅₀ values.

The overall activity of DCB 3503 can be seen in Figure 50. DCB 3503 dose–response curves (all cell lines) showed a concise drop for all cancer cells at 10⁻⁰⁸ M. The direction of that curve is important, because it indicates that almost all cancer cells were inhibited to 50% growth at 10⁻⁰⁸ M. It is important to indicate that DCB 3503 has the lowest GI₅₀ among all our DCB analogs; therefore, it holds the highest activity. The following Table 14 shows some of the relevant cancer cell lines that were inhibited by DCB 3503. The complete table can be seen in Figures 53, 54, 55, and 56.

Table 14: DCB 3503 some relevant cell line and growth percent

Panel/Cell Line	GI ₅₀ (E ⁻⁰⁸)
Colon Cancer (COLO 205)	1.00
Renal Cancer (786-0)	1.00
Melanoma (SK-MEL-2)	1.00
Melanoma (SK-MEL-5)	1.00

Additionally, Dr. Gao did additional biological testing of DCB 3503 at Yale University. DCB 3503 also exerted potent growth-inhibitory effects against HepG2

(human hepatocellular carcinoma) and KB (human nasopharyngeal carcinoma) cell line's.³

Treatment of nude mice bearing HepG2 tumor xenografts by i.p. injections of DCB 3503 at 6 mg/kg every 8 h on days 0 and 3 resulted in significant tumor growth suppression ($P < 0.0001$). Unlike conventional antitumor drugs, 3 μM DCB 3503 did not cause DNA breaks or apoptosis in HepG2 cells.

This tylophorine analog is a member of a unique class of antitumor compounds that have a mode of action different from known antitumor drugs. Early mechanistic studies demonstrated that tylophorine analogs irreversibly inhibit protein synthesis at the elongation stage of the translation cycle. The phenanthroindolizidine alkaloids tylophorine have been shown to be powerful inhibitors of the incorporation of leucine into protein in Ehrlich ascites-tumor cells (a transplantable, poorly differentiated malignant tumor which appeared originally as a spontaneous breast carcinoma in mice. It grows in both solid and ascitic forms by 50% at 10^{-6} M, but does not inhibit the incorporation of uracil into nucleic acids at 10^{-5} M.⁶

In 1960, tylocrebine was advanced to clinical trial but failed due to its significant CNS toxicity, manifested as disorientation and ataxia. Dr. Staerk proposed to synthesize more polar analogs that could minimize the side effects, because these polar analogs would not pass through the blood–brain barrier. Therefore, DCB 3503 is an excellent candidate to overcome this problem, because it contains a secondary alcohol at C14, which provides polarity (see Figure 53).

Figure 53: Structures of tylophorine, tylocrebine, and DCB 3503.

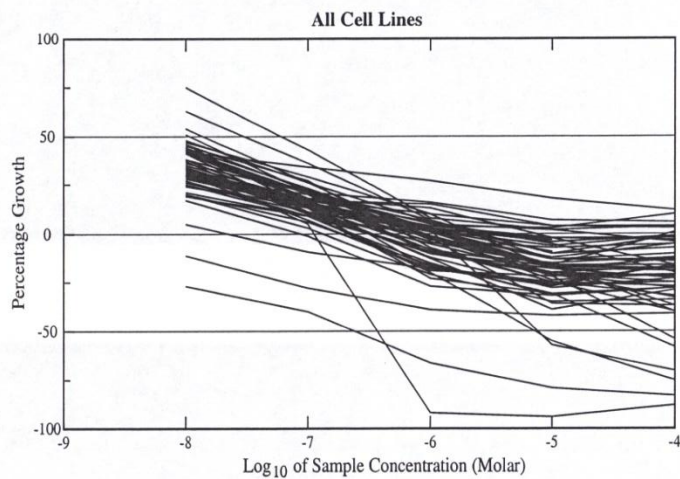


Figure 54: DCB 3503 mean graph.

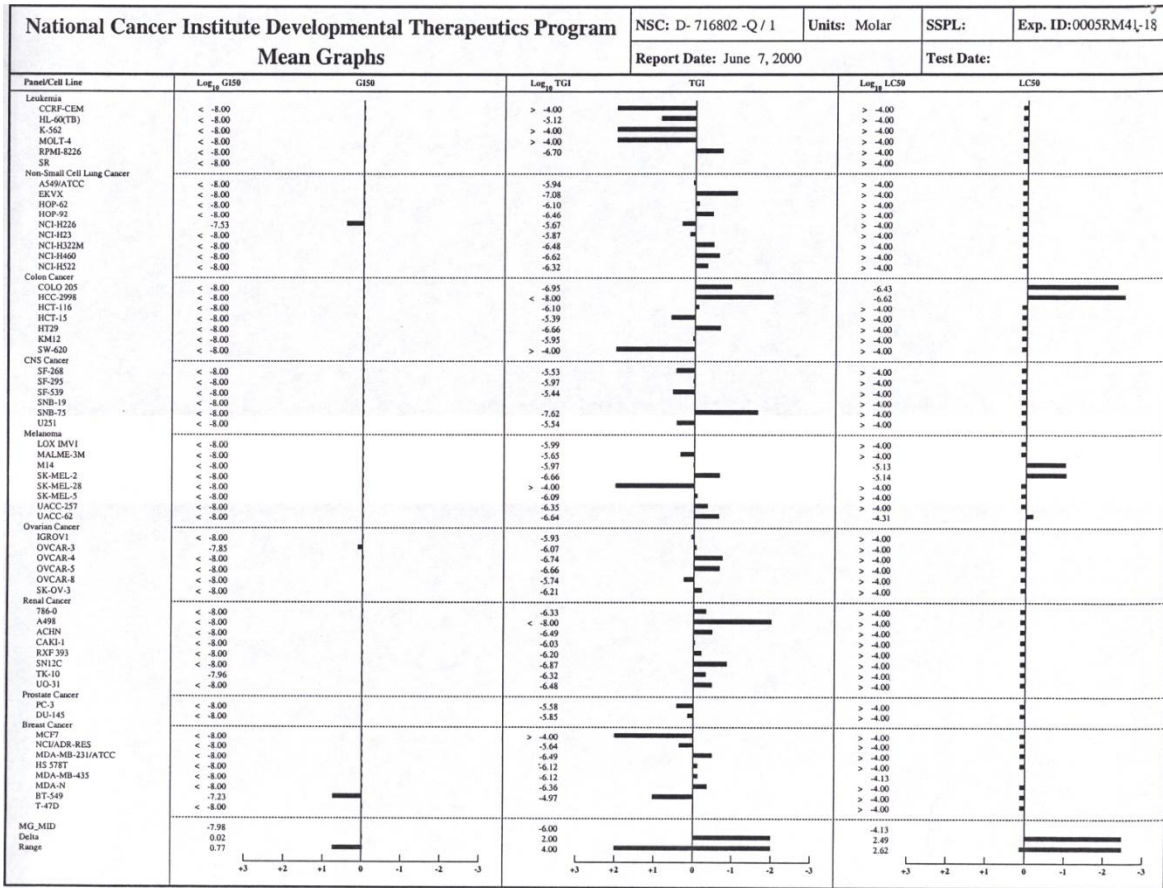


Figure 55: DCB 3503 dose-response curves (all cell lines).

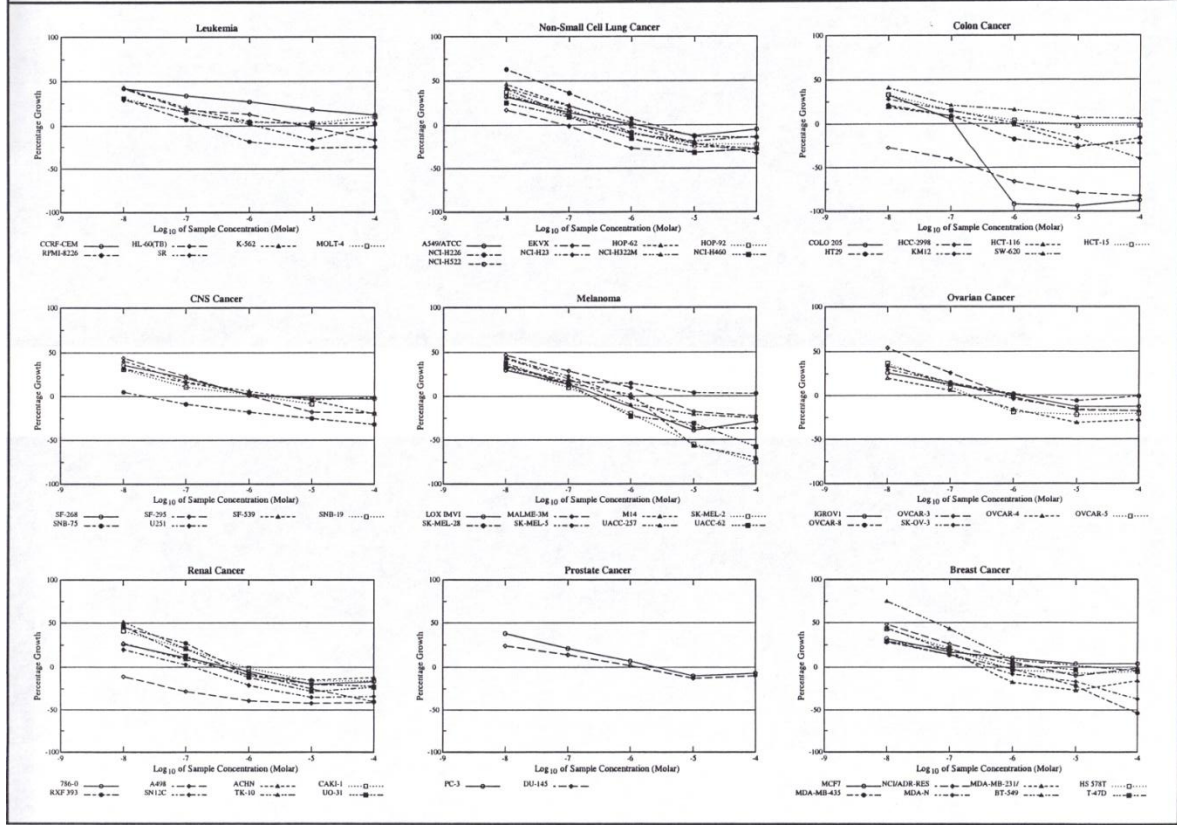


Figure 56: DC B 35 03 dose response curves (by cell line).

National Cancer Institute Developmental Therapeutics Program			
In-Vitro Testing Results			
NSC: D-716802-Q/1	Experiment ID: 0005RM41-18	Test Type: 08	Units: Molar
Report Date: June 7, 2000	Test Date:	QNS:	MC:
COMI:	Stain Reagent: SRB Dual-Pass	SSPL:	

Panel/Cell Line	Time Zero	Log10 Concentration								GI50	TGI	LC50			
		Ctrl	-8.0	-7.0	-6.0	-5.0	-4.0	-3.0	-2.0				-1.0		
Leukemia															
CCRF-CEM	0.102	0.498	0.267	0.238	0.208	0.173	0.151	42	34	27	18	12	<1.00E-08	>1.00E-04	>1.00E-04
HL-60(TB)	0.443	2.116	1.150	0.741	0.667	0.435	0.371	42	18	13	-2	-16	<1.00E-08	7.60E-06	>1.00E-04
K-562	0.294	1.827	0.946	0.595	0.378	0.324	0.361	43	20	5	2	4	<1.00E-08	>1.00E-04	>1.00E-04
MOLT-4	0.198	1.046	0.459	0.326	0.231	0.226	0.287	31	15	4	3	10	<1.00E-08	>1.00E-04	>1.00E-04
RPMI-8226	0.543	1.861	0.939	0.642	0.447	0.403	0.408	30	7	-18	-26	-25	<1.00E-08	1.98E-07	>1.00E-04
SR	0.211	1.261	0.513	0.382	0.229	0.178	0.219	29	16	2	-16	1	<1.00E-08	.	>1.00E-04
Non-Small Cell Lung Cancer															
A549/ATCC	0.422	1.842	0.879	0.624	0.432	0.372	0.401	32	14	1	-12	-5	<1.00E-08	1.14E-06	>1.00E-04
EKVX	0.342	0.674	0.400	0.337	0.251	0.231	0.246	17	-1	-27	-32	-28	<1.00E-08	8.37E-08	>1.00E-04
HOP-62	0.542	1.413	0.939	0.733	0.529	0.430	0.388	46	22	-2	-21	-28	<1.00E-08	7.97E-07	>1.00E-04
HOP-92	0.533	1.953	0.690	0.575	0.488	0.420	0.416	37	10	-9	-21	-22	<1.00E-08	3.46E-07	>1.00E-04
NCI-H226	0.645	1.092	0.925	0.805	0.675	0.561	0.554	63	36	7	-13	-14	2.95E-08	2.16E-06	>1.00E-04
NCI-H23	0.379	1.321	0.771	0.581	0.409	0.301	0.256	42	21	3	-21	-33	<1.00E-08	1.36E-06	>1.00E-04
NCI-H322M	0.336	0.995	0.605	0.409	0.302	0.276	0.294	41	11	-10	-18	-13	<1.00E-08	3.32E-07	>1.00E-04
NCI-H460	0.369	2.049	0.790	0.521	0.314	0.260	0.266	25	9	-15	-32	-28	<1.00E-08	2.39E-07	>1.00E-04
NCI-H522	0.347	0.948	0.547	0.451	0.319	0.252	0.254	33	17	-8	-25	-27	<1.00E-08	4.77E-07	>1.00E-04
Colon Cancer															
COLO 205	0.467	1.805	0.909	0.528	0.039	0.027	0.055	33	5	-92	-94	-88	<1.00E-08	1.12E-07	3.69E-07
HCC-2998	0.379	0.508	0.276	0.228	0.127	0.081	0.066	-27	-40	-66	-79	-83	<1.00E-08	<1.00E-08	2.41E-07
HCT-116	0.164	1.107	0.344	0.245	0.163	0.124	0.130	19	9	-1	-24	-21	<1.00E-08	8.00E-07	>1.00E-04
HCT-15	0.247	1.732	0.737	0.475	0.304	0.241	0.243	33	15	4	-2	-2	<1.00E-08	4.08E-06	>1.00E-04
HT29	0.218	1.266	0.434	0.313	0.181	0.161	0.183	21	9	-17	-26	-16	<1.00E-08	2.21E-07	>1.00E-04
KM12	0.327	1.474	0.648	0.504	0.337	0.274	0.196	28	15	1	-16	-40	<1.00E-08	1.12E-06	>1.00E-04
SW-620	0.189	1.273	0.631	0.414	0.361	0.268	0.257	41	21	16	7	6	<1.00E-08	>1.00E-04	>1.00E-04
CNS Cancer															
SF-268	0.260	0.943	0.509	0.401	0.271	0.256	0.251	36	21	2	-2	-3	<1.00E-08	2.95E-06	>1.00E-04
SF-295	0.661	2.074	1.281	0.988	0.670	0.544	0.537	44	23	1	-18	-19	<1.00E-08	1.08E-06	>1.00E-04
SF-539	0.260	1.049	0.581	0.391	0.310	0.247	0.207	41	17	6	-5	-20	<1.00E-08	3.60E-06	>1.00E-04
SNB-19	0.295	0.964	0.501	0.368	0.307	0.268	0.298	31	11	2	-9	.	<1.00E-08	.	>1.00E-04
SNB-75	0.649	0.884	0.662	0.593	0.532	0.489	0.445	5	-9	-18	-25	-32	<1.00E-08	2.39E-08	>1.00E-04
U251	0.283	1.365	0.626	0.461	0.320	0.272	0.280	32	16	3	-4	-1	<1.00E-08	2.86E-06	>1.00E-04
Melanoma															
LOX IMVI	0.271	1.686	0.690	0.465	0.278	0.166	0.193	30	14	.	-39	-29	<1.00E-08	1.03E-06	>1.00E-04
MALME-3M	0.451	0.956	0.691	0.598	0.501	0.371	0.348	47	29	10	-18	-23	<1.00E-08	2.26E-06	>1.00E-04
M14	0.263	0.994	0.509	0.370	0.274	0.112	0.080	34	15	2	-57	-70	<1.00E-08	1.06E-06	7.48E-06
SK-MEL-2	0.803	1.794	1.134	0.907	0.640	0.363	0.204	33	10	-20	-55	-75	<1.00E-08	2.19E-07	7.24E-06
SK-MEL-28	0.428	1.258	0.718	0.573	0.557	0.461	0.455	35	17	15	4	3	<1.00E-08	>1.00E-04	>1.00E-04
SK-MEL-5	0.538	2.624	1.448	1.018	0.527	0.347	0.342	44	23	-2	-36	-37	<1.00E-08	8.22E-07	>1.00E-04
UACC-257	0.582	1.397	0.930	0.743	0.522	0.460	0.436	43	20	-10	-21	-25	<1.00E-08	4.51E-07	>1.00E-04
UACC-62	0.718	1.801	1.125	0.858	0.554	0.492	0.299	38	13	-23	-31	-58	<1.00E-08	2.29E-07	4.87E-05
Ovarian Cancer															
IGROV1	0.172	0.771	0.326	0.249	0.178	0.149	0.151	26	13	1	-13	-13	<1.00E-08	1.17E-06	>1.00E-04

Figure

e 57: DCB 3503 in-vitro testing results.

6.4 DCB 3507 cytotoxic analysis and structure–activity relationships

Evaluation of DCB 3507 for the National Cancer Institute tumor screen showed a potent inhibition of cell growth in some of the cell lines with an overall $GI_{50} \sim 10^{-6}$ M, with notable selectivity toward several refractory cell lines in melanoma and renal cancer (see Table 15).

Table 15: DCB 3507 relevant cell line, GI_{50} , and growth percent

Panel/Cell Line	$GI_{50} E^{-06}$	Growth Percent
Colon Cancer (COLO 205)	1.12	-54.78
Renal Cancer (786-0)	3.58	-56.30
Melanoma (SK-MEL-2)	3.03	-54.67
Melanoma (SK-MEL-5)	1.07	-70.34

Even though DCB 3507 showed high activity, it has lower activity when compared to DCB 3503. DCB 3507 presented interesting activity with melanoma1 and renal cancer at $GI_{50} = 10^{-6}$ M, but DCB 3503 had a $GI_{50} = 10^{-08}$ M against the same tumor.

DCB 3507 clearly showed its lower activity in the graph: dose–response curves (all cell lines) in Figure 57, 58, 59, 60, and 61. These graphs indicated straight inactivity lines from 10^{-08} M until 10^{-06} M, only after 10^{-06} M inhibition of cancer cells start to grow by an overall drop of cell lines. Due to this lower activity any further analysis or modification for DCB 3507 has been terminated.

Although DCB 3507 had low reactivity, it gave positive and conclusive structure–activity relationship (SAR) results.

First: The DCB 3503 analog must have at least four methoxy groups to increase biological activity. The exact positions could be in R2, R3 for the top part of the phenanthrene ring, and R5,R6 or R6,R7 for the bottom part of the aromatic system as seen in Figure 58. The possibility to increase activity in R5, R6 analog instead of an analog substituted in the R6, R7 position was indicated by tylocrebine's high activity, because it had the methoxy groups in R5, R6 position. However, little is known about the precise mode of action of these compounds, and similar structures may not have similar modes of action, a point recently made in the study by Y.-C. Cheng and co-workers. So far, we had used methoxy groups, but it would be interesting to make ethoxy groups or long/short aliphatic chains with polar functional groups at the end

replacing methoxy groups to study their biological activities. Therefore, DCB 3508 has been synthesized.

It is likely that the ring's electron density affects the binding at the indolizidine system, which is more likely the pharmacophore.

It is important to indicate that all these biological data are investigation about potency, but these data gave limited information on any results any adverse effects. At this time, we do not know if DCB 3503 is more toxic in vivo or is able to produce more negative side effects in the human body than DCB 3507. Our main goal is both to increase potency and decrease adverse effects, such as addictive properties.

Figure 58: Tylophorine derivative with R substituents

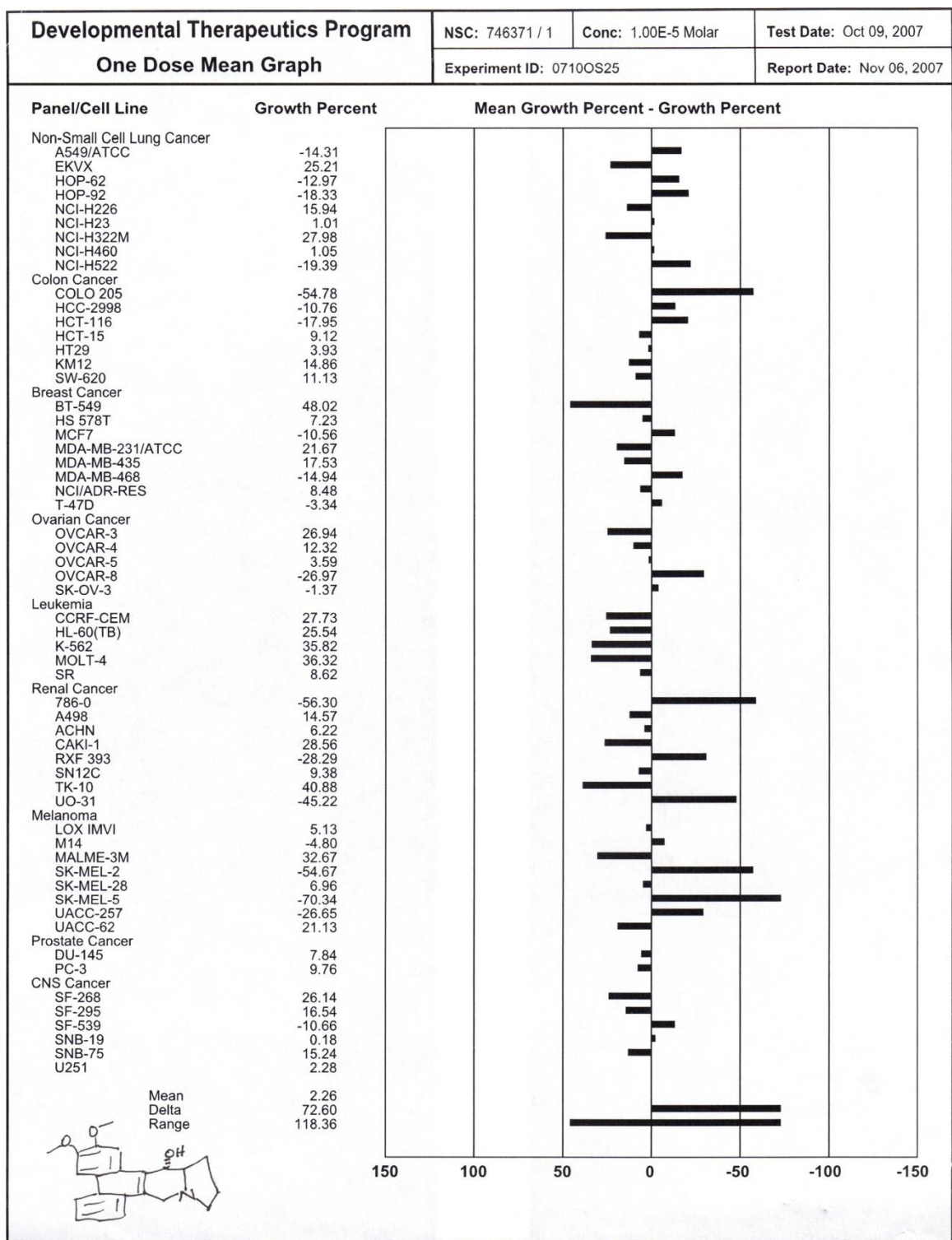


Figure 59: DCB 3507 One-dose mean graph.

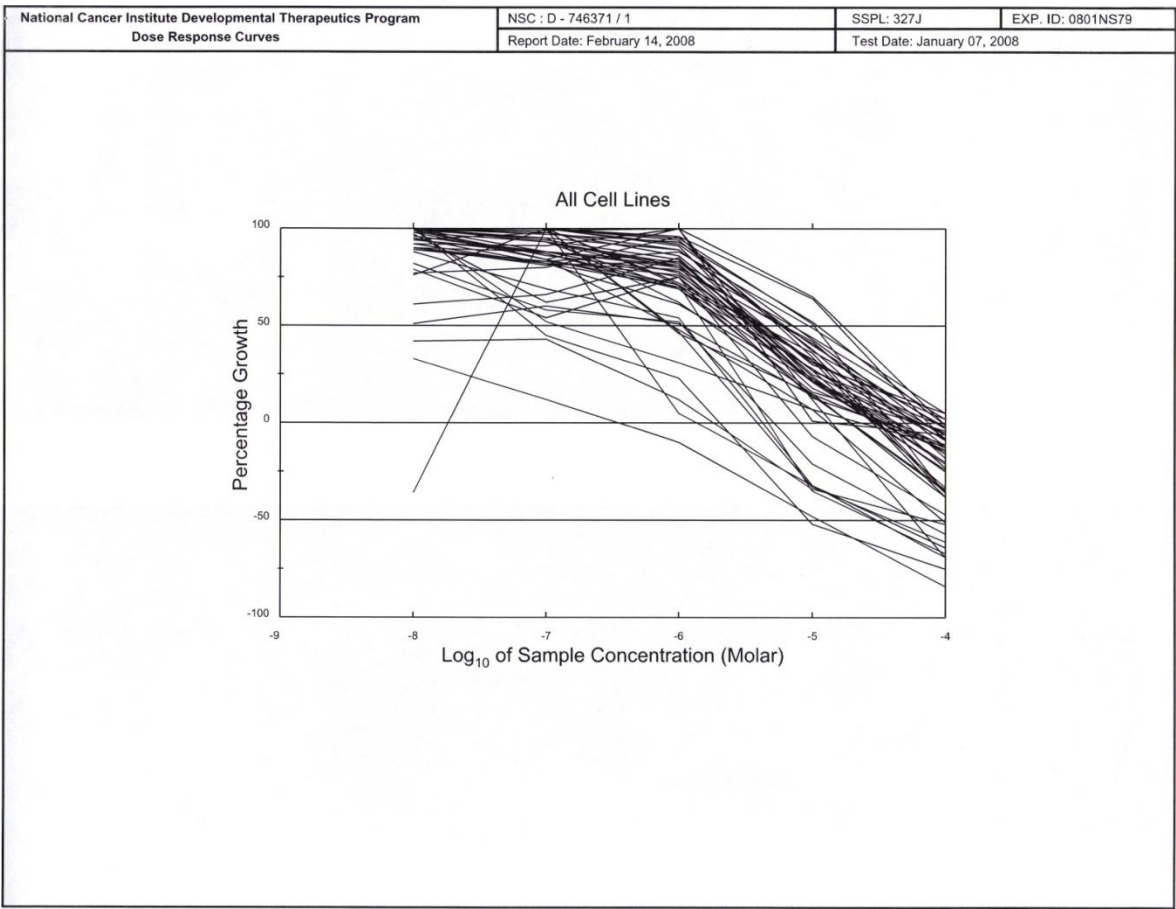


Figure 60: DCB 3507 dose–response curves (all cell lines).

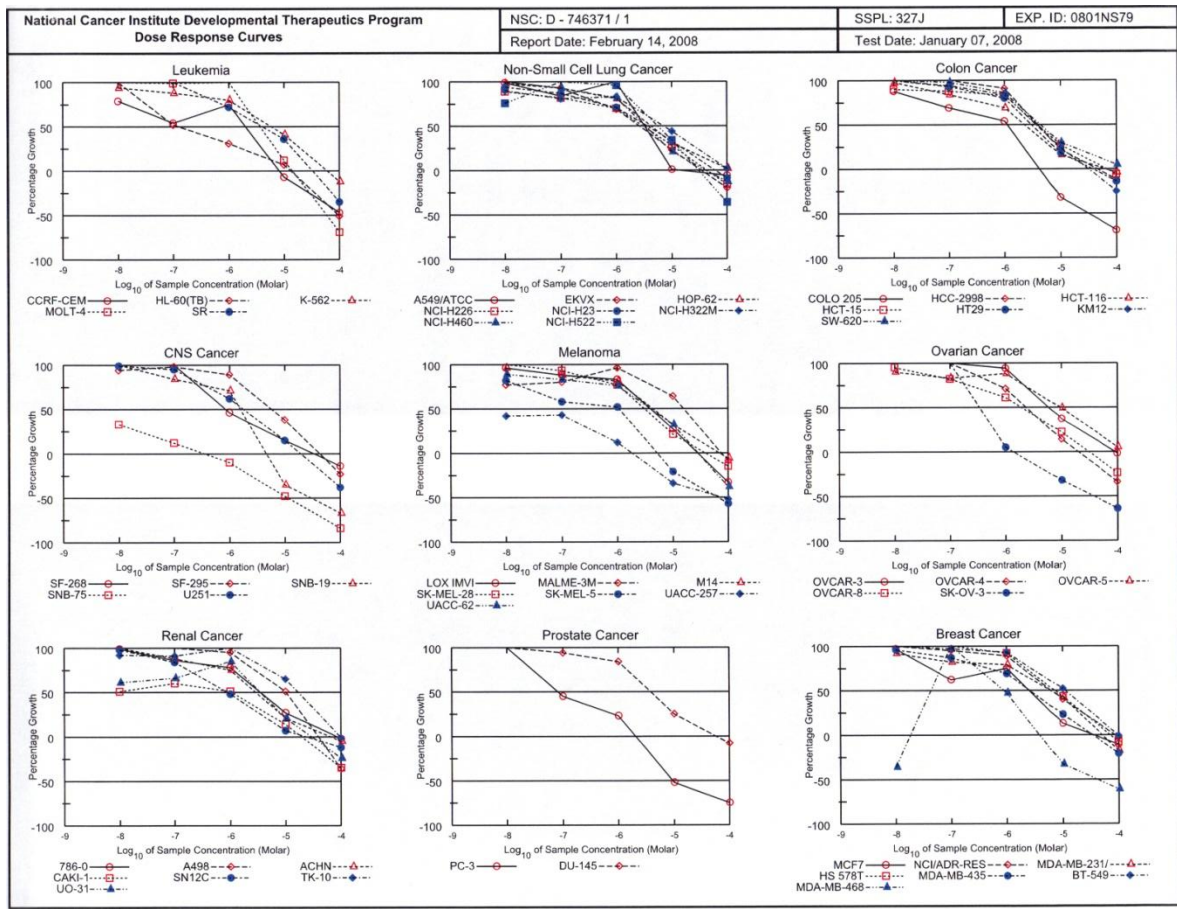


Figure 61: DCB 3507 dose-response curves (by cell line).

**National Cancer Institute Developmental Therapeutics Program
In-Vitro Testing Results**

NSC : D - 746371 / 1		Experiment ID : 0801NS79				Test Type : 08		Units : Molar							
Report Date : February 14, 2008		Test Date : January 07, 2008				QNS :		MC :							
COMI : DCB-3507 (69490)		Stain Reagent : SRB Dual-Pass Related				SSPL : 327J									
Panel/Cell Line	Time	Log10 Concentration						Percent Growth				GI50	TGI	LC50	
		Zero	Ctrl	-8.0	-7.0	-6.0	-5.0	-4.0	-8.0	-7.0	-6.0				-5.0
Leukemia															
CCRF-CEM	0.307	0.683	0.606	0.510	0.590	0.287	0.162	79	54	75	-7	-47	2.04E-6	8.32E-6	> 1.00E-4
HL-60(TB)	0.978	1.845	1.865	1.429	1.249	1.043	0.475	102	52	31	7	-51	1.25E-7	1.34E-5	9.46E-5
K-562	0.205	1.283	1.222	1.152	1.072	0.643	0.180	94	88	80	41	-12	5.81E-6	5.83E-5	> 1.00E-4
MOLT-4	0.423	1.465	1.664	1.458	1.509	0.549	0.131	119	99	104	12	-69	3.88E-6	1.41E-5	5.82E-5
SR	0.285	0.898	0.910	1.005	0.728	0.506	0.185	102	117	72	36	-35	4.11E-6	3.21E-5	> 1.00E-4
Non-Small Cell Lung Cancer															
A549(ATCC)	0.158	0.574	0.571	0.508	0.572	0.162	0.149	99	84	100	1	-6	3.18E-6	1.33E-5	> 1.00E-4
EKVX	0.446	1.237	1.243	1.184	0.995	0.624	0.357	101	93	69	23	-20	2.59E-6	3.38E-5	> 1.00E-4
HOP-62	0.287	1.294	1.275	1.221	1.098	0.603	0.303	98	93	81	31	2	4.17E-6	> 1.00E-4	> 1.00E-4
NCI-H226	0.692	1.823	1.702	1.618	1.484	1.013	0.580	89	82	70	28	-16	3.02E-6	4.32E-5	> 1.00E-4
NCI-H23	0.386	1.142	1.094	1.045	0.922	0.635	0.352	94	87	71	33	-9	3.56E-6	6.15E-5	> 1.00E-4
NCI-H322M	0.595	1.589	1.490	1.400	1.419	1.036	0.613	90	81	83	44	2	7.13E-6	> 1.00E-4	> 1.00E-4
NCI-H460	0.261	1.825	1.980	1.714	1.548	0.586	0.227	110	93	82	21	-13	3.35E-6	4.12E-5	> 1.00E-4
NCI-H522	0.538	1.464	1.238	1.651	1.430	0.857	0.345	76	120	96	34	-36	5.60E-6	3.09E-5	> 1.00E-4
Colon Cancer															
COLO 205	0.402	0.668	0.636	0.584	0.546	0.274	0.124	88	69	54	-32	-69	1.12E-6	4.27E-6	3.07E-5
HCC-2998	0.378	1.248	1.358	1.288	1.173	0.571	0.332	113	105	91	22	-12	3.97E-6	4.42E-5	> 1.00E-4
HCT-116	0.135	1.244	1.217	1.063	0.900	0.308	0.129	98	84	69	16	-4	2.26E-6	6.00E-5	> 1.00E-4
HCT-15	0.213	1.202	1.107	1.085	1.031	0.485	0.201	90	88	83	27	-6	3.91E-6	6.76E-5	> 1.00E-4
HT29	0.249	1.336	1.411	1.258	1.117	0.446	0.215	107	93	80	18	-14	3.05E-6	3.72E-5	> 1.00E-4
KM12	0.236	1.212	1.263	1.155	1.058	0.473	0.178	105	94	84	24	-25	3.73E-6	3.14E-5	> 1.00E-4
SW-620	0.174	1.114	1.116	1.100	0.984	0.461	0.218	100	98	86	30	5	4.46E-6	> 1.00E-4	> 1.00E-4
CNS Cancer															
SF-268	0.364	1.201	1.227	1.209	0.747	0.488	0.314	103	101	46	15	-14	8.36E-7	3.30E-5	> 1.00E-4
SF-295	0.385	1.027	0.991	1.013	0.958	0.630	0.297	94	98	89	38	-23	5.85E-6	4.20E-5	> 1.00E-4
SNB-19	0.906	1.196	1.369	1.149	1.112	0.590	0.295	160	84	71	-35	-67	1.58E-6	4.68E-6	2.91E-5
SNB-75	0.645	0.971	0.754	0.685	0.583	0.338	0.106	33	12	-10	-48	-84	< 1.00E-8	3.62E-7	1.16E-5
U251	0.241	1.320	1.304	1.268	0.912	0.398	0.149	99	95	62	15	-38	1.80E-6	1.88E-5	> 1.00E-4
Melanoma															
LOX IMVI	0.289	1.860	1.802	1.674	1.595	0.713	0.194	96	88	83	27	-33	3.89E-6	2.82E-5	> 1.00E-4
MALME-3M	0.640	1.217	1.085	1.102	1.193	1.008	0.582	77	80	96	64	-9	1.55E-5	7.51E-5	> 1.00E-4
M14	0.283	1.175	1.135	1.066	1.002	0.567	0.267	96	88	81	32	-6	4.25E-6	7.07E-5	> 1.00E-4
SK-MEL-28	0.346	1.022	1.041	0.975	0.865	0.490	0.295	103	93	77	21	-15	3.03E-6	3.88E-5	> 1.00E-4
SK-MEL-5	0.745	1.468	1.339	1.163	1.122	0.592	0.324	82	58	52	-21	-57	1.07E-6	5.22E-6	6.57E-5
UACC-257	0.639	0.836	0.722	0.723	0.663	0.421	0.307	42	43	12	-34	-52	< 1.00E-8	1.83E-6	7.77E-5
UACC-62	0.564	1.994	1.839	1.749	1.658	1.016	0.350	89	83	76	32	-38	3.89E-6	2.85E-5	> 1.00E-4
Ovarian Cancer															
OVCAR-3	0.326	1.081	1.118	1.100	1.035	0.603	0.321	105	103	94	37	-2	5.85E-6	9.04E-5	> 1.00E-4
OVCAR-4	0.583	1.527	1.867	1.559	1.250	0.719	0.385	136	103	71	14	-34	2.33E-6	1.98E-5	> 1.00E-4
OVCAR-5	0.446	1.137	1.066	1.018	1.055	0.787	0.479	90	83	88	49	5	9.59E-6	> 1.00E-4	> 1.00E-4
OVCAR-8	0.264	1.152	1.103	0.995	0.807	0.463	0.200	95	82	61	22	-24	1.94E-6	3.01E-5	> 1.00E-4
SK-OV-3	0.829	1.210	1.261	1.250	0.847	0.561	0.300	114	111	5	-32	-64	3.73E-7	1.33E-6	3.63E-5
Renal Cancer															
786-0	0.322	1.601	1.592	1.421	1.321	0.673	0.317	99	86	78	27	-2	3.58E-6	8.74E-5	> 1.00E-4
A498	0.697	1.379	1.385	1.395	1.344	1.042	0.450	101	102	95	51	-36	1.02E-5	3.87E-5	> 1.00E-4
ACHN	0.327	1.348	1.352	1.228	1.098	0.539	0.311	100	88	75	21	-5	2.92E-6	6.38E-5	> 1.00E-4
CAKI-1	0.335	0.508	0.423	0.439	0.423	0.360	0.218	51	60	51	14	-35	1.03E-6	1.94E-5	> 1.00E-4
SN12C	0.293	1.155	1.140	1.017	0.708	0.356	0.257	98	84	48	7	-12	8.83E-7	2.34E-5	> 1.00E-4
TK-10	0.593	1.343	1.280	1.278	1.405	1.077	0.588	92	91	108	65	-1	1.67E-5	9.68E-5	> 1.00E-4
UO-31	0.198	0.692	0.499	0.527	0.616	0.304	0.150	61	66	85	21	-24	3.53E-6	2.95E-5	> 1.00E-4
Prostate Cancer															
PC-3	0.480	0.681	0.831	0.570	0.526	0.230	0.122	175	45	23	-52	-75	9.09E-8	2.01E-6	9.38E-6
DU-145	0.267	1.031	1.063	0.987	0.910	0.462	0.245	104	94	84	25	-8	3.82E-6	5.64E-5	> 1.00E-4
Breast Cancer															
MCF7	0.354	1.328	1.303	0.961	1.080	0.482	0.316	97	62	75	13	-11	2.51E-6	3.54E-5	> 1.00E-4
NCI/ADR-RES	0.403	1.417	1.420	1.362	1.305	0.810	0.391	100	95	89	40	-3	6.26E-6	8.48E-5	> 1.00E-4
MDA-MB-231/ATCC	0.570	1.338	1.273	1.200	1.177	0.896	0.465	92	82	79	42	-18	6.20E-6	4.98E-5	> 1.00E-4
HS 578T	0.451	1.081	1.135	1.144	1.029	0.720	0.415	109	110	92	43	-8	7.09E-6	6.96E-5	> 1.00E-4
MDA-MB-435	0.274	1.099	1.068	0.992	0.845	0.464	0.216	96	87	69	23	-21	2.60E-6	3.31E-5	> 1.00E-4
BT-549	0.930	1.753	1.854	1.727	1.694	1.359	0.918	112	97	93	52	-1	1.09E-5	9.46E-5	> 1.00E-4
MDA-MB-468	0.469	0.616	0.298	0.790	0.538	0.312	0.185	-36	219	47	-33	-61			4.08E-5

Figure 62: DCB 3507 In-vitro testing results.

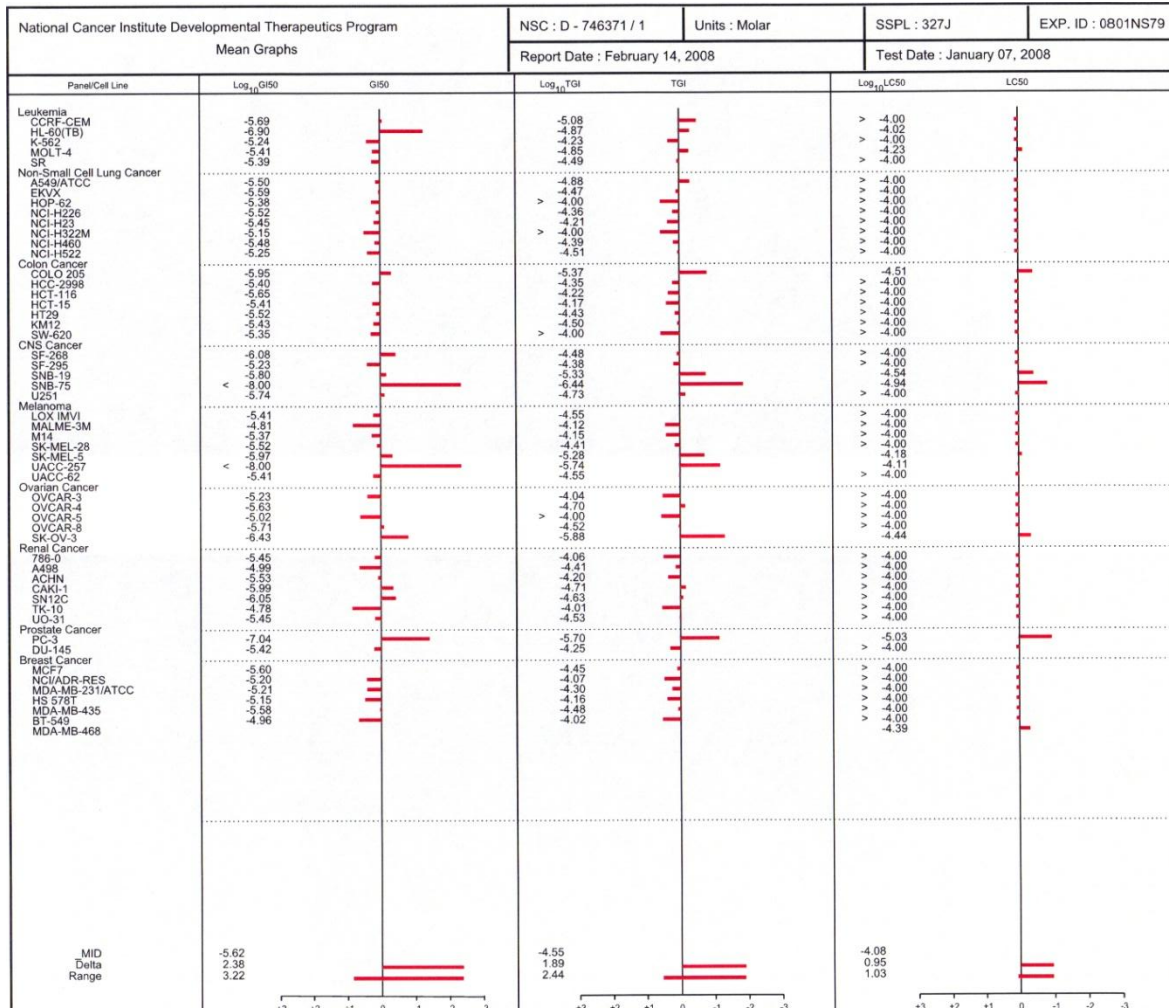


Figure 63: DCB 3507 mean graphs.

6.5 DCB 3508 cytotoxic analysis and structure–activity relationships

Evaluation of DCB 3508 in the National Cancer Institute tumor screen did not show potent inhibition of cell growth in the cell lines ($GI_{50} \sim 10^{-5}$ M) (see figure 64) with an interesting selectivity toward several refractory cell lines in leukemia, (see Table 16).

Table 16: DCB 3508 relevant cell line and growth percent

Panel/Cell Line	Growth Percent
Leukemia (MOLT-4)	-46.10
Leukemia (SR)	-50.57
Renal Cancer (ACHN)	-50.09
Renal Cancer (SN12C)	-49.37
Melanoma (LOX IMVI)	-46.03

This low reactivity allowed one draw certain conclusions about structure–activity relationships (SAR).

First: the tylophorine system must be complete and have a closed cyclohexyl ring (see Scheme 42) in order to be active (GI_{50} , 10^{-6} M, for example).

Figure 64: DCB 3503 and DCB 3508 structures.

Second: there may be a configurational dependence at C14 for anticancer activity. The (*S*)-epimer (DCB 3503) is more active than the (*R*)-epimer (DCB 3501), and the activity of DCB 3507, whose-OH group is relatively free to rotate and assume a variety of conformations, is further diminished.

Given the fact that the 14-OH group in DCB 3503 increases in vivo activity over that of tylophorine (DCB 3500), which lacks a C14 hydroxy group.

The 14-OH could be modified by its bioisosteres, that is functional groups with similar chemical activity and as consequence similar biological activity. The possible bioisosteres are CH₃, NH₂, F, and Cl.³⁶ The chiral C14 carbon with stereochemistry (*S*) could not be modified, because it was proven that (*S*) chiral was more active than (*R*). The 5-membered ring could also be modified (without removing the N) by incorporating a 6-membered ring.

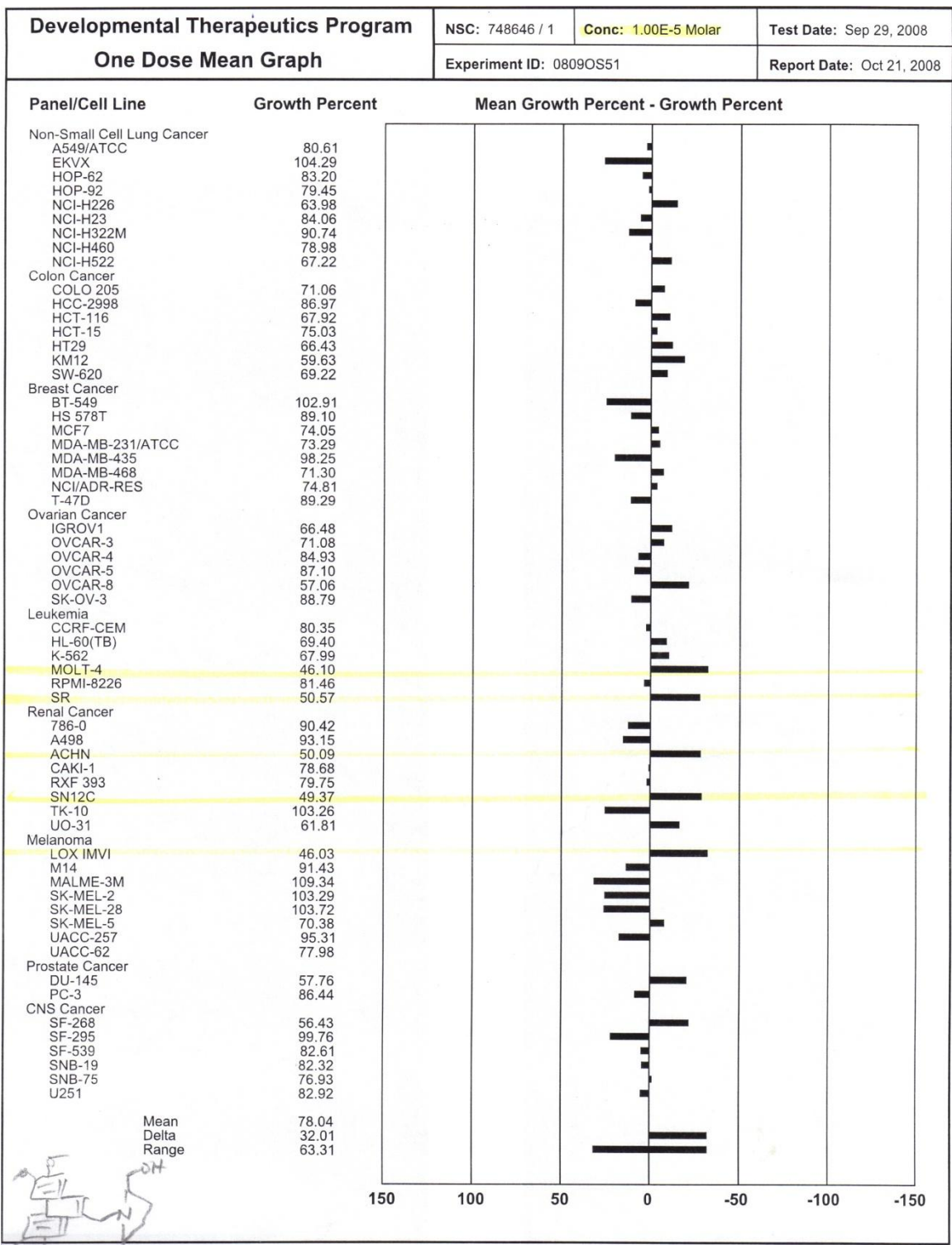


Figure 65: DCB 3508 One-dose mean graph.

6.6 DCB 3509 cytotoxic analysis and structure–activity relationships.

The biological activity of DCB 3509 will be obtained from NCI within 3-4 months. The potency has been predicted to be high by the CoMFA molecular modeling program, using structures and biological data from DCB 3503, DCB 3507, and DCB 3508. These considerations, the author decided to synthesize DCB 3509 with a short saturated straight chain of three carbons with a polar hydroxyl group at the end (see Figure 66). The length of the chain will be varied if DCB 3509 turns out to be highly active.

Figure 66: Structure of DCB 3509.

6.7 Synthesis of biotinylated tylophorine analog cytotoxic analysis and structure–activity relationship

The biological activity of this biotinylated tylophorine analog will be available in a near future. Dr. Y. -C Cheng at Yale University will be conducting the biological studies.

6.6 Conclusions

The improved synthesis of DCB 3503 has provided the means to produce DCB 3503 in 200–400 mg amount in one batch, which in the past was limited to 60 mg in one batch. The most expensive chemicals were replaced with cheaper reagents that were commercially available. These reactions gave also higher yields and were suitable for at least a 4 g scale. These new reactions or improved steps eliminated the need to run chromatography columns to purify products; therefore, the use of expensive solvents such as EtOAc and hexanes were not needed to purify scale-up reactions up to 4 g.

The syntheses of DCB 3503, DCB 3506, DCB 3507, DCB 3508, DCB 3509, and the biotinylated chain to DCB 3506 were carried out to develop the structure–activity relationships and to study the mechanism of reaction with tumor cells. We were also interested in pharmacokinetic, and pharmacodynamics in the cellular level to identify the pharmacophore that binds to cancer cells.

I. Structure–Activity Relationships.

All compounds were evaluated in the 60-cell panel of human-derived tumor cells at the National Cancer Institute. These results offered important information about their structure–activity relationships (SAR). These analogs were modified by replacing methoxy groups (DCB 3503) with hydrogen (DCB 3507), opening cyclic rings (DCB 3508), and attaching a short aliphatic chain (DCB 3509). These modifications either increased or lowered activity.

Tylophorine is considered a structurally specific drug. These drugs, which most drugs are, act with specific sites such as a protein receptor or enzyme. Tylophorine's activity and potency was shown to be susceptible to small changes in chemical structure. Therefore, changing chemical groups gave us an idea what groups were responsible for evoking a biological effect in the living organism.

II. Pharmacokinetics.

It is known that more than three-quarters of drug candidates do not make it to clinical trials because of problems with pharmacokinetics in animals.³⁷ Only less than 10% of drug candidates in clinical trials become marketed products. One of the main obstacles is pharmacokinetic problems, which manifest themselves as poor oral bioavailability or short plasma half-life. Low water solubility of a compound (high

lipophilicity) is a limiting factor in oral bioavailability, and highly lipophilic compounds are easily metabolized or tend to bind to plasma proteins. Moreover, low lipophilicity leads to poor permeability through membranes. Therefore, we need to balance the pharmacokinetic properties of the tylophorine analogs to modify and increase potency.

Pharmacokinetics is important for drug discovery, and in 1997 Lipinski proposed “the rule of five” as guide to improve oral bioavailability during modifications. It has been shown that more than 90% of the compounds with two or more of these points will have poor oral absorption or distribution properties:

1. Molecular weight is >500.
2. The log *P* is < 5.
3. There are more than 5 H-bond donors.
4. There are more than 10 H-bond acceptors.



Figure 67: DCB 3503, 3507, 3508, and 3509.

Table 17: Lipinski's "rule of five" applied to DCB analogs

	DCB 3503	DCB 3507	DCB 3508	DCB 3509
Molecular weight	409.189	349.168	453.215	411.205
Log <i>P</i>	2.92	3.18	2.51	3.24
5 H-bond donors	1	1	1	2
10 H-bond acceptors	6	4	6	7

Analysis of Lipinski's "rule of five" applied to DCBs can be seen in Table 17. The molecular weight for DCB 3503, 3507 3508, and 3509 are all below 500. As mentioned before, the side chain of DCB 3509 could be increased up to 6 carbons and its molecular weight would still below 500.

Log *P* values, the partition coefficients, for all tylophorine analogs are below 5. The partition coefficient is useful to estimate distribution of drugs within the body.

The number of H-bond donors is expressed as the sum of OH and NH. All our tylophorine analogs contained less than 2. The number of H-acceptors is expressed as the sum of N and O. All our tylophorine analogs are below 7. As result, all tylophorine analogs would pass the Lipinski's rule of five, which predicts a good oral absorption.

Chapter seven: Experimental

Experimental procedure to scale-up DCB 3503

General Methods

All reactions were monitored using thin-layer chromatography (TLC). Absorption chromatography was carried out using Sorbent Technologies silica gel plates with a 200 mm thickness. All NMR spectroscopy was used the Varian 300 MHz NMR. Melting points were determined on a Thomas-Hoover capillary melting point apparatus. Positive-ion electrospray mass spectra were acquired on Accutof DART, MALDI, and QUATRO-II quadrupole instrument.

Preparation of (*E*)-2,3-bis(3,4-dimethoxyphenyl)acrylic acid (**3**).

3,4-Dimethoxybenzaldehyde (**1**, 99+%, 15.0 g, 90.3 mmol) was stirred in Ac₂O (55 mL) and TEA (40 mL) until solution was completely dissolved, then (3,4-dimethoxyphenyl)acetic acid (**2**, 99%, 20.0 g, 102.0 mmol) was added. The solution was heated slowly to 100 °C and left stirring overnight. The mixture was cooled to room temperature, and water (50 mL) was added dropwise. An increase in temperature was expected, so addition of water was stopped momentarily until temperature dropped to room temperature. Then, a solution of K₂CO₃ (75 g) in water (250 mL) was added dropwise. From experience, it is recommended to stop adding the K₂CO₃ solution momentarily if formation of sticky oily brown substance started to appear on the walls and bottom of the beaker; then, continue adding K₂CO₃ solution dropwise. If formation of sticky substance was formed and stopped the stir bar, then the solution must be left stand for 30-60 minutes at room temperature until it turned solid and stir bar was again able to spin. The mixture was refluxed until all solids dissolved. Then, mixture was cooled to room temperature and left spinning overnight. Mixture was separated with Et₂O (2 x 100 mL) and aqueous phase was collected (bottom). The aqueous layer was acidified with 2 N HCl, which was added dropwise until pH 1 was reached. If a sticky substance is formed, then the mixture must be left spinning for 30-60 minutes at room temperature, at which time all should solidify; acidification was then continued. The precipitation was recrystallized using MeOH to obtain 35.0 g of **3** (>90.0 % yield). mp: 208 °C. ¹H NMR (CDCl₃): δ 3.46 (3H, s), 3.80 (3H, s), 3.83 (3H, s), 3.88 (3H, s), 6.54 (1H, s), 6.73 (1H, d), 6.78 (1H, s), 6.81 (1H, d), 6.84 (1H, d), 6.9 (1H, d), 7.83 (1H, d);

^{13}C (NMR CDCl_3): δ 55.42, 55.90, 55.92, 56.08, 111.83, 112.65, 112.85, 116.80, 116.82, 142.52. EIMS calcd for $\text{C}_{19}\text{H}_{20}\text{O}_6$ m/z 344.13; found 345.126

Preparation of (*E*)-methyl 2,3-bis(3,4-dimethoxyphenyl)acrylate (4)

To a solution of compound **3** (13.0 g, 37.77 mmol) in MeOH (500 mL) stirred at 60 °C was added dropwise H_2SO_4 (15 mL) and the solution was stirred overnight under reflux. The mixture was concentrated by rotary evaporation at 35-40 °C (do not heat above 50 °C lest a purple oily product form) and a liquid-solid residue formed. This crude product was filtrated and washed quickly with cold MeOH. This solid was purified by column chromatography (2:0.5 EtOAc:hexane), but most of the time it was not necessary. Yield: 13.05 g of **4** (>90%) mp: 125 °C. ^1H NMR (CDCl_3): δ 3.49 (3H, s), 3.80 (3H, s), 3.82 (3H, s), 3.85 (3H, s), 3.90 (3H, s), 6.53 (1H, s), 6.73 (1H, m), 6.81 (1H, m), 6.84 (1H, m), 6.78 (1H, m), 6.90 (1H, m), 7.70 (1H, s); ^{13}C NMR (CDCl_3): δ 52.59, 55.42, 55.92, 56.00, 56.08, 110.49, 111.49, 112.49, 112.98, 122.43, 125.43, 140.53. EIMS calcd for $\text{C}_{20}\text{H}_{22}\text{O}_6$ m/z 348.14; found 349.136

Preparation of methyl 2,3,6,7-tetramethoxyphenanthrene-9-carboxylate (5)

Method A: Using FeCl_3

A solution of compound **4** (4.0 g, 11.17 mmol) in DCM (250 mL) was cooled to -10 °C. Then a solution of anhydride FeCl_3 (13 g, 80.83 mmol) in EtOAc (250 mL) was added dropwise. The solution was stirred overnight, but the reaction was completed as soon as $\text{FeCl}_3/\text{EtOAc}$ solution was added. The TLC was used to confirm completion of the reaction (2:0.5 EtOAc:hexanes). The product's spot must be bright blue with spray/heat development with anisaldehyde-sulfuric acid. † The presence of a small brown spot on the TLC plate (spots of product and starting material overlap), is indicative of the presence of starting material. If this is the case, then the temperature of the solution was lowered using an ice bath at -10 °C and a solution of FeCl_3 anhydride in EtOAc was added, the amount depending on the size of the brown spot. To quench the reaction, water (250 mL) was added to the solution and mixture was allowed to stir for 3 hours or until it turned dark yellow, if the solution had a dark green color, then more water was added. The solution was extracted with CHCl_3 (3 x 50 mL) and dried with Na_2SO_4 . The mixture was filtered and solvent was evaporated at ≤ 35 °C, because the final compound is heat sensitive. The crude product was purified by column chromatography

(2:0.5 EtOAc:hexanes) to give 3.86 g **5** (>90%) mp. . ¹HNMR (CDCl₃): δ 4.01 (1H, s), 4.04 (1H, s), 4.07 (1H, s), 4.12 (1H, s), 4.14 (1H, s), 7.27 (1H, s), 7.77 (1H, s), 7.80 (1H, s), 8.42 (1H, s), 8.65 (1H, s); ¹³(CDCl₃): δ 52.26, 52.5, 56.08, 56.09, 56.25, 56.26, 102.70, 102.87, 107.02, 109.50. EIMS calcd for C₂₀H₂₀O₆ *m/z* 356.13; found 357.132

Method: VOF₃

To a compound **4** (1.86, 5.19 mmol) was added DCM (18 mL), and mixture was stirred at -10 °C. Then, a solution of VOF₃ (2 g, 16.14 mmol), DCM (35 mL), EtOAc (17.5 mL), TFA (1 mL), and TFAA (3 drops) was added dropwise with stirring. The solution was stirred for 5 h at -10 °C. To quench the reaction, the mixture was poured onto ice and extracted with CHCl₃ (3 x 50 mL). The organic phase was dried with Na₂SO₄ and filtered, and solvent was evaporated. The crude product was purified by column chromatography (2:0.5 EtOAc:hexanes) to give 1.55 g (80%) of **5**. TLC showed a bright blue color under anisaldehyde TLC stain. In our experience, VOF₃ is a toxic powder that has to be open quickly inside a hood. The VOF₃ solution stains glassware with a green color that can be removed with 2 N HCl. This organic waste must be disposed of in a separate container.

Preparation of (2,3,6,7-tetramethoxyphenylphenanthren-9-yl)methanol (6**)**

For this reduction, a three-neck round flask was outfitted to be maintained under an N₂ atmosphere. To a mixture of LiAlH₄ (3.5 g, 92.22 mmol) in THF (280 mL) at -10 °C was added dropwise a solution of **5** (3.95 g, 11.09 mmol) in THF. Ice bath was removed, and the mixture was stirred at room temperature overnight. The mixture was again cooled to -10 °C and EtOAc (100 mL) was added dropwise, then Na₂SO₄·10H₂O (around 10 g) was added slowly until solution stopped bubbling and turned yellow. The mixture was stirred overnight. Alternatively, 2 N HCl can be used instead of Na₂SO₄·10H₂O to quench the reaction, but lower yield generally resulted. The mixture was filtered, and the solvent was evaporated by rotary evaporation. The crude product was purified by column chromatography (2:0.5 EtOAc:hexanes) to give 3.18 g **6** (>90%) mp: 184 ° C. ¹HNMR (CDCl₃): δ 4.03 (3H, s), 4.07 (3H, s), 4.12 (3H, s), 4.14 (3H, s), 5.14 (2H, s), 7.22 (1H, s), 7.56 (1H, s), 7.60 (1H, s), 7.78 (1H, s), 7.84 (1H, s); ¹³C NMR (CDCl₃): δ 56.00, 56.08, 56.10, 56.25, 65.04, 103.03, 103.37, 105.02, 108.67, 124.24. EIMS calcd for C₁₉H₂₀O₅ *m/z* 328.13; found 329.128.

Preparation of (S)-methyl 5-oxo-1-((2,3,6,7-tetramethoxyphenanthren-9-yl)methyl)pyrrolidine-2-carboxylate (**7**)

This reaction required three steps:

Step 1: A solution of compound **6** (3.4 g, 10.35 mmol) in freshly distilled CHCl_3 (200 mL) was cooled to $-10\text{ }^\circ\text{C}$. (Using non-distilled CHCl_3 increased side reactions). Then a solution of PBr_3 (4.8 mL, 17.93 mmol) in CHCl_3 (5 mL) was added dropwise. Iced bath was removed and solution was stirred at room temperature for 1.5 h. Then, the solution was poured over ice and stirred until ice was completely melted. The product was extracted with CHCl_3 and dried over Na_2SO_4 . The mixture was filtered, and solvent was evaporated by rotary evaporation to obtain **6.1** as a yellow solid. Mp: $184\text{ }^\circ\text{C}$. ^1H NMR (CDCl_3): δ 4.02 (3H, s), 4.11 (3H, s), 4.12 (3H, s), 4.13 (3H, s), 4.99 (2H, s), 7.52 (1H, s), 7.67 (1H, s), 7.76 (1H, s), 7.18 (1H, s), 7.83 (1H, s); ^{13}C NMR (CDCl_3): δ 56.01, 56.05, 56.07, 56.08, 33.85, 102.87, 103.53, 105.02, 108.50.

Step 2: The crude product **6.1** was added DMF (200 mL), glutamic acid dimethyl ester **27** (6 g, 28.35 mmol) and allowed to dissolve completely. Then K_2CO_3 (10 g) was added, and the mixture was stirred at $65\text{ }^\circ\text{C}$ overnight. At higher or lower temperature, side reactions were noted.

Step 3: The solvent was evaporated by high vacuum (~ 1 torr) rotary evaporation. The residue was extracted with CHCl_3 , and the extract was washed with water and dried with Na_2SO_4 . The organic extract was filtered, and solvent was removed by rotary evaporation. The crude product was dissolved in MeOH (80 mL) and AcOH (80 mL) and stirred at $45\text{ }^\circ\text{C}$ overnight. At higher or lower temperature, side reactions were formed. The solvent was removed by rotary evaporation, then high-vacuum rotary evaporation (~ 1 torr) to obtain a yellow solid. The crude product was purified by column chromatography (2:0.5 EtOAc:hexanes) to give 3.4 g of **7** (>90 % yield). ^1H NMR (CDCl_3): δ 2.08 (1H, m, $J = 3.22$ Hz), 2.12 (1H, m, $J = 3.22$ Hz), 2.24 (1H, m, $J = 3.22$), 2.48 (1H, m, $J = 3.22$ Hz), 3.46 (3H, s), 3.84 (1H, dd, 3.23, 9.05 Hz), 4.03 (3H, s), 4.034 (3H, s), 4.12 (3H, s), 4.13 (3H, s) 4.4 (1H, m, $J = 14.58$ Hz), 5.49 (1H, m, 14.58 Hz), 7.19 (1H, s), 7.41 (1H, s), 7.61 (1H, s), 7.76 (1H, s), 7.81 (1H, s); ^{13}C NMR (CDCl_3): δ 22.89, 24.88, 44.79, 52.43, 56.08, 56.74, 56.91, 58.73, 103.03, 103.19, 105.35, 108.34, 127.09. EIMS calcd for $\text{C}_{25}\text{H}_{27}\text{NO}_7$ m/z 453.18; found 454.171

Preparation of (S)-5-oxo-1-((2,3,6,7-tetramethoxyphenanthren-9-yl)pyrrolidine-2-carboxylic acid (8)

Compound **7** (8.0 g, 17.65 mmol) was stirred in solution of 1,4-dioxane (100 mL), 2 N KOH (200 mL), and MeOH (100 mL) for 1.5 h at room temperature. The solution was acidified with 2 N HCl until pH 1, and extracted with CHCl₃ and Et₂O. Alternatively, phosphoric acid can be used to quench the reaction, and a precipitate was formed. The solvent was removed by rotary evaporation to give **8** 7.4 g (80 % yield) mp 220-225 °C. ¹H NMR (CDCl₃): δ 2.10 (2H, m), 2.40 (2H, m), 3.69 (1H, m), 4.30 (1H, m), 4.00 (3H, m), (4.02 (3H, s), 4.10 (3H, m), 4.12 (3H, m), 5.64 (1H, m), 7.16 (1H, s), 7.44 (1H, s), 7.59 (1H, s), 7.74 (1H, s), 7.78 (1H, s)); ¹³C NMR (CDCl₃): δ 21.90, 24.74, 51.10, 56.00, 56.08, 56.41, 56.24, 67.36, 102.87, 103.34, 104.26, 105.36, 108.51. EIMS calcd for C₂₄H₂₅NO₇ *m/z* 439.16; found 440.179.

Preparation of (S)-2,3,6,7-tetramethoxy-13,13a-dihydrodibenzo[f,h]pyrrolo[1,2-b]isoquinoline-11,14(9H,12H)-dione (9)

Method A1: TFAA and BF₃·Et₂O

TFAA (4.0 mL) was added to a solution of compound **8** (0.58 g, 1.32 mmol) and 1,2-dichloroethane (45 mL). It was noted that starting material did not dissolve in 1,2-dichloroethane until TFAA was added. The solution was stirred at room temperature for 1 h. Then, BF₃·Et₂O (4 mL) was added and solution was stirred overnight at room temperature. The majority of solvent was removed by rotary evaporation and DCM (50 mL) was added slowly. Then, a solution of saturated K₂CO₃ in water was added dropwise until release of CO₂ stopped and solution turned yellow from a dark green color. The solution was stirred overnight at room temperature (or for at least 5 hours). Then, the mixture was filtrated, and the organic phase was extracted with CHCl₃ and water. The solvent was removed by rotary evaporation and purified by column chromatography (2:1:0.3 CHCl₃:EtOAc:MeOH) to give **9** 0.4 g as a yellow powder. If product became oily due to heating on the rotary evaporator, then EtOAc was added until the product dissolved, and small amount of hexanes were added to precipitate product. TLC typically showed the product as a yellow spot after it was developed in anisaldehyde-H₂SO₄ TLC stain (65 %yield) mp. ¹H NMR (CDCl₃): δ 2.30 (1H, m), 2.40 (1H, m), 2.60 (1H, m), 2.62 (1H, m), 3.51 (3H, s), 3.91 (1H, m), 3.96 (3H, s), 4.05 (3H,

m), 4.06 (3H, s), 4.35 (1H, s), 5.44 (1H, s), 7.09 (1H, s), 7.32 (1H, s), 7.53 (1H, s), 7.72 (1H, s); ^{13}C NMR (CDCl_3): δ 30.07, 55.02, 55.07, 56.02, 56.06, 56.17, 56.32, 58.49, 61.17, 102.61, 102.99, 105.22, 108.14. EIMS calcd for $\text{C}_{24}\text{H}_{23}\text{NO}_6$ m/z 421.15; found 422.157.

Method A2: Oxalyl chloride and SnCl_4

Compound **8** (0.5 g, 11.39 mmol) was dissolved in DCM (40 mL) and $(\text{CO})\text{Cl}_2$ (0.4 mL, 3.15 mmol) was added dropwise, followed by the addition of a catalytic amount of DMF (1-2 drops). Mixture was stirring for 1.5 h at room temperature, then, it was brought to 35 °C and SnCl_4 (0.6 mL, 2.30 mmol) was added. The mixture was stirred for 4 h under an N_2 atmosphere at 35 °C. The reaction was cooled to room temperature and was added cold 2 N HCl (3.5 mL). TLC showed a yellow spot as product after it was dipped in anisaldehyde TLC reagent.

Preparation of (13a*S*,14*S*)-14-hydroxy-2,3,6,7-tetramethoxy-12,13,13a,14-tetrahydrobenzo[*f,h*]pyrrolo[1,2-*b*]isoquinolin-11(9*H*)-one (10)

A solution of compound **9** (3.76 g, 4.85 mmol) in dry THF (25 mL) under an N_2 atmosphere was cooled to -10 °C. Then either K-selectride or L-selectride (1.0 M solution in THF) (3.1 mL, 13.95 mmol) was added, and stirred for 5 h at -35 °C. The reaction was quenched by the addition of 2 N HCl (2 mL), and the product was partitioned between CHCl_3 and water. The organic solvent was removed by rotary evaporation and the crude product was purified by column chromatography to give **10** (2.95 g, 75%). TLC (2:1:0.3 CHCl_3 :EtOAc:MeOH) generally showed an orange/red spot for the product after the plate was developed with anisaldehyde- H_2SO_4 mp. ^1H NMR (CDCl_3): δ 2.30 (1H, m), 2.36 (1H, m), 2.62 (1H, m), 2.63 (1H, m), 2.80 (1H, m), 3.94 (3H, s), 3.97 (1H, m), 4.09 (3H, s), 4.11 (3H, s), 4.12 (3H, s), 4.49 (1H, m), 5.19 (1H, m), 6.98 (1H, s), 7.59 (1H, s), 7.75 (1H, s), 7.70 (1H, s); ^{13}C NMR (CDCl_3): δ 30.20, 32.60, 40.02, 55.90, 56.06, 58.62, 64.69, 103.53, 103.60, 103.70, 104.46, 175.40. EIMS calcd for $\text{C}_{24}\text{H}_{25}\text{NO}_6$ m/z 423.17; found 424.179

Preparation of (13a*S*, 14*S*)-2,3,6,7-tetramethoxy-9,11,12,13,13a,14-hexahydrobenzo[*f,h*]pyrrolo[1,2-*b*]isoquinolin-13-ol (11)

For this reduction, a three-neck round-bottom flask outfitted for an N₂ atmosphere was used. To a mixture of LiAlH₄ (0.2 g, 7.11 mmol) in THF (60 mL) at -10 °C was added dropwise a solution of **10** (0.27 g, 0.638 mmol) in THF. Ice bath was removed and solution was stirred at room temperature overnight. The solution was brought back to -10°C, and EtOAc (50 mL) was added dropwise, then Na₂SO₄·10H₂O was added slowly until the mixture stopped bubbling and turned yellow. (The mixture should not be left spinning for more than 4 hours. The use of 2 N HCl to quench the reaction proved to lower the yield.) The solution was filtered and solvent was removed by rotary evaporation. The crude product was purified by column chromatography (2:1:0.5 CHCl₃:EtOAc:MeOH) to give **11** 0.15 g (60 % yield) mp. ¹H NMR (CDCl₃): δ 1.84 (1H, m), 2.16 (1H, m), 2.20 (1H, m), 2.21 (1H, m), 2.82 (1H, m), 3.13 (1H, m), 3.77 (3H, s), 3.28 (1H, m), 4.10 (3H, s), 4.11 (3H, m) 4.16 (3H, m), 6.06 (1H, s), 7.37 (1H, s), 7.59 (1H, s), 7.89 (1H,s); ¹³C NMR (CDCl₃): δ 23.93, 24.02, 53.29, 55.71, 55.75, 55.92, 56.08, 64.93, 65.62, 102.2, 102.54, 102.7, 105.36. EIMS calcd for C₂₄H₂₇NO₅ *m/z* 409.19; found 410.197

Preparation of (S)-1,5-dimethoxy-1,5-dioxopentan-2-aminium chloride (BMPAC) (27)

To a solution of L(+)-glutamic acid **26** (6 g, 40.80 mmol) in MeOH (300 mL) at -10 °C was added dropwise SOCl₂ (40 mL). Then, the solution was heated at 35 °C overnight. Heating the solution at higher temperature produced a green or orange oil. The green oil worked perfectly, but the orange oil was not the product expected. Solvent was removed by rotary evaporation at 35 °C as yellow oil that hardened into white solid under vacuum overnight.

Experimental procedure for DCB 3503

Preparation of (*E*)-2,3-bis(3,4-dimethoxyphenyl)acrylic acid (**3**).

3,4-Dimethoxybenzaldehyde (**1**, 99+%, 15.0 g, 90.3 mmol) was stirred in Ac₂O (55 mL) and TEA (40 mL) until solution was completely dissolved, then (3,4-dimethoxyphenyl)acetic acid (**2**, 99%, 20.0 g, 102.0 mmol) was added. The solution was heated slowly to 100 °C and left stirring overnight. The mixture was cooled to room temperature, and water (50 mL) was added dropwise. Then, a solution of K₂CO₃ (75 g) in water (250 mL) was added dropwise. The mixture was refluxed until all solid dissolved. Then, mixture was cooled to room temperature and left stirring overnight. Mixture was separated with Et₂O (2 x 100 mL) and water phase was collected (bottom). The aqueous layer was acidified with 2 N HCl, which was added dropwise until pH 1 was reached. The precipitation was recrystallized using MeOH to obtain **3** (35.0 g, >90.0 % yield). mp 218 °C (lit.¹ 215-216 °C); ¹H NMR (CDCl₃): δ 3.46 (3H, s), 3.80 (3H, s), 3.83 (3H, s), 3.88 (3H, s), 6.54 (1H, s), 6.73 (1H, d), 6.78 (1H, s), 6.81 (1H, d), 6.84 (1H, d), 6.9 (1H, d), 7.83 (1H, d); ¹³C (NMR CDCl₃): δ 55.42, 55.90, 55.92, 56.08, 111.83, 112.65, 112.85, 116.80, 116.82, 142.52. EIMS calcd for C₁₉H₂₀O₆ *m/z* 344.126; found 345.126.

Preparation of (*E*)-methyl 2,3-bis(3,4-dimethoxyphenyl)acrylate (**4**)

Compound **3** (13.0 g, 37.77 mmol) was added to MeOH (500 mL) and the solution was stirred at 60 °C. Then, H₂SO₄ (15 mL) was added dropwise and solution was stirred overnight. The solvent was removed by rotary evaporation at 40 °C and a precipitate solid/liquid was formed. This product was filtrated and washed quickly with cold MeOH. This solid was purified by column chromatography (2:0.5 EtOAc:hexane). To obtain **4** (13.05 g, >90%) mp 125 °C (lit.² 126 -127 °C). ¹H NMR (CDCl₃): δ 3.49 (3H, s), 3.80 (3H, s), 3.82 (3H, s), 3.85 (3H, s), 3.90 (3H, s), 6.53 (1H, s), 6.73 (1H, m), 6.81 (1H, m), 6.84 (1H, m), 6.78 (1H, m), 6.90 (1H, m), 7.70 (1H, s); ¹³C NMR (CDCl₃): δ 52.59, 55.42, 55.92, 56.00, 56.08, 110.49, 111.49, 112.49, 112.98, 122.43, 125.43, 140.53. EIMS calcd for C₂₀H₂₂O₆ *m/z* 358.142; found 359.136.

Preparation of methyl 2,3,6,7-tetramethoxyphenanthrene-9-carboxylate (**5**)

Method: FeCl₃

Compound **4** (4.0 g, 11.17 mmol) was added to DCM (250 mL) at -10 °C. Then a solution of FeCl₃ anhydride (13 g, 80.83 mmol) in EtOAc (250 mL) was added dropwise and solution was stirred overnight. To quench the reaction, water (250 mL) was added to the solution and allowed to stir for three hours. The solution was extracted with CHCl₃ (3 x 50 mL) and dried with Na₂SO₄. The solution was filtered and solvent was removed by rotary evaporation. The crude product was purified by column chromatography (2:0.5 EtOAc:hexanes) to give **5** (3.86 g, >90%) mp: 202 °C (lit.³ 203-205 °C). ¹HNMR (CDCl₃): δ 4.01 (1H, s), 4.04 (1H, s), 4.07 (1H, s), 4.12 (1H, s), 4.14 (1H, s), 7.27 (1H, s), 7.77 (1H, s), 7.80 (1H, s), 8.42 (1H, s), 8.65 (1H, s); ¹³(CDCl₃): δ 52.26, 52.5, 56.08, 56.09, 56.25, 56.26, 102.70, 102.87, 107.02, 109.50. EIMS calcd for C₂₀H₂₀O₆ *m/z* 356.126; found 357.132.

Method: VOF₃

Compound **4** (1.86, 5.19 mmol) was added DCM (18 mL) at stirred at -10 °C. Then, the following solution was added dropwise: VOF₃ (2 g, 16.14 mmol), DCM (35 mL), EtOAc (17.5 mL), TFA (1 mL), and TFAA (3 drops). The solution was stirred for 5 h at -10 °C. To quench the reaction, it was poured on ice and organic phase separated with CHCl₃ (3 x 50 mL). The solution was dried with Na₂SO₄, filtered, and solvent was removed by rotary evaporation. The crude product was purified by column chromatography (2:0.5 EtOAc:hexanes) to give **5** (1.55 g, >90%) mp: 202 °C (lit.³ 203-205 °C). VOF₃ stains glassware with a green color that can be removed with 2 N HCl.

Preparation of (2,3,6,7-tetramethoxyphenylphenanthren-9-yl)methanol (6**)**

To a mixture of LiAlH₄ (3.5 g, 92.22 mmol) in THF (280 mL) at -10 °C was added dropwise a solution of **5** (3.95 g, 11.09 mmol) in THF. Ice bath was removed and solution was stirred at room temperature overnight. The solution was brought back to -10 °C and EtOAc (100 mL) was added dropwise, then Na₂SO₄·10H₂O (around 10 g) was added slowly. The solution was left stirred overnight. The solution was filtered and solvent was removed by rotary evaporation. The crude product was purified by column chromatography (2:0.5 EtOAc:hexanes) to give **6** (3.18 g, >90%) mp: 184 °C (lit.⁴ 184-185 °C). ¹HNMR (CDCl₃): δ 4.03 (3H, s), 4.07 (3H, s), 4.12 (3H, s), 4.14 (3H, s), 5.14 (2H, s), 7.22 (1H, s), 7.56 (1H, s), 7.60 (1H, s), 7.78 (1H, s), 7.84 (1H, s); ¹³C NMR

(CDCl₃): δ 56.00, 56.08, 56.10, 56.25, 65.04, 103.03, 103.37, 105.02, 108.67, 124.24. EIMS calcd for C₁₉H₂₀O₅ m/z 328.131; found 329.128.

Preparation of (S)-methyl 5-oxo-1-((2,3,6,7-tetramethoxyphenanthren-9-yl)methyl)pyrrolidine-2-carboxylate (7)

This reaction required three steps:

Step 1: Compound **6** (3.4 g, 10.35 mmol) was added freshly distilled CHCl₃ (200 mL) at -10 °C. Using regular CHCl₃ increased side reactions. Then a solution of PBr₃ (4.8 mL, 17.93 mmol) in CHCl₃ (5 mL) was added dropwise. Iced bath was removed and solution was stirred at room temperature for 1.5 h. Then, the solution was poured over ice and stirred until ice was completely melted. The organic phase was separated by extraction using CHCl₃ and dried over Na₂SO₄. The solution was filtered and solvent was removed by rotary evaporation to obtain **6.1** as a yellow solid 9-(bromomethyl)-2,3,6,7-tetramethoxyphenanthrene. ¹H NMR (CDCl₃): δ 4.02 (3H, s), 4.11 (3H, s), 4.12 (3H, s), 4.13 (3H, s), 4.99 (2H, s), 7.52 (1H, s), 7.67 (1H, s), 7.76 (1H, s), 7.18 (1H, s), 7.83 (1H, s); ¹³C NMR (CDCl₃): δ 56.01, 56.05, 56.07, 56.08, 33.85, 102.87, 103.53, 105.02, 108.50.

Step 2: The crude product **6.1** was added DMF (200 mL), glutamic acid dimethyl ester **27** (6 g, 28.35 mmol), and K₂CO₃ (10 g). The mixture was stirred at 65 °C overnight.

Step 3: The solvent was removed by high vacuum rotary evaporation. Extraction with CHCl₃ and water was used to obtain organic phase. Then, it was dried with Na₂SO₄, filtered, and solvent was removed by rotary evaporation. The crude product was dissolved in MeOH (80 mL) and AcOH (80 mL) and stirred at 45 °C overnight. The solution was removed by rotary evaporation and high vacuum rotary evaporation to obtain a yellow solid. The crude product was purified by column chromatography (2:0.5 EtOAc:hexanes) to give **7** (3.4 g, >90 % yield) mp 215 °C (lit.⁵ 210-215 °C). ¹H NMR (CDCl₃): δ 2.08 (1H, m, J = 3.22 Hz), 2.12 (1H, m, J = 3.22 Hz), 2.24 (1H, m, J = 3.22), 2.48 (1H, m, J = 3.22 Hz), 3.46 (3H, s), 3.84 (1H, dd, 3.23, 9.05 Hz), 4.03 (3H, s), 4.034 (3H, s), 4.12 (3H, s), 4.13 (3H, s), 4.4 (1H, m, J = 14.58 Hz), 5.49 (1H, m, 14.58 Hz), 7.19 (1H, s), 7.41 (1H, s), 7.61 (1H, s), 7.76 (1H, s), 7.81 (1H, s); ¹³C NMR (CDCl₃): δ 22.89, 24.88, 44.79, 52.43, 56.08, 56.74, 56.91, 58.73, 103.03, 103.19, 105.35, 108.34, 127.09. EIMS calcd for C₂₅H₂₇NO₇ m/z 453.179; found 454.171.

Preparation of (S)-5-oxo-1-((2,3,6,7-tetramethoxyphenanthren-9-yl)pyrrolidine-2-carboxylic acid (8)

Compound **7** (8.0 g, 17.65 mmol) was stirred in solution of 1,4-dioxane (100 mL), 2 N KOH (200 mL), and MeOH (100 mL) for 1.5 h at room temperature. The solution was acidified with 2 N HCl until pH = 1, and extracted with CHCl₃ and Et₂O. The solvent was removed by rotary evaporation to give **8** (7.4 g, 80 % yield) mp: 290-300 °C (lit.⁵ 300-302 °C). ¹HNMR (CDCl₃): δ 2.10 (2H, m), 2.40 (2H, m), 3.69 (1H, m), 4.30 (1H, m), 4.00 (3H, m), (4.02 (3H, s), 4.10 (3H, m), 4.12 (3H, m), 5.64 (1H, m), 7.16 (1H, s), 7.44 (1H, s), 7.59 (1H, s), 7.74 (1H, s), 7.78 (1H, s); ¹³C NMR (CDCl₃): δ 21.90, 24.74, 51.10, 56.00, 56.08, 56.41, 56.24, 67.36, 102.87, 103.34, 104.26, 105.36, 108.51. EIMS calcd for C₂₄H₂₅NO₇ *m/z* 439.163; found 440.179.

Preparation of (S)-2,3,6,7-tetramethoxy-13,13a dihydrodibenzo[*f,h*]pyrrolo[1,2-*b*]isoquinoline-11,14(9*H*,12*H*)-dione (9)

Method TFAA and BF₃·Et₂O

TFAA (4.0 mL) was added to a solution of compound **8** (0.58 g, 1.32 mmol) and 1,2-dichloroethane (45 mL). The solution was stirred at room temperature for 1 h. Then, BF₃·Et₂O (4 mL) was added and solution was stirred overnight at room temperature. Majority of solvent was removed by rotary evaporation and DCM (50 mL) was added slowly. Then, a solution of saturated K₂CO₃ in water was added dropwise. The solution was stirred overnight at room temperature. Then, it was filtrated and organic phase was extracted with CHCl₃ and water. The solvent was removed by rotary evaporation and purified by column chromatography (2:1:0.3 CHCl₃:EtOAc:MeOH) to give **9** (0.4 g, 65 % yield) mp 225 °C (lit.⁵ 228-230 °C). ¹HNMR (CDCl₃): δ 2.30 (1H, m), 2.40 (1H, m), 2.60 (1H, m), 2.62 (1H, m), 3.51 (3H, s), 3.91 (1H, m), 3.96 (3H, s), 4.05 (3H, m), 4.06 (3H, s), 4.35 (1H, s), 5.44 (1H, s), 7.09 (1H, s), 7.32 (1H, s), 7.53 (1H, s), 7.72 (1H, s); ¹³C NMR (CDCl₃): δ 30.07, 55.02, 55.07, 56.02, 56.06, 56.17, 56.32, 58.49, 61.17, 102.61, 102.99, 105.22, 108.14. EIMS calcd for C₂₄H₂₃NO₆ *m/z* 421.153; found 422.157.

Method Oxalyl chloride and SnCl₄

Compound **8** (0.5 g, 11.39 mmol) was dissolved in DCM (40 mL) and (CO)₂Cl₂ (0.4 mL, 3.15 mmol) was added dropwise with DMF (1-2 drops). Mixture was stirring for 1.5 h at room temperature. Then, it was brought to 35 °C, to add SnCl₄ (0.6 mL, 2.30 mmol) for 4 h under N₂ atmosphere. The reaction was cooled to room temperature and was added cold 2 N HCl (3.5 mL). The solution was extracted with CHCl₃ and H₂O. The organic phase was separated and dried with Na₂SO₄, filtered, and solvent removed by rotary evaporation. Crude product was purified by column chromatography (2:1:0.3 CHCl₃:EtOAc:MeOH) to give **9** 0.35 g. (60-75 % yield) mp 225 °C.

Preparation of (13aS,14S)-14-hydroxy-2,3,6,7-tetramethoxy-12,13,13a,14-tetrahydrobenzo[*f,h*]pyrrolo[1,2-*b*]isoquinolin-11(9*H*)-one (10)

Compound **9** (3.76 g, 4.85 mmol) was added THF (25 mL) under N₂ gas at -10 °C. Then K-selectride (1.0 M solution in tetrahydrofuran) (3.1 mL, 13.95 mmol) was added and stirred for 5 h. The solution was added 2 N HCl (2 mL). Then, organic phase was extracted with CHCl₃ and water. The solvent was removed by rotary evaporation and purified by column chromatography. (2:1:0.3 CHCl₃:EtOAc:MeOH) to give **10** (2.95 g, 75 % yield) mp 260 °C (lit.⁵ 262 °C). ¹H NMR (CDCl₃): δ 2.30 (1H, m), 2.36 (1H, m), 2.62 (1H, m), 2.63 (1H, m), 2.80 (1H, m), 3.94 (3H, s), 3.97 (1H, m), 4.09 (3H, s), 4.11 (3H, s), 4.12 (3H, s), 4.49 (1H, m), 5.19 (1H, m), 6.98 (1H, s), 7.59 (1H, s), 7.75 (1H, s), 7.70 (1H, s); ¹³C NMR (CDCl₃): δ 30.20, 32.60, 40.02, 55.90, 56.06, 58.62, 64.69, 103.53, 103.60, 103.70, 104.46, 175.40. EIMS calcd for C₂₄H₂₅NO₆ *m/z* 423.168; found 424.179.

Preparation of (13aS, 14S)-2,3,6,7-tetramethoxy-9,11,12,13,13a,14-hexahydrobenzo[*f,h*]pyrrolo[1,2-*b*]isoquinolin-13-ol (11)

To a mixture of LiAlH₄ (0.2 g, 7.11 mmol) in THF (60 mL) at -10 °C was added dropwise a solution of **10** (0.27 g, 0.638 mmol) in THF. Ice bath was removed and solution was stirred at room temperature overnight. The solution was brought back to -10°C and EtOAc (50 mL) was added dropwise, then Na₂SO₄·10H₂O was added. The use of 2 N HCl to quench the reaction proved to lower the yield. The solution was filtered and solvent was removed by rotary evaporation. The crude product was purified by column chromatography (2:1:0.5 CHCl₃:EtOAc:MeOH) to give **11** 0.15 g (60 % yield) mp 268 °C (lit.⁵ 270 °C). ¹H NMR (CDCl₃): δ 1.84 (1H, m), 2.16 (1H, m), 2.20 (1H, m), 2.21 (1H, m),

2.82 (1H, m), 3.13 (1H, m), 3.77 (3H, s), 3.28 (1H, m), 4.10 (3H, s), 4.11 (3H, m) 4.16 (3H, m), 4.81 (1H,s), 6.06 (1H, s), 7.37 (1H, s), 7.59 (1H, s), 7.89 (1H,s); ^{13}C NMR (CDCl₃): δ 23.93, 24.02, 53.29, 55.71, 55.75, 55.92, 56.08, 64.93, 65.62, 102.2, 102.54, 102.7, 105.36. EIMS calcd for C₂₄H₂₇NO₅ m/z 409.189; found 410.189.

Preparation of (S)-1,5-dimethoxy-1,5-dioxopentan-2-aminium chloride (BMPAC) (27)

To a solution of L(+)-glutamic acid **26** (6 g, 40.80 mmol) in MeOH (300 mL) at -10 °C was added dropwise SOCl₂ (40 mL). Then, the solution was heated at 35 °C overnight. Solvent was removed by rotary evaporation at 35 °C as yellow oil. A white precipitate was formed in vacuum overnight.

Preparation of anisaldehyde TLC stain

This clear stain was prepared by dissolving *p*-anisaldehyde (9.2 mL) in EtOH (338 mL) containing conc. H₂SO₄ (12.5 mL) and acetic acid (3.75 mL). The plate was developed by heating on a hot plate/drier.

Experimental procedure for DCB 3507

Synthesis of (*E*)-3-(3,4-dimethoxyphenyl)-2-phenylacrylic acid (**13**)

3,4-dimethoxybenzaldehyde (**1**, 99+%, 15.0 g, 90.3 mmol) was stirred in Ac₂O (55 mL) and TEA (40 mL), then 2-phenylacetic acid **12** (20.0 g, 147.0 mmol) was added. The solution was heated to 100 °C and left stirring overnight. The mixture was cooled to room temperature and water (50 mL) was added dropwise. Then, a solution of K₂CO₃ (75 g) in water (250 mL) was added dropwise. The solution was refluxed until all solid dissolved and left spinning overnight at room temperature. The mixture was separated with Et₂O (2 x 100 mL) and water phase was collected. The aqueous layer was acidified with 2 N HCl until pH = 1 was reached. The precipitation was recrystallized using MeOH to obtain **13** (35.0 g, >90.0 % yield). mp 220 °C. ¹H NMR (CDCl₃): δ 3.36 (3H, s), 3.84 (3H, s), 6.41 (1H, s), 6.74 (1H, d), 6.88 (1H, d), 7.29 (1H, m), 7.34 (1H, m), 7.39 (1H, m), 7.42 (1H, d), 7.81 (1H, s); ¹³C NMR (CDCl₃): δ 55.25, 55.91, 110.83, 112.32, 126.26, 128.25, 129.08, 130.24, 130.26, 142.68, 172.89. EIMS calcd for C₁₇H₁₆O₄ *m/z* 284.105; found 285.111.

Synthesis of (*E*)-methyl 3-(3,4-dimethoxyphenyl)-2-phenylacrylate (**14**)

Compound **13** (13.0 g, 45.76 mmol) was added MeOH (500 mL) and the solution was stirred at 60 °C. Then, H₂SO₄ (15 mL) was added dropwise, and solution was stirred overnight. The solvent was removed by rotary evaporation at 35 °C and a precipitate formed. This product was washed with cold MeOH. The precipitate was purified by column chromatography (2:0.5 EtOAc:hexane). To obtain **14** (13.05 g, >90%) mp 160 °C. ¹H NMR (CDCl₃): δ 3.50 (3H, s), 3.82 (3H, s), 3.90 (3H, s), 5.74 (1H, d), 6.48 (1H, d), 6.77 (1H, d), 6.79 (1H, t), 6.83 (1H, t), 6.91 (1H, t), 6.93 (1H, d), 7.26 (1H, s), 7.75 (1H, s); ¹³C NMR (CDCl₃): δ 52.30, 55.34, 55.92, 111.48, 112.04, 114.06, 122.21, 126.97, 140.56, 145.84, 148.56, 149.27. EIMS calcd for C₁₈H₁₈O₄ *m/z* 298.121; found 299.123.

Synthesis of methyl 2,3-dimethoxyphenanthrene-9-carboxylate (**15**)

Method FeCl₃ and SiO₂

Compound **14** (3.2 g, 10.73 mmol) was added DCM (320 mL) at room temperature. Then, a fresh mixture of FeCl₃:SiO₂ (11 g: 11 g) was added to the solution to be ran for two days at room temperature. The solution was filtered and mixture was separated with

CHCl₃. The solvent was removed by rotary evaporation at 35 °C. SiO₂ was dried overnight to obtain higher yield. This product was purified by column chromatography (2:0.5 EtOAc:hexane). To obtain **15** as a yellow powder (1.43 g, >90%) mp 128 °C. ¹H NMR (CDCl₃): δ 4.03 (3H, s), 4.05 (3H, s), 4.14 (3H, s), 7.25 (1H, d), 7.62 (1H, t), 7.64 (1H, t), 7.98 (1, s), 8.44 (1H, s), 8.55 (1H, s), 8.99 (1H, d); ¹³C NMR (CDCl₃): δ 52.13, 55.98, 56.05, 103.04, 109.21, 126.44, 126.54, 126.69, 130.03, 168.13. EIMS calcd for C₁₈H₁₆O₄ *m/z* 296.105; found 297.086.

Method VOF₃ and TFA

Compound **14** (2.5, 8.38 mmol) was added DCM (35 mL) and stirred at -10 °C. Then, the following solution was added dropwise: VOF₃ (2.5 g, 20.17 mmol), DCM (58 mL), EtOAc (35 mL), TFA (2 mL), and TFAA (3 drops). The solution was stirred for 5 h at -10 °C. To quench the reaction, it was poured on ice and organic phase separated with CHCl₃ (3 x 50 mL). The solution was dried with Na₂SO₄, filtered, and solvent was removed by rotary evaporation. The crude product was purified by column chromatography (2:0.5 EtOAc:hexanes) to obtain **15** as a yellow powder (3.07 g, > 90%) mp 128 °C. EIMS calcd for C₁₈H₁₆O₄ *m/z* 296.105; found 297.106.

Synthesis of (2,3-dimethoxyphenanthren-9-yl)methanol (16)

To a mixture of LiAlH₄ (0.5 g, 13.15 mmol) in THF (48 mL) at -10 °C was added dropwise a solution of **15** (1.2 g, 4.05 mmol) in THF. Ice bath was removed and solution was stirred at room temperature overnight. The solution was brought back to -10 °C and was added EtOAc (50 mL) dropwise, then Na₂SO₄·10H₂O was added until solution turned yellow. Alternatively, 2 N HCl can be used to quench the reaction, but Na₂SO₄·10H₂O gave a better yield. The solution was filtered and solvent was removed by rotary evaporation. The crude product was purified by column chromatography (2:0.5 EtOAc:hexanes) to **16** as a yellow powder (1.14 g, >90%) mp 150 °C. ¹H NMR (CDCl₃): δ 4.05 (3H, s), 4.13 (3H, s), 5.19 (2H, s), 5.60 (1H, s), 7.71 (1H, s), 7.23 (1H, s), 7.60 (1H, t), 7.67 (1H, t), 8.00 (1H, s), 8.19 (1H, d), 8.60 (1H, d); ¹³C NMR (CDCl₃): δ 64.19, 103.53, 108.67, 122.94, 124.77, 125.27, 126.00, 126.59. EIMS calcd for C₁₈H₁₆O₄ *m/z* 268.110; found 269.109.

Synthesis of (S)-methyl 1-((2,3-dimethoxyphenanthren-9-yl)methyl)-5-oxopurrolidine-2-carboxylate (17)

Step 1: Compound **16** (1.14 g, 4.25 mmol) was added freshly distilled CHCl_3 (98 mL) at -10°C . Then a solution of PBr_3 (1 mL, 3.65 mmol) in CHCl_3 (20 mL) was added dropwise. Iced bath was removed and solution was stirred at room temperature for 1.5 h. Then, it was poured over ice and stirred until ice was completely melted. The organic phase was separated by extraction using CHCl_3 and dried over Na_2SO_4 . The solution was filtered and solvent was removed by rotary evaporation.

Step 2: The crude product was added DMF (118 mL), glutamic acid dimethyl ester **27** (3.2 g, mmol), and allowed to dissolve completely. Then K_2CO_3 (3.2 g) was added and the mixture was stirred at 65°C overnight.

Step 3: The solvent was removed by high vacuum rotary evaporation. Extraction with CHCl_3 and water was used to obtain organic phase. Then, it was dried with Na_2SO_4 , filtered, and solvent was removed by rotary evaporation. The crude product was dissolved in MeOH (63 mL) and AcOH (63 mL) and stirred at 45°C overnight. The solution was removed by rotary evaporation and high vacuum rotary evaporation. The crude product was purified by column chromatography (2:1 EtOAc:hexanes) to give **17** as a yellow powder (1.06 g, >90 % yield). mp 148°C . $^1\text{H NMR}$ (CDCl_3): δ 1.94 (1H, m, $J = 9.4$ Hz), 2.07 (1H, m, $J = 9.4$ Hz), 2.41 (1H, m, $J = 9.4$ Hz), 3.76 (1H, dd, $J = 2.98, 9.15$ Hz), 4.08 (3H, s), 3.99 (3H, s), 3.47 (3H, s), 4.42 (1H, d, $J = 14.63$ Hz), 5.47 (1H, d, $J = 14.63$ Hz), 7.09 (1H, s), 7.44 (1H, t, $J = 7.9$ Hz), 7.50 (1H, s), 7.56 (1H, t, $J = 7.9$ Hz), 7.89 (1H, s), 8.01 (1H, t, $J = 7.9$ Hz), 8.5 (1H, d, $J = 7.9$ Hz); $^{13}\text{C NMR}$ (CDCl_3): δ 22.81, 30.03, 44.47, 52.26, 52.26, 56.08, 58.74, 103.36, 108.34, 122.94, 124.93, 126.42, 126.59, 128.58, 171.6, 172.7. EIMS calcd for $\text{C}_{23}\text{H}_{23}\text{NO}_5$ m/z 393.158; found 394.164

Synthesis of (S)-1-((2, 3-dimethoxyphenanthren-9-yl)-5-oxopyrrolidine-2-carboxylic acid (18)

Compound **17** (1.06 g, 2.69 mmol) was stirred in solution of 1,4-dioxane (40 mL), 2 N KOH (25 mL), and MeOH (40 mL) for 2 h at room temperature. The solution was acidified with 2 N HCl until pH 1, and extracted with CHCl_3 and Et_2O . The solvent was removed by rotary evaporation to give **18** (1.04 g, >90 %) mp 160°C . $^1\text{H NMR}$ (CDCl_3) δ 1.90 (1H, m), 2.0 (1H, m), 2.41 (1H, m), 2.60 (1H, m), 3.8 (1H, m), 4.42 (1H, m), 5.74

(1H, m), 6.93 (1H, s), 7.57 (1H, s), 7.63 (1H, t), 7.67 (1H, t), 8.01 (1H, s), 8.10 (1H, d), 8.57 (1H, d); ^{13}C NMR (CDCl_3): δ 21.05, 30.01, 41.3, 59.6, 110.2, 119.0, 121.5, 121.8, 122.4, 122.6, 123.4, 176.4, 178.4. EIMS calcd for $\text{C}_{22}\text{H}_{21}\text{NO}_5$ m/z 379.142; found 380.150.

Alternative method to quench reaction **18**: DOWEX 50 (H^+) resin

To prepare resin: (use wet resin)

Dovex 50 was washed with diluted 4:1 HCl:water. Then, it was washed with DI water until neutral. The solution $\text{RCOO}^- \text{K}^+$ was added until pH is 1-2, and resin was filtered off. Product was extracted and dried in rotary evaporation to obtain white powder.

Synthesis of (S)-2,3-dimethoxy-13,13a-dihydrodibenzo[*f,h*]pyrrolo[1,2-*b*]isoquinoline-11,14(9*H*, 12*H*)-dione (19)

Method TFAA and $\text{BF}_3\cdot\text{Et}_2\text{O}$

TFAA (1.5 mL) was added to a solution of compound **18** (1.32 g, 3.48 mmol) and 1,2-dichloroethane (30 mL). The solution was stirred at room temperature for 1 h. Then, $\text{BF}_3\cdot\text{Et}_2\text{O}$ (1.5 mL) was added and solution was stirred overnight at room temperature. Majority of solvent was removed by rotary evaporation and DCM (15 mL) was added slowly. Then, a solution of saturated K_2CO_3 in water was added dropwise until release of CO_2 stopped and solution turned yellow from a dark green color. Solution was stirred overnight at room temperature or at least five hours. Then it was filtrated and organic phase extracted with CHCl_3 and water. Solvent was removed by rotary evaporation and purified by column chromatography (2:1:0.3 CHCl_3 :EtOAc:MeOH) to give **19** (0.93 g, 50-70 %) mp 155 °C. ^1H NMR (CDCl_3) δ 2.57 (1H, m), 2.59 (1H, m), 2.60 (1H, m), 2.62 (1H, m), 4.09 (3H, s), 4.12 (3H, s), 4.43 (1H, m), 4.79 (1H, m), 5.86 (1H, m), 7.64 (1H, t), 7.78 (1H, t), 7.97 (1H, s), 8.12 (1H, d), 9.03 (1H, s); ^{13}C NMR (CDCl_3): δ 20.74, 30.59, 40.82, 61.4, 55.92, 56.08, 103.0, 107.9, 124.8, 125.0, 125.1, 128.6. EIMS calculated for $\text{C}_{22}\text{H}_{21}\text{NO}_4$ m/z 361.131, found 362.138

Method Oxalyl chloride and SnCl_4

Compound **18** (0.5 g, 1.32 mmol) was dissolved in DCM (40 mL) and $(\text{CO})_2\text{Cl}_2$ (0.4 mL, 3.18 mmol) was added dropwise with DMF (1-2 drops). Mixture was stirring for 1.5 h at room temperature. Then, it was brought to 35 °C, to add SnCl_4 (0.6 mL, 2.31 mmol) for 4 h under N_2 atmosphere. The reaction was cooled to room temperature and was added

cold 2 N HCl (mL). The solution was extracted with CHCl₃ and H₂O. The organic phase was separated and dried with Na₂SO₄, filtered, and solvent removed by rotary evaporation. Crude product was purified by column chromatography (2:1:0.3 CHCl₃:EtOAc:MeOH) to give (**19** g, 60-75 % yield) mp 155 °C.

Synthesis of (13aS, 14S)-14-hydroxy-2,3-dimethoxy-12.13,13a,14-tetrahydrodibenzo[*f,h*]pyrrolo[1,2-*b*]isoquinolin-11(9*H*)-one (20)

Compound **19** (0.9 g, 2.49 mmol) was added THF (26 mL) under N₂ gas at -10 °C. Then K-selectride (1.0 M solution in tetrahydrofuran) (4.5 mL, mmol) was added and stirred for 5 h. Solution was added 2 N HCl (0.7 mL). Then organic phase was extracted with CHCl₃ and water. Solvent was removed by rotary evaporation and purified by column chromatography (2:1:0.3 CHCl₃:EtOAc:MeOH) to give **20** (0.47 g, >90 %) mp 118 °C. ¹H NMR (CDCl₃): δ 2.30 (1H, m), 2.32 (1H, m), 2.49 (1H, *J* = 4.38 Hz), 2.58 (1H, m), 3.96 (1H, m), 4.07 (3H, s), 4.08 (3H, s), 4.52 (1H, d, *J* = 17.49 Hz), 5.17 (1H, m), 5.42 (1H, d, *J* = 17.62 Hz), 7.52 (1H, t), 7.53 (1H, t), 7.60 (1H, s), 7.84 (1H, d), 7.93 (1H, s), 8.50 (1H, d, *J* = 8.34 Hz); ¹³C NMR (CDCl₃): δ 30.94, 31.03, 40.03, 41.01, 56.23, 56.19, 58.47, 58.47, 65.95, 103.77, 104.47, 122.82, 123.59, 126.62, 128.14. EIMS calculated for C₂₂H₂₁NO₄ *m/z* 363.147, found 364.136

Synthesis of (13aS, 14S)-2,3-dimethoxy-9,11,12,13a,14-hexahydrodibenzo[*f,g*]pyrrolo[1,2-*b*]isoquinolin-14-ol (21)

To a mixture of LiAlH₄ (1.2 g, mmol) in THF (33 mL) at -10 °C was added dropwise a solution of **20** (0.47 g, 1.29 mmol) in THF. Ice bath was removed and solution was stirred at room temperature overnight. The solution was brought back to -10 °C and EtOAc (33 mL) was added dropwise, then Na₂SO₄·10H₂O was added until solution turned yellow, but it should not be left spinning for more than four hours. The solution was filtered and solvent was removed by rotary evaporation. The crude product was purified by column chromatography (2:1:0.5 CHCl₃:EtOAc:MeOH) to give **21** (0.40 g, 60-70 %) mp 168 °C. ¹H NMR (CDCl₃): δ 1.75 (1H, m), 1.79 (1H, m), 1.90 (1H, m), 2.03 (1H, m), 2.13 (1H, m, *J* = 4.42 Hz), 2.30 (1H, m), 2.93 (1H, d, *J* = 15.42 Hz), 2.95 (1H, m), 3.2 (1H, d, *J* = 15.42 Hz), 4.04 (3H, s), 4.1 (3H, s), 4.75 (1H, m, 1.78 Hz), 6.80 (1H, d, *J* = 8.12 Hz), 7.05 (1H, m, *J* = 7.29 Hz), 7.39 (1H, m, *J* = 7.34 Hz), 7.81 (1H, s), 7.87

(1H, s), 8.29 (1H, d, $J = 8.32$ Hz); ^{13}C NMR (CDCl_3): 21.4, 24.06, 53.43, 55.42, 55.92, 56.25, 64.87, 103.36, 105.36, 122.28, 122.61, 125.59, 126.26. EIMS calculated for $\text{C}_{22}\text{H}_{23}\text{NO}_3$ m/z 349.17, found 350.191.

Experimental procedure for DCB 3508

Synthesis of (S)-2-(methoxycarbonyl)pyrrolidinium chloride (23)

To a solution of L(-)-proline **22** (4.6 g, 39.98 mmol) in MeOH (40 mL) at -30 °C was added SOCl₂ (4 mL). The solution was heated at reflux for 1 h. Solvent was removed by rotary evaporation as a yellow oil and precipitate was formed in vacuum overnight.

Synthesis of (S)-methyl 1-(2,3,6,7-tetramethoxyphenanthren-9-yl)methylpyrrolidine-2-carboxylate (24)

To a solution of **6.1** (0.3 g, 0.77 mmol) and acetone (30 mL) was added **23** (0.2 g, 1.21 mmol) and NaI (1g). The solution was refluxed for 48 h. Solvent was removed by rotary evaporation to obtain an oily compound, which was precipitated by adding EtOAc and hexanes (70:30 v/v) to give **24** (0.4 g, > 90%) mp 197 °C. ¹H NMR (CDCl₃): δ 1.18 (1H, m), 1.89 (1H, m), 1.68 (1H, m), 2.12 (1H, m), 2.28 (1H, m), 2.78 (1H, m), 3.19 (1H, m), 3.53 (1H, m), 3.61 (1H, m), 4.03 (3H, s), 4.04 (3H, s), 4.05 (3H, m), 4.48 (3H, s), 4.49 (1H, s), 7.08 (1H, s), 7.37 (1H, s), 7.68 (1H, s), 7.70 (1H, s), 8.09 (1H, s); ¹³C NMR (CDCl₃): 22.89, 29.53, 51.76, 55.92, 56.18, 56.20, 56.24, 58.74, 102.86, 102.70, 106.68, 125.43. EIMS: calcd for C₂₅H₂₉NO₆ m/z 439.199; found 440.205.

Synthesis of (S)-1-((2,3,6,7-tetramethoxyphenanthren-9-yl)methylpyrrolidin-2-yl)methanol (25)

To a mixture of LiAlH₄ (1.7g, 44.79 mmol) in THF (100 mL) at -10 °C was added dropwise a solution of **24** (0.94g, 2.14 mmol) in THF. Ice bath was removed and solution was stirred at room temperature overnight. The solution was brought back to -10 °C and was added EtOAc (50 mL) dropwise, then Na₂SO₄·10H₂O was added until solution turned yellow. The solution was filtered and solvent was removed by rotary evaporation. The crude product was purified by column chromatography (2:1:0.5 CHCl₃:EtOAc:MeOH) to give **25** (0.9 g, >90 %) mp 201 °C. ¹H NMR (CDCl₃): δ 1.73 (1H,m), 1.86 (1H,m), 1.89 (1H,m), 2.03 (1H,m), 2.43 (1H,m), 2.89 (1H,m), 2.92 (1H,m), 3.49 (1H, d), 3.75 (1H, d), 3.77 (1H,m), 4.04 (3H, s), 4.08 (3H, s), 4.12 (3H, s), 4.13 (3H, s), 4.49 (1H, d), 7.21 (1H, s), 7.54 (1H, s), 7.61 (1H, s), 7.79 (1H, s), 7.84 (1H, s); ¹³C NMR (CDCl₃): 50.77, 54.59, 55.92, 56.08, 56.22, 59.23, 62.55, 65.21, 103.3, 104.86, 108.34, 125.76. EIMS calculated for C₂₄H₂₉NO₅ m/z 411.205; found 412.209.

Experimental procedure for DCB 3506

Synthesis of (*E*)-3-(4-acetoxy-3-methoxyphenyl)-2-(3,4-dimethoxy)acrylic acid (**27**).

3-hydroxy-4-methoxybenzaldehyde (**26**, 99+%, 15.0 g, 98.6 mmol) was stirred in Ac₂O (55 mL) and TEA (40 mL) until solution was completely dissolved, then (3,4-dimethoxyphenyl)acetic acid (**2**, 99%, 20.0 g, 102.0 mmol) was added. The solution was heated slowly to 100 °C and left stirring overnight. The mixture was cooled to room temperature, and water (50 mL) was added dropwise. Then, a solution of K₂CO₃ (75 g) in water (250 mL) was added dropwise. The mixture was refluxed until all solid dissolved. Then, mixture was cooled to room temperature and left stirring overnight. Mixture was separated with Et₂O (2 x 100 mL) and water phase was collected (bottom). The aqueous layer was acidified with 2 N HCl, which was added dropwise until pH 1 was reached. The precipitation was recrystallized using MeOH to obtain **27** (39.0 g, >90.0 % yield). mp 172.9 °C (lit.⁶ 170.9-176.2 °C); ¹H NMR (CDCl₃): δ 2.28 (3H, s), 3.46 (3H, s), 3.82 (3H, s), 3.89 (3H, s), 6.66 (1H, s), 6.77 (1H, m), 6.84 (1H, m), 6.89 (1H, m), 6.90 (1H, m), 6.92 (1H, m), 7.86 (1H, s); ¹³C (NMR CDCl₃): δ 55.42, 55.90, 55.92, 56.08, 111.52, 112.75, 113.93, 114.20, 119.60, 142.63, 195.91. EIMS calcd for C₂₀H₂₀O₇ *m/z* 372.121; found 373.126.

Synthesis of (*E*)-methyl 2-(3,4-dimethoxyphenyl)-3-(4-hydroxy-3-methoxy)acrylate (**28**)

Compound **27** (13.0 g, 34.93 mmol) was added to MeOH (500 mL) and the solution was stirred at 60 °C. Then, H₂SO₄ (15 mL) was added dropwise and solution was stirred overnight. The solvent was removed by rotary evaporation at 40 °C and a precipitate solid/liquid was formed. This product was filtrated and washed quickly with cold MeOH. This solid was purified by column chromatography (2:0.5 EtOAc:hexane). To obtain **28** (12.50 g, >90%) mp 126 °C (lit.⁶ 121.7 -123.5 °C). ¹H NMR (CDCl₃): δ 3.50 (3H,s), 3.79 (3H, s), 3.82 (3H, s), 3.90 (3H, s), 6.66(1H, s), 6.76 (1H, m), 6.77 (1H, s), 6.78 (1H, m), 6.91 (1H, m), 7.75 (1H, s), 7.87 (1H, m); ¹³C NMR (CDCl₃): δ 55.29, 55.32, 55.90, 111.47, 112.89, 114.09, 122.19, 126.96, 140.55, 142.63, 195.91. EIMS calcd for C₁₉H₂₀O₆ *m/z* 344.126; found 345.122.

Synthesis of (E)-methyl 3-(4-acetoxy-3-methoxyphenyl)-2-(3,4-dimethoxyphenyl)acrylate (29)

Compound **28** (2.5 g, 7.26 mmol) was added TEA (20 mL) and Ac₂O (15 mL) and solution was left stirring for 1 h at room temperature. The product 29 precipitated as yellow powder. In case product would not precipitate, the reagents (TEA and Ac₂O) were evaporated using high vacuum, and product was filtrated to give 29 (2.8 g, >90%) mp: 108 °C (lit.⁶ 110.5-114.8 °C). ¹H NMR(CDCl₃): δ 2.27 (3H, s), 3.46 (1H, s), 3.80 (3H, s), 3.81 (3H, s), 3.89 (3H, s), 6.23 (1H, m), 6.62 (1H, m), 6.89 (1H, m), 6.88 (1H, s), 6.90 (1H, s), 7.76 (1H, s); ¹³C(CHCl₃): δ 52.34, 55.34, 55.90, 55.91, 110.12, 111.43, 113.76, 122.11, 122.16, 124.17, 140.27, 170.64. EIMS calcd for C₂₁H₂₂O₇ *m/z* 386.136; found 387.132.

Synthesis of methyl 3-acetoxy-2,6,7-trimethoxyphenanthrene-9-carboxylate (30)

Compound **28** (1.86, 48.17 mmol) was added DCM (18 mL) at stirred at -10 °C. Then, the following solution was added dropwise: VOF₃ (2 g, 16.14 mmol), DCM (35 mL), EtOAc (17.5 mL), TFA (1 mL), and TFAA (3 drops). The solution was stirred for 5 h at -10 °C. To quench the reaction, it was poured on ice and organic phase separated with CHCl₃ (3 x 50 mL). The solution was dried with Na₂SO₄, filtered, and solvent was removed by rotary evaporation. The crude product was purified by column chromatography (2:0.5 EtOAc:hexanes) to give **30** (1.55 g, >90%) mp: 122 °C (lit.⁶ 121.7-123.5 °C). VOF₃ stains glassware with a green color that can be removed with 2 N HCl. ¹H NMR (CDCl₃): δ 2.40 (3H, s), 3.96 (3H, s), 4.05 (3H, s), 4.08 (3H, s), 4.09 (3H, s), 7.34 (1H, s), 7.76 (1H, s), 8.12 (1H, s), 8.40 (1H, s); ¹³C(CDCl₃): δ 20.76, 52.10, 52.18, 55.13, 55.98, 102.71, 106.70, 110.26, 116.11, 129.90. EIMS calcd for C₂₁H₂₀O₇ *m/z* 384.121; found 385.132.

Synthesis of 9-(hydroxymethyl)-2,6,7-trimethoxyphenanthren-3-ol (31)

To a mixture of LiAlH₄ (3.5 g, 92.22 mmol) in THF (280 mL) at -10 °C was added dropwise a solution of **30** (3.95 g, 10.28 mmol) in THF. Ice bath was removed and solution was stirred at room temperature overnight. The solution was brought back to -10 °C and EtOAc (100 mL) was added dropwise, then Na₂SO₄·10H₂O (around 10 g) was added slowly. The solution was left stirred overnight. The solution was filtered and solvent was removed by rotary evaporation. The crude product was purified by column

chromatography (2:0.5 EtOAc:hexanes) to give **31** (3.20 g, >90%) mp: 189 °C (lit.⁶ 189.4-192.1 °C). ¹HNMR (CDCl₃): δ 4.05 (3H, s), 4.08 (3H, m), 4.09 (3H, s), 5.95 (1H, s), 7.11 (1H, s), 7.19 (1H, s), 7.52 (1H, s), 7.56 (1H, s), 7.84 (1H, s), 7.96 (1H, s); ¹³C NMR (CDCl₃): δ 56.00, 56.10, 56.12, 63.4, 104.00, 104.70, 104.80, 109.00. EIMS calcd for C₁₈H₂₈O₅ *m/z* 314.115; found 315.118.

Synthesis of 1-((3-hydroxy-2,6,7-trimethoxyphenanthren-9-yl)methyl)-5-oxopyrrolidine-2-carboxylate (32)

This reaction required three steps:

Step 1: Compound **31** (3.5 g, 11.14 mmol) was added freshly distilled CHCl₃ (200 mL) at -10 °C. Using regular CHCl₃ increased side reactions. Then a solution of PBr₃ (4.8 mL, 17.93 mmol) in CHCl₃ (5 mL) was added dropwise. Iced bath was removed and solution was stirred at room temperature for 1.5 h. Then, the solution was poured over ice and stirred until ice was completely melted. The organic phase was separated by extraction using CHCl₃ and dried over Na₂SO₄. The solution was filtered and solvent was removed by rotary evaporation to obtain the brominated intermediate as a yellow solid

Step 2: The crude product intermediate was added DMF (200 mL), glutamic acid dimethyl ester (6 g, 28.35 mmol), and K₂CO₃ (10 g). The mixture was stirred at 65 °C overnight.

Step 3: The solvent was removed by high vacuum rotary evaporation. Extraction with CHCl₃ and water was used to obtain organic phase. Then, it was dried with Na₂SO₄, filtered, and solvent was removed by rotary evaporation. The crude product was dissolved in MeOH (80 mL) and AcOH (80 mL) and stirred at 45 °C overnight. The solution was removed by rotary evaporation and high vacuum rotary evaporation to obtain a yellow solid. The crude product was purified by column chromatography (2:0.5 EtOAc:hexanes) to give **32** (3.8 g, >90 % yield) mp 215 °C (lit.⁶ 210-215 °C). ¹HNMR (CDCl₃): δ 2.34 (1H, s), 2.62 (2H, m), 3.57 (3H, s), 3.82 (1H, m), 4.03 (3H, s), 4.05 (3H, m), 4.08 (3H, m), 4.43 (1H, d), 5.52 (1H, d), 7.16 (1H, s), 7.38 (1H, s), 7.59 (1H, s), 7.83 (1H, s), 7.96 (1H, s); ¹³C NMR (CDCl₃): 22.90, 29.70, 47.60, 56.00, 56.10, 56.22, 66.1, 104.30, 108.00, 108.30, 109.00, 171.12. EIMS calcd for C₂₄H₂₅NO₇ *m/z* 439.163; found 440.166.

Synthesis of 1-((3-hydroxy-2,6,7-trimethoxyphenanthren-9-yl)methyl)-5-oxopyrrolidine-2-carboxylic acid (33)

Compound **32** (8.0 g, 18.22 mmol) was stirred in solution of 1,4-dioxane (100 mL), 2 N KOH (200 mL), and MeOH (100 mL) for 1.5 h at room temperature. The solution was acidified with 2 N HCl until pH = 1, and extracted with CHCl₃ and Et₂O. The solvent was removed by rotary evaporation to give **33** (7.8 g, 80 % yield) mp: 318 °C (lit.⁶ 320 °C). ¹HNMR (CDCl₃): δ 2.26 (2H, m), 2.47 (2H, m), 3.59 (1H, d), 3.85 (3H, s), 3.88 (3H, s), 3.91 (3H, s), 4.19 (1H, d), 5.51 (1H, d), 7.16 (1H, s), 7.37 (1H, s), 7.41 (1H, s), 7.74 (1H, s), 8.32 (1H, s); ¹³C NMR (CDCl₃): δ 23.00, 29.94, 44.35, 56.10, 56.22, 58.57, 58.60, 104.44, 105.51, 107.64, 109.22, 126.72, 175.89. EIMS calcd for C₂₃H₂₃NO₇ *m/z* 425.147; found 426.149.

Synthesis of (S)-3-hydroxy-2,6,7-trimethoxy-13,13a-dihydrodibenzo[*f,h*]pyrrolo[1,2-*b*]isoquinoline-11,14(9*H*,12*H*)-dione (34)

Compound **33** (0.5 g, 1.18 mmol) was dissolved in DCM (40 mL) and (CO)₂Cl₂ (0.4 mL, 3.15 mmol) was added dropwise with DMF (1-2 drops). Mixture was stirring for 1.5 h at room temperature. Then, it was brought to 35 °C, to add SnCl₄ (0.6 mL, 2.30 mmol) for 4 h under N₂ atmosphere. The reaction was cooled to room temperature and was added cold 2 N HCl (3.5 mL). The solution was extracted with CHCl₃ and H₂O. The organic phase was separated and dried with Na₂SO₄, filtered, and solvent removed by rotary evaporation. Crude product was purified by column chromatography (2:1:0.3 CHCl₃:EtOAc:MeOH) to give **34** 0.35 g. (60-75 % yield) mp: 220 °C (lit.⁶ 220 °C). ¹HNMR (CDCl₃): δ 2.14 (2H, m), 2.39 (2H, m), 4.01 (3H, s), 4.05 (3H, s), 4.12 (3H, s), 4.37 (1H, d), 4.67 (1H, d), 5.72 (1H, d), 7.23 (1H, s), 7.72 (1H, s), 8.09 (1H, s), 9.16 (1H, s); ¹³C NMR (CDCl₃): δ 20.68, 29.64, 40.71, 55.89, 56.27, 61.07, 103.44, 103.46, 104.39, 120.98, 195.13, 173.71. EIMS calcd for C₂₃H₂₁NO₆ *m/z* 407.137; found 408.137.

Synthesis of (13*aS*,14*S*)-3,14-dihydroxy-2,6,7-trimethoxy-12,13,13*a*,14-tetrahydrodibenzo[*f,h*]pyrrolo[1,2-*b*]isoquinolin-11(9*H*)-one (35)

Compound **34** (3.81 g, 9.36 mmol) was added THF (25 mL) under N₂ gas at -10 °C. Then K-selectride (1.0 M solution in tetrahydrofuran) (3.1 mL, 13.95 mmol) was added and stirred for 5 h. The solution was added 2 N HCl (2 mL). Then, organic phase was extracted with CHCl₃ and water. The solvent was removed by rotary evaporation and

purified by column chromatography. (2:1:0.3 CHCl₃:EtOAc:MeOH) to give **35** (3.25 g, 75 % yield) mp 160 °C (lit.⁶ 160 °C). ¹H NMR (CDCl₃): δ 2.09 (2H, m), 2.28 (2H, m), 2.86 (1H, m), 4.45 (1H, d), 5.15 (1H, d), 5.52 (1H, d), 7.17 (1H, s), 7.52 (1H, s), 7.81 (1H, s), 7.97 (1H, s); ¹³C NMR (CDCl₃): δ 21.72, 30.02, 45.51, 60.51, 67.55, 104.01, 104.71, 108.81, 108.92. EIMS calcd for C₂₃H₂₃NO₆ *m/z* 409.153; found 410.155.

Synthesis of (13aS, 14S)-2,6,7-trimethoxy-9,11,12,13,13a,14-hexahydrodibenzo[*f,h*]pyrrolo[1,2-*b*]isoquinoline-3,14-diol (36)

To a mixture of LiAlH₄ (0.2 g, 7.11 mmol) in THF (60 mL) at -10 °C was added dropwise a solution of **35** (0.27 g, 0.66 mmol) in THF. Ice bath was removed and solution was stirred at room temperature overnight. The solution was brought back to -10°C and EtOAc (50 mL) was added dropwise, then Na₂SO₄·10H₂O was added. The use of 2 N HCl to quench the reaction proved to lower the yield. The solution was filtered and solvent was removed by rotary evaporation. The crude product was purified by column chromatography (2:1:0.5 CHCl₃:EtOAc:MeOH) to give **11** 0.15 g (60 % yield) mp 168 °C (lit.⁶ 170 °C). ¹H NMR (CDCl₃): δ 2.08 (2H, m), 2.24 (2H, m), 2.40 (1H, m), 2.47 (2H, m), 3.40 (1H, d), 3.94 (3H, s), 3.98 (3H, s), 3.99 (3H, s), 5.13 (1H, d), 7.19 (1H, s), 7.60 (1H, s), 7.89 (1H, s), 8.04 (1H, s); ¹³C NMR (CDCl₃): δ 23.03, 23.04, 53.85, 55.57, 55.66, 55.70, 55.72, 65.80, 65.83, 103.70, 103.72, 103.86, 105.22. EIMS calcd for C₂₃H₂₅NO₅ *m/z* 395.173; found 396.173.

Experimental procedure for DCB 3509

Synthesis of (13a*S*, 14*S*)-3-(3-hydroxypropoxy)-2,6,7-trimethoxy-9,11,12,13,13a,14-hexahydrodibenzo[*f,h*]pyrrolo[1,2-*b*]isoquinolin-14-ol (**37**)

To a solution of **36** (30 mg, 75.92 μmol) in acetone (15 mL) was added 3-bromopropanol (60 mg, 434.88 μmol) and K_2CO_3 (0.1 g). The solution was heated to 65 $^\circ\text{C}$ for 48 hours. At room temperature, the solution was filtered and washed with CHCl_3 . The solvent was removed by rotary evaporation and concentrated to obtain an oil. The crude product was purified by column chromatography CHCl_3 :EtOAc:MeOH (2:1:0.5) to give **37** (30-60 mg, >90 % yield) as powder. mp 265 $^\circ\text{C}$. EIMS calculated for $\text{C}_{26}\text{H}_{31}\text{NO}_6$ m/z 453.215; found: 454.219

Experimental procedure for biotinylated tylophorine analog

Synthesis of (13aS, 14S)-3-(6-bromohexyloxy)-14-hydroxy-2,6,7-trimethoxy-12,13,13a,14-tetrahydrodibenzo[*f,h*]pyrrolo[1,2-*b*]isoquinolin-11(9*H*)-one (38)

To a solution of intermediate **35** (0.07 mg, 0.17 mmol) and acetone (100 mL) was added 1,6-dibromohexane (0.2 mL, 0.83 mmol) and K₂CO₃ (0.4 g). The solution was refluxed to 70 °C for 48 hours. At room temperature, the solution was filtered and washed with CHCl₃. The solvent was removed by rotary evaporation and concentrated to obtain an oil. The crude product was added EtOAc:hexanes:Et₂O (2:1:1) and left stirring for 30 minutes, then product precipitated to give **38** (70-100 mg, >90 % yield) as yellow powder. mp 287 °C. ¹H NMR (CDCl₃): δ 1.3 (2H,m), 1.61 (2H,m), 1.8 (2H,m), 1.98 (2H,m), 2.3 (1H,m), 2.32 (1H,m), 2.5 (1H,m), 2.52 (1H,m), 2.62 (1H,m), 3.5 (2H, m), 3.8 (3H, s), 3.91 (1H,m), 4.05 (3H,s), 4.08 (3H, s), 4.24 (2H, t), 4.43 (1H, s), 5.12 (1H,m), 5.22 (1H,s), 6.84 (1H,s), 7.63 (1H,m), 7.71 (1H, s), 7.78 (1H, s); ¹³C NMR (CDCl₃): δ 28.4, 29.04, 31.69, 32.6, 32.69, 34.01, 40.1, 41.15, 56.06,56.07,56.08, 61.2, 65.87, 69.35, 103.19, 103.37, 104.86, 105.19, 175.56. EIMS calculated for C₂₄H₂₉NO₅ *m/z* 571.157, found: 572.167, 5.74.167.

Synthesis of 3-(6-azidohexyloxy)-14-hydroxy-2,6,7-trimethoxy-12,12,13a,14-tetrahydrodibenzo[*f,h*]pyrrolo[1,2-*b*]isoquinolin-11(9*H*)-one (39)

To a solution of intermediate **38** (30 mg, 56.15 μmol) and DMF (3 mL) was added NaN₃ (0.1g). The solution was left refluxing to 80 °C overnight. The solvent was removed by high vacuum evaporation. The crude product was purified by column chromatography (2:1:0.5) CHCl₃:EtOAc:MeOH to give **39** as an oil (30-70 mg, 70 - 90 %). mp 295 °C. ¹H NMR (CDCl₃): δ 1.30 (2H,m), 1.53 (1H,m), 1.61 (1H,m), 1.69 (1H,m), 1.79 (2H,m), 1.99 (1H,m), 2.29 (1H,m), 2.50 (1H,m), 2.59 (1H,m), 2.60 (1H,m), 2.72 (1H,m), 3.40 (2H,t), 3.83 (1H,m), 3.92 (3H,s), 4.06 (3H,s), 4.08 (3H,s), 4.23 (2H,t), 4.43 (1H,d), 5.16 (1H,s), 5.22 (1H,d), 6.88 (1H,s), 7.60 (1H,s), 7.69 (1H,s), 7.77 (1H,s); ¹³C NMR (CDCl₃): δ 19.41, 26.71, 26.72, 29.20, 31.03, 34.84, 41.15, 55.92, 56.20, 56.25, 58.57, 61.00, 65.70, 69.19, 103.03, 103.30, 104.53, 104.86, 175.50. EIMS calcd for C₂₉H₃₄N₄O₆ *m/z* 534.25; found 535.25

Synthesis of (13aS,14S)-3-(6-aminohexyloxy)-2,6,7-trimethoxy-9,11,12,13,13a,14-hexahydrodibenzo[*f,h*]pyrrolo[1,2-*b*]isoquinolin-14-ol (40)

To a mixture of LiAlH_4 (0.15g, 3.94 mmol) in THF (10 mL) at -10°C was added dropwise a solution of 39 (50 mg, 93.59 μmol) in THF. Ice bath was removed and solution was stirred at room temperature overnight. The solution was brought back to -10°C and was added EtOAc (20 mL), H_2O (10 mL), 3 M NaOH (7.5 mL), and H_2O (10 mL) dropwise. The solution was filtered with celite and solvent was removed by vacuum evaporation at room temperature. The crude product was used for the next step without any purification. The amine test using ninhydrin turned positive: purple. EIMS calculated for $\text{C}_{29}\text{H}_{38}\text{N}_2\text{O}_5$ m/z 494.28; found 495.29.

Synthesis of N-(6-((13a*S*,14*S*-14-hydroxy-2,6,7-trimethoxy-9,11,12,13,13a,14-hexahydrodibenzo[*f,h*]pyrrolo[1,2-*b*]isoquinolin-3-yl)oxy)hexyl)-5-((3a*S*,4a*S*,6a*R*)-2-oxohexahydro-1*H*-thieno[3,4-*d*]imidazol-4-yl)pentanamide (41)

A solution of biotin (0.01g, 0.04 mmol) in DMF (2 mL) under N_2 gas was added HBTU (0.01, 0.03 mmol), and DIPEA (0.05 mL). This solution was left stirring overnight at room temperature. Then, intermediate 40 (0.01g, 0.02 mmol) in DMF (1 mL) was added dropwise. The whole solution was left stirring at room temperature overnight. DMF was evaporated under high vacuum pressure at room temperature, then the following solvents were added: MeOH: Et_2O (2:10) and left in the refrigerator overnight to form a white precipitate. EIMS calculated for $\text{C}_{39}\text{H}_{52}\text{N}_4\text{O}_7\text{S}$ m/z 720.36; found $[\text{M}+\text{Na}]^+ = 743.35$

References

- (1) Akué-Gédu, R.; Al Akoum Ebrik, S.; Witczak-Légrand, A.; Fasseur, D.; El Ghammarti, S.; Couturier, D.; Decroix, B.; Othman, M.; Debacker, M.; Rigo, B. *Tetrahedron* **2002**, *58*, 9239-9247.
- (2) Buckley, T. F.; Rapoport, H. *J. Org. Chem.* **1983**, *48*, 4222-4232.
- (3) Gao, W.; Lam, W.; Zhong, S.; Kaczmarek, C.; Baker, D. C.; Cheng, Y.-C. *Cancer Res.* **2004**, *64*, 678-688.
- (4) Li, Z.; Jin, Z.; Huang, R. *Synthesis* **2001**, *2001*, 2365-2378.
- (5) Liepa Andris J, S. R. E. *J. Chem. Soc., Chem. Commun.* **1977**, 826-827.
- (6) Donaldson, G. R.; Atkinson M. R.; Murray A. W. *Biochem. Biophys. Res. Commun.* **1968**, *31*, 104-109.
- (7) Chauncy, B. *Aust. J. Chem.* **1970**, *23*, 2503-2516.
- (8) Tanner, U. Wiegrebé, W. *Arch. Pharm.* **1993**, *326*, 67-72.
- (9) Shi, L. M.; Fan, Y.; Lee, J. K.; Waltham, M.; Andrews, D. T.; Scherf, U.; Paull, K. D.; Weinstein, J. N. *J. Chem. Inf. Comput. Sci* **2000**, *40*, 367-379.
- (10) Yang, C.-W.; Chen, W.-L.; Wu, P.-L.; Tseng, H.-Y.; Lee, S.-J. *Mol Pharmacol.* **2006**, *69*, 749-758.
- (11) Gao, W.; Bussom, S.; Grill, S. P.; Gullen, E. A.; Hu, Y.-C.; Huang, X.; Zhong, S.; Kaczmarek, C.; Gutierrez, J.; Francis, S.; Baker, D. C.; Yu, S.; Cheng, Y.-C. *Bioorg. Med. Chem. Lett.* **2007**, *17*, 4338-4342.
- (12) Khatri, N. A.; Schmitthenner; H. F.; Shringarpure, J.; Weinreb, S. M. *J. Am. Chem. Soc* **1981**, *103*, 6387-6393.
- (13) Hedges, S. H.; Herbert, R. B.; Knagg, E.; Pasupathy, V. *Tetrahedron Lett.* **1988**, *29*, 807-810.
- (14) Gao, W.; Chen, A. P.-C.; Leung, C.-H.; Gullen, E. A.; Fürstner, A.; Shi, Q.; Wei, L.; Lee, K.-H.; Cheng, Y.-C. *Bioorg. Med. Chem. Lett.* **2008**, *18*, 704-709.
- (15) Kaczmarek, C., The University of Tennessee, 2004.
- (16) Wang, K.-L.; Lü, M.-Y.; Wang, Q.-M.; Huang, R.-Q. *Tetrahedron* **2008**, *64*, 7504-7510.
- (17) Jin, Z.; Wang, Q.; Huang, R. **2004**, *34*, 119 - 128.
- (18) Halton, B.; Maidment, A. I.; Officer, D. L.; Warnes, J. M. *Aust. J. Chem.* **1984**, *37*.
- (19) Schaumberg, J. P.; Hokanson, G. C.; French, J. C.; Smal, E.; Baker, D. C. *J. Org. Chem.* **1985**, *50*, 1651-1656.
- (20) Friebolin, H. *Basic One- and Two-Dimensional NMR Spectroscopy*; Third revised edition ed.; Wiley-VCH: Weinheim, 1998.
- (21) Bourry, A.; Akué-Gédu, R.; Hénichart, J.-P.; Sanz, G.; Rigo, B. *Tetrahedron Lett.* **2004**, *45*, 2097-2101.
- (22) Bourry, A.; Couturier, D.; Sanz, G.; Hijfte, L. V.; Hénichart, J.-P.; Rigo, B. *Tetrahedron* **2006**, *62*, 4400-4407.
- (23) Martin, L. L.; Scott, S. J.; Agnew, M. N.; Setescak, L. L. *J. Org. Chem* **1986**, *51*, 3697-3700.
- (24) Fülep, G. H.; Hoesl, C. E.; Höfner, G.; Wanner, K. T. *Eur. J. Med. Chem.* **2006**, *41*, 809-824.
- (25) Cui, D.-M.; Kawamura, M.; Shimada, S.; Hayashi, T.; Tanaka, M.

- Tetrahedron Lett.* **2003**, *44*, 4007-4010.
- (26) Kubo, A.; Nakai, T.; Koizumi, Y.; Kitahara, Y.; Saito, N.; Mikami, Y.; Yazawa, K.; Uno, J. *Heterocycles* **1996**, *42*, 195-211.
- (27) Pearson, W. H.; Walavalkar, R. *Tetrahedron* **1994**, *50*, 12293-12304.
- (28) Jempty, T. C.; Gogins, K. A. Z.; Mazur, Y.; Miller, L. L. *J. Org. Chem* **1981**, *46*, 4545-4551.
- (29) Jempty, T. C.; Miller, L. L.; Mazur, Y. *J. Org. Chem* **1980**, *45*, 749-751.
- (30) Krishna, P. R.; Lavanya, B.; Mahalingam, A. K.; Reddy, V. V. R.; Sharma, G. V. M. *Lett. Org. Chem.* **2005**, *2*, 360-363.
- (31) Nygren, C.; Zhong S.; Kaczmarek, C.; Turner, J. F. C.; Baker, D. C. *Acta Crystallogr.* **2004**, o208-o210.
- (32) Vanecko, J. A.; West, F. G. *Tetrahedron* **2005**, *7*, 2949-2952.
- (33) Govindachari, T. R.; Lakshmikantham, M. V.; Rajadurai, S. *Tetrahedron* **1961**, *14*, 284-287.
- (34) Wei, L.; Brossi, A.; Kendall, R.; Bastow, K. F.; Morris-Natschke, S. L.; Shi, Q.; Lee, K.-H. *Bioorg. Med. Chem.* **2006**, *14*, 6560-6569.
- (35) Silverstein, R. M. *Spectroscopic Identification of Organic Compounds*; Sixth ed.; Wiley: New York, 1998.
- (36) Silverman, R. B. *The Organic Chemistry of Drug Design and Drug Action*; Second ed.; Elsevier: Amsterdam, 2004.
- (37) von Corswant, C; Thoren, P. ; Engström, S. *J. Pharm. Sci.* **1998**, *87*, 200-208.

Appendix

Chapter Two: Synthesis of DCB 3507

2.2.1 Synthesis of (*E*)-2,3-bis(3,4-dimethoxyphenyl)acrylic acid (13)

2.2.1.1 Condensation reaction to give C

Experimental conditions and observations in detail:

Scheme 39: Condensation reaction to obtain C

First step: the solution was left stirring until it reached room temperature.

Second step: Water (150 mL) was added to decompose the unreacted Ac_2O . The temperature increased quickly, so the water had to be added slowly. It could get as high as 60 °C.

Third step: An aqueous solution of K_2CO_3 (150g/500 mL) was added, which caused foaming (CO_2 evolution). This solid/liquid solution was reheated until reflux to ensure completely dissolved; then, the solution was left stirring overnight at room temperature. Potassium carbonate was added to eliminate water and form the alkene. Scheme

Fourth step: The organic phase was separated with ethyl ether. The aqueous layer contained the cationic product. The organic layer was washed three times.

Fifth step: The aqueous solution was quenched with concentrated HCl. The acid was added dropwise with stirring. At the beginning the solution had a pH 10. As the solution became more acidic, it formed a sticky brown solid that stopped the stirring bar. In order to avoid this problem, the addition of HCl had to be slowly. A yellow precipitate started to form at pH 4.5–6. The addition of HCl continued until pH 1. The solution was left stirring overnight to maximize the conversion to product C. This precipitate was

separated and recrystallized with methanol at 65 °C. The final percent yield was between 70–80% after recrystallization.

2.2.1.2 Condensation reaction to give (13)

Experimental conditions and observations in detail:

Scheme 40: Condensation reaction to obtain 13

The same first, second, third, fourth, and fifth steps we repeated to synthesize **13**. The product **13** was consistently improved until a constant 95% yield. It was noticed that during quenching the reaction with HCl at pH ~ 5-7, a large amount of precipitate was formed which, seemed the right product; however, as the pH decrease to approximately pH 4-5, a yellowish sticky solid, formed that was unmanageable. A first attempt to avoid this problem to quenched at pH 5.5 and recrystallized the product. This white crystalline product partially dissolved in CHCl₃. It was determined that this product was a mixture of salts and did not give a satisfactory esterification reaction in the next step.

A second attempt to overcome this problem was to add all reagents slowly. The first, second, and third steps were gradually carried out. Normally, it took two hours to complete the four steps, but in this case the addition of water and aqueous solution of K₂CO₃ were added dropwise. It took five hours for the first three steps. For the fourth step, the aqueous solution was quenched in an ice bath and HCl was added dropwise. It took two hours to decrease the pH 1. At pH 1, the solution did not form any sticky solid and precipitated a clean yellow product.

As final review about this Perkin reaction, the addition of water and aqueous solution of K₂CO₃ must be added slowly. Then, the acidic quenching must be taken to

pH 1 with diluted HCl solution (2 N HCl), which is added dropwise to avoid the formation of any sticky solid.

VITA

Julio Gutierrez was born in Lima, Peru on March 10th, 1978. He graduated from high school in 1995. He started his chemistry career in the Universidad Nacional Mayor de San Marcos (University of San Marcos) in 1997. In 1999, he moved to the United States of America to continue his career at Columbus State University in Columbus, GA. He graduated in 2003 and joined Dr. David Baker group in 2004 at the University of Tennessee as a graduate student, after two consecutive undergraduate summer research in his synthetic laboratory (2002-2003). After graduation in August 2009, he will work as a post-doctoral fellow under the direction of Professor Thomas Tobin at the University of Kentucky.